

Electronic Thesis and Dissertation Repository

12-18-2020 10:00 AM

Impact of Extremely Low-Frequency Magnetic and Electric Stimuli on Vestibular-Driven Outcomes

Nicolas Bouisset, *The University of Western Ontario*

Supervisor: Alexandre Legros, *The University of Western Ontario*

A thesis submitted in partial fulfillment of the requirements for the Doctor of Philosophy degree in Kinesiology

© Nicolas Bouisset 2020

Follow this and additional works at: <https://ir.lib.uwo.ca/etd>



Part of the [Kinesiology Commons](#)

Recommended Citation

Bouisset, Nicolas, "Impact of Extremely Low-Frequency Magnetic and Electric Stimuli on Vestibular-Driven Outcomes" (2020). *Electronic Thesis and Dissertation Repository*. 7562.

<https://ir.lib.uwo.ca/etd/7562>

This Dissertation/Thesis is brought to you for free and open access by Scholarship@Western. It has been accepted for inclusion in Electronic Thesis and Dissertation Repository by an authorized administrator of Scholarship@Western. For more information, please contact wlsadmin@uwo.ca.

Abstract

The vestibular system is extremely sensitive to electric fields (E-Fields). Indeed, vestibular hair cells are graded potential cells and this property makes them very susceptible to small membrane potential modulations. Studies show that extremely low-frequency magnetic fields (ELF-MF) induced E-Fields impact postural control in which the vestibular system plays an important role. However, the knowledge of whether this is indeed a vestibular specific effect is still pending.

Considering its crucial role and the specific neurophysiological characteristics of its hair cells, the vestibular system emerges as an ELF-MF likely target

The three studies presented in this thesis aimed to further address whether ELF-MF modulate vestibular-driven outcomes.

Studies 1 and 2 aimed to investigate postural responses while more specifically targeting the vestibular system. However, we did not find any modulation in either study. Nonetheless, based on both studies, study 3 aimed to determine whether the orientation and frequency of our stimulations were more likely to target the otoliths. Therefore, the third study looked at the subjective visual vertical. Here, we found a potential ELF-MF utricular modulation.

This thesis is the first steppingstone in a new field of research. Further investigations regarding the interaction between the ELF-MF and the vestibular system will have to look at more reflexives vestibular outcomes. Nonetheless, this thesis provides valuable information that will need to be taken into consideration when writing future international guidelines and standards related to ELF-MF.

Keywords

Electromagnetic induction, Extremely Low-Frequency Magnetic Fields (ELF-MFs), human vestibular system, Electric vestibular stimulations, postural control, subjective visual vertical.

Summary for Lay Audience

Without noticing it, because of electricity generation and use, electromagnetic fields surround us in our daily lives. When sufficiently strong, these fields generate electrical currents inside the body. Such currents can modulate the physiologic electric information transiting in the form of electrical signals propagating inside the nerves. This impact raises health and safety concerns regarding the interactions between these fields and human neurophysiology. The most constant and sensitive response to electromagnetic fields resulting from power generation and transport is the perception of flickering lights appearing in the peripheral visual field. It underlines an interaction with cells in the retina. This phenomenon is used as the model for the interaction between the so-called extremely low frequency electromagnetic fields (ELF-MF) and the brain and is adopted as the basis for international guidelines and standards, setting the exposure limits to avoid adverse human effects. However, there are still several gaps in our overall knowledge of the threshold effects and our understanding of the precise interaction mechanisms and looking at the impact on other sensory systems could provide potential answers.

The vestibular system is a little sensory organ nestled within the inner ear. It is known as the balance system. This tiny sensory system has sensors extremely sensitive to electrical stimulations, which are also very close neurophysiologically to the sensors found within the retina. Therefore, the vestibular system seems to be a good alternate model to study the impact of low frequency electromagnetic fields on human neurophysiology.

This thesis explores the impact of electric and magnetic signals applied to the vestibular system by looking at balance in the first two studies and space perception in the third study. We did not find balance differences in outcomes when we stimulated the participants. However, the study on space perception showed that the ELF-MF could have modulated a subsystem within the vestibular system.

Altogether this thesis stresses useful information for the safety of both the public and the workers subjected to ELF-MF. Finally, this thesis is the first steppingstone in this relatively new research avenue and further research related to the vestibular system will need to be investigated in the future.

Co-Authorship Statement

On all manuscripts, Nicolas Bouisset is the first author and both Dr Sébastien Villard and Dr Alexandre Legros are co-authors.

Acknowledgments

Why do you consider going to graduate school?

I cannot recount how many times I was asked that first question. Indeed, as a physiotherapist having his private practice, a lot of my patients, colleagues, and friends were puzzled by the idea of me going back to school. Indeed, that meant, extra work, less income and for sure more “problems”! Why indeed would any sane person make such a choice, especially at the time when two daughters were born?

Why are you here?

This second question was asked by some of my professors, once I started my master’s degree in Montpellier, France. They were also perplexed as to why I was pursuing a research degree, given the fact that obviously, it would not make any difference as a clinical physiotherapist, and that there was little doubt I was too old to learn or start something new.

Without even knowing it, they all the more motivated me. Thank you!

My thanks also go to Alexandre Legros. You never judged my choices and you did not think my age would be an obstacle. On the contrary, you welcomed me rapidly into your lab, surely estimating I was sufficiently grown up to take responsibility for my actions. You have given my family the opportunity to live a Canadian adventure! Thank you for allowing the “old” physiotherapist a chance to start anew on this Ph.D. journey. Not many were willing to give me that chance...

Surely, the transition from the self-employed clinician to the Ph.D. student has probably been a little rough in the beginning and managing a student in his forties is probably not as easy as supervising a much younger student. Nonetheless, altogether, I can only conclude that things went well, since, after four years, you’re still willing to have me in your lab.

I now thank you for offering me my first research job opportunity!

Seb ...

Let me here express my gratitude and consideration for everything you did for me during the last four years.

First, thank you for leaving everything that you cherished in Minneapolis to come to London Ontario and start educating me without even knowing who I was!! 😊

Second, you have taught me the “joys” of programming by first introducing me to Matlab and R. Then came Python, as you consider it to be the most versatile programming language and, therefore, worth studying. Much more work is needed, and I still have a lot to learn! Nonetheless, I feel more confident.

Then, you have taught me that science is not done quickly but needs rigor and precision in analyzing the data. I have lost count of how many times you told me to check and verify the codes, to plot the data, nor can I recount the number of times we went through the analyses to make sure I wasn't mistaking, forgetting a step, and that the results were correct.

Yes, science can be frustrating at times... not to mention writing it!

Thanks for your patience and your constructive feedback.

I wish all the best to you and your family back in Minneapolis. I feel if it is time for you to move back, it probably means you feel confident with the idea that I'm now ready to “fly” by myself. Otherwise, I am sure you would have stayed much longer to back me up...

More than a “supervisor”, more than a colleague, you have been a friend. Always present in the good times but also the bad ones.

Thank you!

I'll miss our stormy and heated debates!

Bon vent l'ami!

Of course, my Ph.D. wouldn't have been possible without the financial funding and support from our industry sponsors and research support: MITACS Accelerate Funding, Lawson Internal Research Fund, Western Graduate Research Scholarship, Hydro-Quebec, Électricité de France (EDF), Réseau de Transport d'Électricité (RTE) and Electric Power Research Institute (EPRI).

It would not have been possible either without the knowledge and skills of Lynn Keenlside, who designed and produced all the material and ELF-MF stimulation devices we used in our protocols.

Special thanks also go to all the teachers, professors, and researchers, for educating me and for taking the time to help me along this journey.

Thank you to all the participants for willingly letting me “fry” their brains and vestibular systems with our magnetic and electrical stimulations. Thank you also for your time.

To my brother Fred and his family. I'm happy we're on the same side of the pond now!

A thought goes to my parents for everything they have done for me and for what they have taught me. I hope to be as good as a parent for my children.

A thought goes to my children. To Sarah, Salomé, Timothé, and the little one to come, sorry for my lack of patience and my absences. I hope someday you will realize that this was done for you. To Gaël, Raphaël, and Michel for looking over me and giving me the strength needed in the difficult times...

Finally, to my wife Amandine... probably the “craziest” of us all for leaving everything behind without looking back: her family, her friends, her career as a pharmacist, and the sunshine of the French Mediterranean coast, to follow me on what was at times a difficult venture. Thank you for your love and support!

Table of Contents

Abstract.....	ii
Summary for Lay Audience.....	iii
Co-Authorship Statement.....	iv
Acknowledgments.....	v
Table of Contents.....	viii
List of Tables.....	xii
List of Figures.....	xiii
List of Appendices.....	xvii
I) General introduction.....	1
1.1 The vestibular system: an overview.....	2
1.2 Magnetic Fields: an overview.....	5
1.2.1 Static Magnetic Fields.....	5
1.2.2 Time-Varying Magnetic Fields.....	6
1.2.3 ELF-MF and electrostimulation: Health and safety concerns.....	7
1.2.4 ELF-MF: Magnetophosphenes and neurophysiological functions.....	8
1.2.5 The vestibular system: a new model to study the ELF-MF impact on neurophysiology?.....	9
1.3 Magnetic Fields and the vestibular system: interaction mechanisms.....	10
1.3.1 The Diamagnetic Susceptibility (DS).....	10
1.3.2 The Magneto-HydroDynamic (MHD) forces.....	10
1.3.3 Induced Galvanic Vestibular Stimulation (iGVS).....	12
1.4 Electric fields, currents and the vestibular systems.....	13
1.4.1 High conductivity.....	14
1.4.2 Transduction mechanism.....	15
1.4.3 Hair cells and E-Fields.....	18

1.4.4	Voltage gated calcium channels and E-Fields	18
1.5	Stimulation thresholds	20
1.5.1	Current intensity thresholds	22
1.5.2	E-Field thresholds	22
1.5.3	DB/dt thresholds	23
1.6	ELF-MF and Galvanic vestibular stimulations: same effects?	25
1.6.1	Vestibulo-thalamo-cortical pathway: sensory perception and cognitive functions.....	25
1.6.2	Vestibulo-ocular pathway: Visual acuity and Visual tracking	29
1.6.3	Vestibulo-autonomous pathway.....	30
1.6.4	Vestibulo-spinal pathway: postural control	31
1.6.5	Summary and caveat	31
1.7	Electromagnetic induction and the vestibular system: a need for new research... 32	
1.7.1	Going beyond MRIs.....	32
1.7.2	Investigating higher frequencies	33
1.7.3	Power-line frequency exclusive ELF-MF postural modulations	33
1.8	Thesis direction and aims – Electric and magnetically induced vestibular-driven effects	34
1.9	References.....	36
2	Human Postural Control Under High Levels of Extremely Low Frequency Magnetic Fields	65
2.1	Introduction.....	65
2.2	Methods.....	67
2.2.1	Participants.....	67
2.2.2	Experimental devices	67
2.2.3	Protocol.....	70
2.2.4	Data analysis	72

2.2.5	Statistical analysis	74
2.3	Results	74
2.3.1	DC Stimulations	74
2.3.2	ELF-MF stimulations	75
2.3.3	Phosphene perceptions	78
2.4	Discussion	78
2.5	Conclusion	83
2.6	References	84
3	Human Postural Responses to High Vestibular Specific Extremely Low-Frequency Magnetic Stimulations	92
3.1	Introduction	92
3.2	Methods	94
3.2.1	Participants	94
3.2.2	Experimental devices	94
3.2.3	Protocol	95
3.2.4	Data analysis	97
3.2.5	Statistical analysis	99
3.3	Results	100
3.3.1	Differences in CTRL conditions	100
3.3.2	Effect of Stimulation device	100
3.3.3	Effects of positive control	100
3.3.4	Effects of AC and MF stimulations	101
3.4	Discussion	103
3.5	Conclusion	109
3.6	References	110
4	Vestibular Extremely low frequency magnetic and electric stimulation effects on human subjective visual vertical perception	118

4.1	Introduction.....	118
4.2	Methods.....	120
4.2.1	Participants.....	120
4.2.2	Stimulations	121
4.2.3	Procedure	123
4.2.4	Data collection and analysis.....	124
4.3	Results.....	125
4.4	Discussion.....	127
4.5	Conclusion	132
4.6	References.....	132
5	General discussion and conclusion	141
5.1	General discussion	141
5.2	General limitations.....	144
5.3	Future studies	147
5.3.1	Eye movement analysis.....	147
5.3.2	Myogenic responses.....	148
5.3.3	Cortical activity.....	148
5.3.4	Autonomous responses	149
5.3.5	Animal models and C-Fos	150
5.4	General conclusion.....	150
5.5	References.....	150
	Appendices.....	164
	Curriculum Vitae	170

List of Tables

Table I-1 ICNIRP and IEEE-ICES ICES reference levels for ELF-MF head exposures	8
Table I-2 Summary of the vestibular thresholds in mA, V/m and T/s depending on the vestibular pathways.....	24
Table 2-1 Descriptive statistics for the DC results (CTRL vs DC). Mean and standard errors (\pm SE) values for Velocities and Variance Explained as well as mean angles and angular deviations (\pm AD) for Theta.....	75
Table 3-1 Descriptive statistics for both stimulation groups (MF and AC) across all frequencies (20, 60, 90,120 and 160 Hz). Mean and standard deviation values for Δ speed and ρ . No information about θ is reported since no mean angle could be computed.....	102
Table 3-2 ELF-MF and AC stimulations estimated peak E-Field values across all frequencies.	105
Table 4-1 Alternating magnetic field intensity (in rms) expressed in mT and $T.s^{-1}$ at 3 cm from the casing of the coil for the four frequency conditions. We intentionally decreased the level of flux density to keep a stable dB/dt across frequency conditions.	122

List of Figures

Figure I-1 Overview of the vestibular system: A. Anatomical structures constituting the two vestibular subsystems. B. The semicircular ducts end in the ampulla containing the hair cell receptors. A rotational acceleration of the head creates an endolymphatic flux displacing the cupula, bending the cilia in the opposite direction of the rotation. C. A linear acceleration or a static head tilt can displace the otolithic membrane creating shear forces bending the otolithic hair cells. Adapted from (8) 2

Figure I-2 Vestibular inputs integrated within the vestibular nuclei (red dot) and distributed through the four vestibular pathways. Adapted from (4), (9), and (10)..... 4

Figure I-3 The Lorentz force mechanism (Adapted from (104)): When interacting with a strong magnetic field (\mathbf{B} - yellow arrow), the utricular ionic current (\mathbf{J} - green arrow) results in a Lorentz force (\mathbf{F} - red arrow) inducing a sufficiently strong endolymph flows (orange arrows) able to act on both the horizontal and superior canal cupulas. The right-hand rule shows the relationship between each vector. Axis represents the Right, Anterior, Superior (RAS) radiological coordinate system [+X/right, +Y/anterior, +Z/superior]. 12

Figure I-4 Left panel shows a classical monaural GVS montages where one electrode is applied to one mastoid process while the second electrode is placed at the C7 spinous process. Right panel shows the location of the vestibular system within a human head where 60 % of the stimulation is still found. Adapted from (68). 14

Figure I-5. Illustration of the six hair cell’s transduction stages. Adapted from (92). 1) Mechanic force deflecting the stereocilia. 2) Potassium entering hair cell. 3) Hair cell basolateral current depolarizing the hair cell. 4) Inward calcium currents. 5) Glutamate release in cleft. 6) Spike encoder. 17

Figure I-6 D’arsonval’ s electromagnetic human stimulations. Source (<http://www.cinq.ulaval.ca/TMS>) 21

Figure 2-1 Stimulation apparatus. Volunteers stood in complete darkness, feet together, arms by their side and eye closed on a 1.5 cm foam pad covering the force plate. Their head was fully stimulated by Helmholtz-like coils centered on their ears, with ELF-MF stimulations at

8.89 T/s, 26.66 T/s and 39.98 T/s (left panel). The binaural bipolar DC montage stimulating both vestibular systems at 2 mA. The cathode is behind the right mastoid process and the anode is behind the left mastoid process (right panel)..... 69

Figure 2-2 Two-dimensional spatial illustration of the MF level distribution around the exposure system computed according to the Bio-Savart law (Left panel). The thick black rectangles represent the outer boundaries of both coils. Small black arrows represent the magnetic vector field. Red and blue lines represent respectively the boundaries of a 1% and 5% flux density variation limit area from the center. Dashed lines represent the lower boundary while solid lines represent the upper boundary. Participants' vestibular systems, illustrated by the yellow structures in the head, lie within a 50 mT ($\pm 0.5\%$) vertically-oriented homogeneous field . Flux density values for full head homogeneous ELF-MF stimulations targeted at 50 mT (right panel). The blue line represents the expected flux density values given by the model along the mediolateral axis. Red and black dots are actual flux density measurements along the mediolateral and anteroposterior axes respectfully 70

Figure 2-3 Schematic representation of the postural control protocol..... 72

Figure 2-4 Graphical representation of dependent variables found with Principal Component Analysis. In all panels, the movement of COP is represented by the black line. In A, the red line represents the main direction of sway at an angle θ symbolized by the grey shaded area. A direction of sway at 90 degrees angle would indicate a pure AP sway. In B and C red ellipses are examples of dispersion of the orientation of sway in space. In B, 52 % of the variance explained is expressed along the first PC whereas, in C, 98 % of the variance explained is expressed along the first PC. 73

Figure 2-5 Mean velocities (A) and Variance explained (B) for CTRL vs all MF experimental conditions. Error bars represent 95% confidence intervals 76

Figure 2-6 Average sway orientation for CTRL vs all MF experimental conditions. The black lines represent the main direction of sway (PC1) at the angle θ . The length of each black line is proportional to the mean quantity of movement expressed by the participants. Ellipses are a representation of the mean area of COP displacement. Shaded areas from light green (CTRL) to dark green (90 Hz) represent the angular deviation as frequency increases..... 77

Figure 2-7 Bottom view of field orientation within a head representation. Both yellow structures are the vestibular systems. The green crosses represent the homogeneous MF increasing towards the top of the head. The light blue circle symbolizes a 5 cm radius Faraday’s loop encompassing both vestibular systems. The dark blue arrows represent the tangential induced E-Fields generated at selected points of the loop. 80

Figure 3-1 Representation of experimental exposition apparatus. The left panel shows a diagram of the custom coils system centered over the mastoid process. The electrodes (yellow circles) delivering the DC and AC currents, were placed in a monaural configuration behind the right mastoid and the C7 spinous process. The right panel shows a volunteer standing on the foam pad, wearing the vest self-sustaining the MF headset device unloading the weight of the coils. 96

Figure 3-2 Graphical representation of postural sway for one participant. Left panels show the Center of Pressure (COP) before (black) and during the stimulation (blue in control condition, CTRL, and red in direct current condition, DC). These COP movements can be summarized on the right panels by their 95% confidence ellipses. The displacement from the ellipses’ barycenter from pre-stimulation to during-stimulation provides distance ρ and the angle θ of the displacement. Finally, the size of the dot characterizes the difference of sway movement (calculated as COP average velocity) between pre- and during stimulation. 98

Figure 3-3 Postural shift of COP barycenters from pre- to during exposure. Pre-exposure barycenters are centered at the origin. Each dot location represents the displacement due to exposure. The dot size shows the absolute difference in Δ speed (amplitude only) while transparency shows actual Δ speed (amplitude and sign: most transparent express higher speed in pre-exposure). 101

Figure 3-4 Postural modulations for AC (left) and MF (right) at 60 Hz compared to control conditions (blue dots). Results at 60 Hz are representative of all experimental conditions. Pre-exposure barycenters are centered at the origin. Each dot location represents the displacement due to exposure. The dot size shows the absolute difference in Δ speed (amplitude only) while transparency shows actual Δ speed (amplitude and sign: most transparent express higher speed in pre-exposure). 102

FIG. 3-5 Representation of a lateral view of E-Fields impacting the right vestibular system (3D grey structures). The upper panels consider a canalithic level while the lower panels represent an otolithic level. The light blue crosses represent the homogeneous MF increasing from the right to the left side of the head. The red circles symbolize the Faraday's loops encapsulating the entire human vestibular system. The red E arrows represent the tangential induced E-Fields generated either at the anterior canal ampulla (upper right panel) or at the utricle (lower right panel). The dark blue E_{col} arrows represent the fractional component of E aligned with the hair cells showing little impact at the canalithic level and greater impact at the utricular level. 106

Figure 4-1 Magnetic flux density distribution around the exposure device for a 20Hz stimulation. On the left panel, the black lines show the outer boundaries casing, and the grey lines show the outer boundaries of the solenoid. The vestibular system (represented as the two yellow structures into the skull) lays approximately 3 cm from the casing of the coil. The right panel shows the dB/dt values along the Mediolateral axis at the level of the vestibular level. The dashed line represents the position of the coil casing (black) and the vestibular system (red) along the mediolateral axis. 122

Figure 4-2 Swarm plot representation of SVV angle assessment for all participants overall experimental stimulations (CTRL: Control, DC: Direct Current, AC: Alternating Current, MF: Magnetic Field) by frequency conditions (from CTRL and DC on the left panel to 160 Hz for AC and MF on the right panel). The solid dots represent the data collected for the 3 participants exhibiting SVV angles $> 2.5^\circ$ in the CTRL condition. The shaded dots represent the measurements of SVV kept in the statistical analysis..... 125

Figure 4-3 Boxplots representation of dSVVmean, dSVVstd, and dVel distributions comparing AC and MF stimulations. Individual measurements are presented as swarm plot over each boxplot. Only dSVVstd and dVel yielded significant differences between AC and MF..... 127

List of Appendices

Appendices 1. Ethics Approval # 106122 for postural studies (Chapters 2 & 3).....	164
Appendices 2. Ethics Approval # 109161 for perception of verticality (Chapters 4).....	165
Appendices 3. Copyright release from IEEE-Access (Chapter 2).....	167
Appendices 4. Copyright releases from IEEE-Access (Chapter 3)	169

I) General introduction

When asked about sensory experiences, people will easily define sight, touch, hearing, taste, and smell. Indeed, inputs from distinct sensory organs, emerge as conscious perceptions after being integrated within the brain. Yet, we often forget about another sensory organ: the vestibular system. Indeed, this system is so humble that it was only considered as a specific sensory organ just a little bit more than a century ago (1), although it is the first sensory system to develop in the womb and is fully operational before birth. Surely, the constant presence of gravity on earth could be a reason for this (2). We might argue that its late discovery would reflect the minor role it plays in our daily lives, but this assumption is far from the truth (3).

Although normally “quiet”, the slightest dysfunction of this minuscule sensory organ produces compelling difficulties spanning from lack of balance to gaze instability (4).

We take for granted living on our feet and moving around without falling, knowing where we are in space. Certainly, most people do not pay attention to the small part of the inner ear, called the vestibular system, responsible for so many proper bodily functions.

Another thing people do not pay attention to is the electromagnetic environments in which they live. Indeed, Extremely Low-Frequency Magnetic Fields (ELF-MFs < 300 Hz) at powerline frequencies (i.e. 60 Hz in North America) are ubiquitous in modern societies due to the generation, distribution, and use of alternating currents (AC). ELF-MF induce electric fields (E-Fields) and currents in exposed conductors and are thus prone to penetrate the human body. Yet, most people are unaware of such Fields.

This thesis stands at the crossroads where the vestibular system and the ELF-MF meet. Within a framework encompassing health risks and safety concerns, this work focuses on identifying whether ELF-MF exposure modulates vestibular function. This is done through the analysis of behavioral outcomes sought after to set and write international standards and guidelines. In this perspective, this thesis is a modest attempt to contribute to our current understanding of how ELF-MF exposure impact human neurophysiology.

1.1 The vestibular system: an overview

The vestibular system lies within the inner ear (one on each side of the head). When working perfectly, the vestibular system is silent and there is no conscious experience of its function. This is why Aristotle [384-322 B.C] did not list it amongst our five other senses, as researchers and clinicians only discovered it's function a little bit more than a century ago (1). Its main structure consists of a labyrinth of membranous tubules filled with endolymph fluid, which is continuous with the auditory component of the inner ear (i.e. cochlea) (FIG. I-1) (5–7). Two distinct subsystems constitute the vestibular system: the semicircular canals and the otolith organs. The formers detect angular accelerations of the head. The latter, found within the utricle and saccule, detect horizontal and vertical linear accelerations of the head, respectively. This is done by transducing mechanical information (i.e. head movement) into electrical information integrated at the Central Nervous System (CNS) level. The sensing elements of the vestibular system, found in both subsystems, are called hair cells. Head movements produce a deflection of the hair cells towards or away from the so-called kinocilium, ultimately triggering a train of action potentials transmitted to the CNS (5,7).

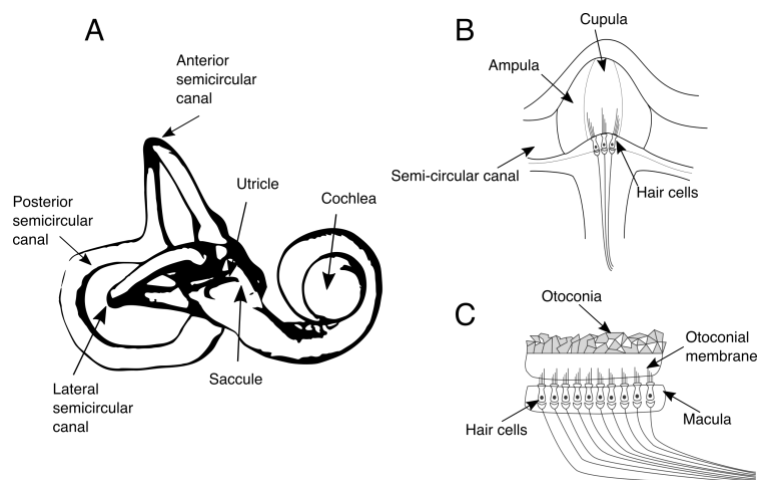


Figure I-1 Overview of the vestibular system: A. Anatomical structures constituting the two vestibular subsystems. B. The semicircular ducts end in the ampulla containing the hair cell receptors. A rotational acceleration of the head creates an endolymphatic flux displacing the cupula, bending the cilia in the opposite direction

of the rotation. C. A linear acceleration or a static head tilt can displace the otolithic membrane creating shear forces bending the otolithic hair cells. Adapted from (8) .

The vestibular system works as a push-pull mechanism. This means that, as the firing rate of one part of the system increases, the firing rate of another part decreases accordingly. The brain compares the difference between the firing rates on both sides and interprets it as head movements.

Once the peripheral vestibular afferent information reaches the vestibular nuclei within the brainstem, it passes through different ascending and descending neurological pathways. There are four main distinctive pathways (FIG. I-2): 1) the vestibulo-ocular, 2) the vestibulospinal, 3) the vestibulo-thalamo-cortical and 4) the vestibulo-autonomous pathways.

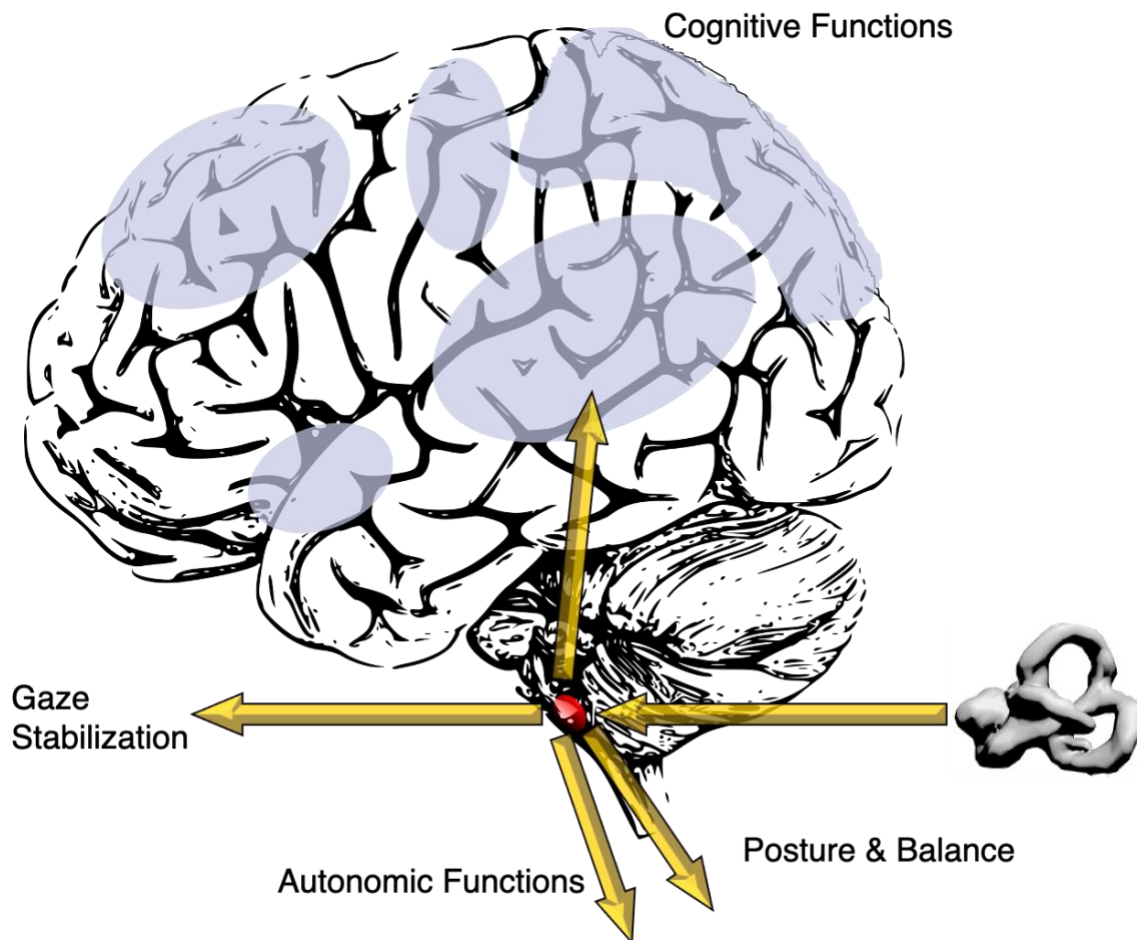


Figure I-2 Vestibular inputs integrated within the vestibular nuclei (red dot) and distributed through the four vestibular pathways. Adapted from (4), (9), and (10)

Therefore, the vestibular system contributes to multiple bodily functions. Indeed, the vestibular system plays an important role in balance (11–14), gait (15,16), control of arm movements (17–20) as well as in gaze stability and eye movements (21–23).

It also handles high cortical tasks (3) such as self-motion estimation (4,24), spatial memory (25), external space representation and space navigation (26,27). Vestibulo-cognitive implications also show the importance of the vestibular system in daily living functions such as decision-making, arithmetic abilities, reading, concentration, and restriction of mobility (28). The vestibular system also plays a role in regulating emotions, affective processes and disorders (3,29) such as anxiety (30), mood (31,32), pain modulation (33–

36) as well as being decisively implicated in embodiment mechanisms linked to body schema construction (37–43).

The otolithic system also regulates circadian rhythms, homeostasis, and body composition possibly due to vestibulo-hypothalamic connections (44). Finally, the vestibular system is linked with autonomic system functions (10,29,45) impacting autonomic reflexes such as the vestibulo-sympathetic reflex (46) modulating blood pressure, heart rate, and cerebral blood flow (10,47–49). The vestibular system is thus much more complex than previously thought (3) and we can discern why it is critical to investigate whether the electromagnetic fields surrounding us daily impact its function.

1.2 Magnetic Fields: an overview

Natural and man-made sources of Magnetic Fields (MF) are omnipresent in our environment (50–52). Although we measure the intensity (H) of MF in Ampere per meter (A/m), we most often report them in terms of their magnetic flux density (B) measured in Tesla (T). The relation between H and B follows equation [1] where μ is a permeability constant equal to $1.256 \cdot 10^{-6}$ Henries per meter (H/m).

$$B = \mu H \quad [1]$$

MF are either steady (i.e. static) or fluctuating over time (i.e. time-varying).

1.2.1 Static Magnetic Fields

Sources of Static Magnetic Fields (SMF) can either be natural or industrial. The earth's surface static geomagnetic field values range between 30 and 70 microTesla (μT) (53) and represents the main natural SMF source. Indeed, we rarely think about the earth's SMF. Yet, looking at our children amazed by a compass needle or astonished when flocks of Canadian geese fly south when winter settles, always remind us that the earth indeed behaves like a magnet.

Artificial or man-made SMF are more diverse. One source of such industrial SMF comes from high voltage direct current used in transporting electric energy over long distances which generate 20 μT (54). Using superconductors' diamagnetic properties, another source of SMF is found in rail transportation for magnetic levitation trains where SMF values can range from 10 to 100 mT close to the trains' engines (54). However, the most common environment in which humans encounter important SMF is in the vicinity of Magnetic Resonance Imaging (MRI) scanners. In this specific environment, the SMF values range between the classical 1.5 T MRI scanner used for clinical imagery reasons and the 14 T super-conducting magnets operated for research purposes (55,56).

1.2.2 Time-Varying Magnetic Fields

Depending on the frequency bandwidth, there are different types of time-varying magnetic fields. In this thesis will we only focus on Extremely Low Frequency Magnetic Fields (ELF-MF < 300 Hz).

Since Michael Faraday's work, in the ELF-MF range, we know that changes in magnetic flux generate electric fields (E-Fields) and currents in conductors. The human body is a conductor. Therefore, any change in the MF flux density over time (dB/dt measured in T/s) induces E-Fields and currents within it. The higher the dB/dt , the higher the E-Fields. This is given by equation [2] where E is the E- field expressed in volts per meter (V/m) and r is the radius of the Faraday's loop (structure of concern) in meters (m) within a homogeneous alternating flux density B of frequency f expressed in hertz (Hz).

$$E = \frac{r}{2} \frac{\partial B}{\partial t} = \pi r f B \quad [2]$$

Also, the MF strength value (B) follows equation [3] where (μ) represents once again the permeability constant described for equation [1], (I) is the current intensity and (r) the distance from the source.

$$B = \frac{\mu I}{2\pi r} \quad [3]$$

Thus, (B) proportionally decreases with increased distance from the source.

ELF-MF can be confronted in two distinct environments. On the one hand, ELF-MF are ubiquitous wherever electricity is produced, transported, or used. Since they result from moving electric charges, time-varying electric currents at powerline frequency (i.e. domestic electricity at 50 or 60 Hz), generate ELF-MF at the same frequencies. On the other hand, in an MRI setting, outside the bore, given equation [3], the strength of the magnetic field decays with distance. This creates an inhomogeneous SMF gradient. Moving through this gradient results in movement-induced ELF-MF which according to equation [2], not only depend on the SMF strength but also on the speed of movement.

Therefore, given the laws of induction, depending on the distance from the source, ELF-MF induce more or less important E-Fields and currents inside the human body. Depending on their strength, they can possibly interfere with the body own physiological electric activity.

1.2.3 ELF-MF and electrostimulation: Health and safety concerns

From a health and safety perspective, electrostimulation through electromagnetic induction is a concern in the ELF range. Thus, it is essential to establish if the exposure levels, to which one is exposed for short or longer periods, potentially provoke biological and/or adverse health effects. In this regard, international agencies such as the International Commission for Non-Ionizing Radiation Protection (ICNIRP) and the International Committee on Electromagnetic Safety of Electrical and Electronics Engineers (IEEE-ICES) carefully review scientific data to publish standards, guidelines, and recommendations (57–60).

The average levels of such public ELF-MF exposures are usually found between $0.1 \mu\text{T}$ and $0.3 \mu\text{T}$ (53). However, they can reach higher levels up to 2 mT for commonly used electrical household appliances (51,61,62). Furthermore, for those working close to high current conductors, such as live-line electric utility workers, exposure levels reach up to 10

mT (53). These values can exceed the ELF-MF restrictions found in both international guidelines (59) and standards (63) (Table I-1). Moreover, the movement-induced ELF-MF within the MRI setting can also generate E-Field values exceeding the basic restrictions highlighted in the guidelines (64).

Being exposed to ELF-MF above guidelines' restrictions means that the generated E-Fields could exceed the 0.075 V/m peak threshold reported to trigger synaptic modulations, potentially leading to sensory experiences as well as adverse effects in the human brain (57).

Table I-1 ICNIRP and IEEE-ICES ICES reference levels for ELF-MF head exposures

	ICNIRP (mT _{rms})			IEEE (mT _{rms})
	20 Hz	50 Hz	60 Hz	20-759 Hz
General Public Guidelines	0.25	0.2	0.2	0.9
Occupational/Controlled Environment Guidelines	1.25	1	1	2.71

1.2.4 ELF-MF: Magnetophosphenes and neurophysiological functions

When exposed to sufficiently strong ELF-MF (65) or alternating electrical stimulations (66–68), participants describe an acute neurophysiological response known as phosphenes. Phosphenes are flickering lights appearing in the peripheral visual field. Electrophosphenes and magnetophosphenes share common mechanisms (69) and evidence shows that they are directly linked to the retinal membrane electrical potential modulation (68,70–72).

Magnetophosphenes are generated by movement-induced ELF-MF in MRI environments (56,73–75), as well as in exclusive ELF-MF settings (65,76,77), and represent to date, the most established and sensitive ELF-MF acute biological responses.

The retina is a part of the central nervous system (CNS) and shares most of the architectural and biological mechanisms found in the brain (70). Both computational models (78–80) as well as human data (81–84), are in favor of an induction impact of ELF-MF on the CNS.

Yet, contrary to the magnetophosphenes studies, the ELF-MF modulation results of CNS structures are miscellaneous (85). Therefore, given the consistency of the retinal responses and the close similarities between the retina and the brain, phosphenes are used as the main model to study the impact of ELF-MF on the CNS to produce the guidelines (57–59).

However, there are still gaps regarding the interaction mechanisms between the ELF-MF and human neurophysiology (86) which questions whether generalizing the retinal outcomes to the entire CNS is appropriate or whether ELF-MF only impact specific sensory cells.

1.2.5 The vestibular system: a new model to study the ELF-MF impact on neurophysiology?

Besides the brain, the retinal cells also share important similarities and common neurophysiological properties with the vestibular hair cells. Indeed, both types of cells use graded potential for signal processing (87) both releasing glutamate gradually from ribbon synapses (88–92), regulated in both systems by the same specialized components known as Usher, RIBEYE and SNARE protein complexes (93–95).

Also, remarkably, when d'Arsonval first reported magnetophosphenes, his participants additionally described having vertigo (65). It is noteworthy to read that electrostimulation from the same ELF-MF stimulations produced two distinct outcomes potentially coming from two distinct sensory system. Furthermore, like the retinal photoreceptors (96), the vestibular system is also sensitive to E-Fields (97).

Therefore, given i) the striking neurophysiological and structural similarities between both the retinal cells and the vestibular hair cells, ii) the known retinal and vestibular sensitivity to E-Fields and iii) the presumed vestibular effects triggered by the ELF-MF in d'Arsonval's study, the question raises whether ELF-MF impact the vestibular system.

Thus, investigations relative to induction on the vestibular system needs to be pushed further.

1.3 Magnetic Fields and the vestibular system: interaction mechanisms

In a seminal paper published in 2007, Glover et al. (98), described three physical mechanisms that could trigger vestibular responses: i) the Diamagnetic Susceptibility (DS), ii) the Magneto-HydroDynamic (MHD) forces and iii) the induced Galvanic Vestibular Stimulation.

1.3.1 The Diamagnetic Susceptibility (DS)

Unlike the vestibular cupula in which there are no crystalline structures, the otoconia located in the utricle and saccule end organs are calcium carbonate bio-crystals. This gives the otolithic subsystem diamagnetic properties. Thus, when subjected to a MF, an induced repulsive force could repel the otolithic membrane in the opposite direction creating a shear force triggering the hair cells (FIG. I-1). However, this mechanism necessitates two conditions: i) high field strength in the order of 7 T (98) and ii) an inhomogeneous MF.

To our knowledge, these conditions can only be met within the magnetic stray fields from MRI scanners. Yet, even in this specific environment, the DS hypothesis has been consistently dismissed as negligible, both in theoretical and experimental works (98–100).

1.3.2 The Magneto-HydroDynamic (MHD) forces

There are two kinds of MHD forces: i) motion induced MHD forces and ii) Static MHD forces also known as Lorentz forces.

1.3.2.1 Motion induced MHD forces

Motion induced MHD forces require a moving conducting fluids (i.e. blood flow or ionic currents) within a high MF environments (101). Therefore, applying this mechanism to the vestibular system necessitates both high-velocity endolymphatic flux (i.e. vigorous head

movements) within a strong MF environment. Taking a flux density of 7 T and an angular velocity of 10 rad/s in their model, Glover et al. (98) found a pressure of 5.5 microPascals (μPa) which is under the threshold necessary to start pushing on the cupula (102). Therefore, this hypothesis was considered irrelevant to the vestibular system.

1.3.2.2 Lorentz Forces (Static MHD)

The generation of Lorentz forces requires a conductive fluid and a high MF strength. In this case, contrary to the Motion induced MHD forces, no movement is required. The vestibular endolymph is an ion-rich fluid and potassium as well as calcium currents constantly flow through the hair cells. The utricle plays an important role in this mechanism for two reasons: i) the higher ionic currents found at its level and ii) its location close to both the anterior and the lateral canals. Indeed, there is approximately 33,000 hair cells at the utricle level. This is 4.5 times more than the number of hair cells found within a canalithic ampullae. Therefore, this is where the highest current density is to be found. When interacting with a high strength SMF, these ionic currents at the utricle level produce a Lorentz force generating a strong enough pressure (99) sensed by the cupulas of the lateral and anterior semicircular canals (103,104) (FIG. I-3). Due to the SMF orientation, the direction of the Lorentz force excites one vestibular system while inhibiting the other (104). The asymmetry between the two vestibular systems simulates a constant head acceleration (105–107), generating clear nystagmus (involuntary reflexive eyes movements) (103–105,108,109). In a 7 T MRI bore, the horizontal component of recorded nystagmus can peak up to 40 deg/sec before generally plateauing around a mean of 10 deg/sec (105). Furthermore that response can last up to 90 min during the entire exposure, while participants lay still in the MRI bore (105).

Up to date, backed up by mathematical modeling (99) and both animal (55,110–115) and human (100,103,104,108) experimental data, the Lorentz force is the more thoroughly understood mechanism explaining the impact of high SMF above 1.5 T (116) on the vestibular system.

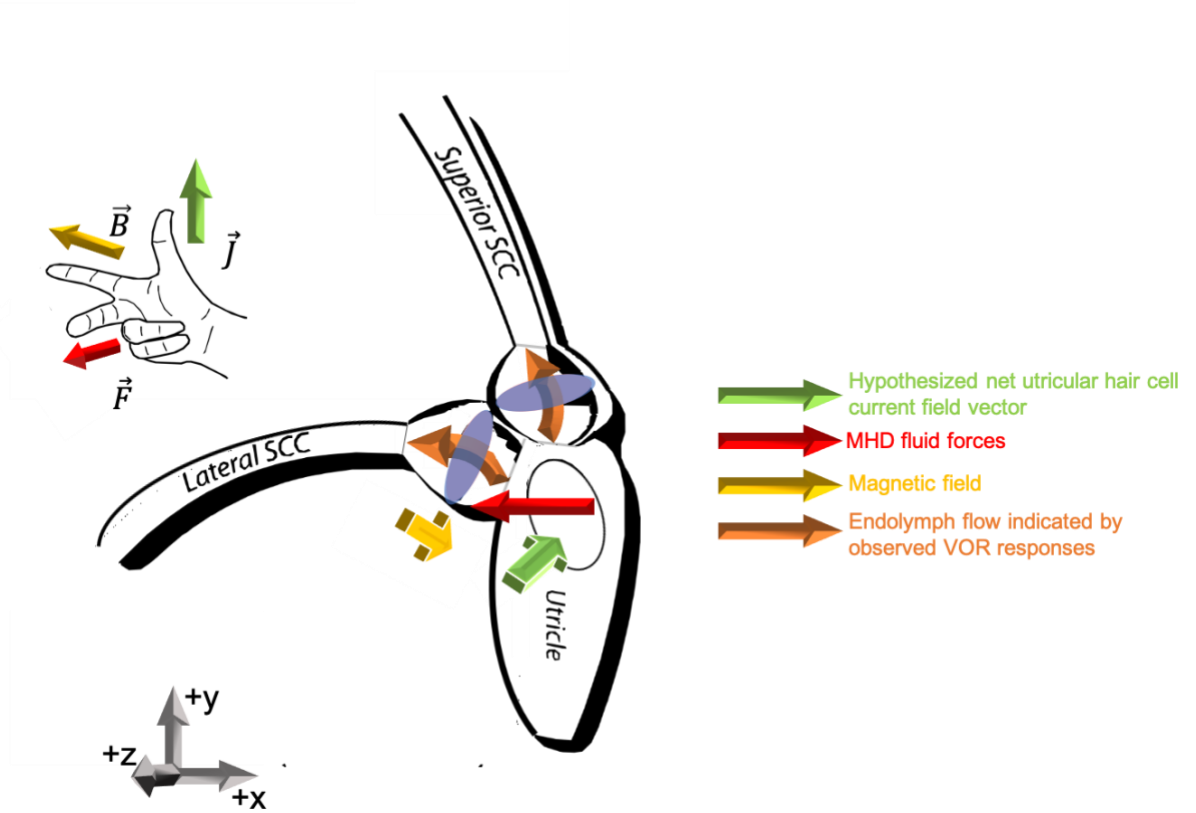


Figure I-3 The Lorentz force mechanism (Adapted from (104)): When interacting with a strong magnetic field (\vec{B} - yellow arrow), the utricular ionic current (\vec{J} - green arrow) results in a Lorentz force (\vec{F} - red arrow) inducing a sufficiently strong endolymph flows (orange arrows) able to act on both the horizontal and superior canal cupulas. The right-hand rule shows the relationship between each vector. Axis represents the Right, Anterior, Superior (RAS) radiological coordinate system [+X/right, +Y/anterior, +Z/superior].

1.3.3 Induced Galvanic Vestibular Stimulation (iGVS)

As seen above, following equation [2], ELF-MF induce E-Field and currents that can impact human neurophysiology. Transcranial electrical stimulation is also a well-known means in which E-Field change cortical excitability. This is done by applying electrodes to the skull to excite the underlying neural structures (117). Such electric stimulations can either use direct or alternating currents. Depending on the types of currents used, the

stimulation is either termed transcranial direct current stimulation (tDCS) or transcranial alternating current stimulation (tACS).

As for the retina, the vestibular system is extremely sensitive to low intensity electric currents (97), often reported in the literature as galvanic vestibular stimulations (GVS) (for review see (14)).

GVS is just a variant of transcranial electrical stimulation where electrodes application is at the mastoid processes on the temporal bones. Such an electrode application triggers specific vestibular outcomes (for reviews see (14,118)). Like tDCS and tACS, GVS can also use direct or alternating currents.

With electric stimulations, the intensity is more often reported in milliamperes (mA). Knowing the intensity, we can easily get the current density (J) in mA per meter squared (mA/m²). Interestingly J relates to the E-Field strength following equation [4] where (s) is the local tissue conductivity expressed in Siemens per meter (S/m).

$$E = J \cdot s \text{ [4]}$$

As seen above with equation [2], E-Fields are also proportional to the dB/dt values expressing the change in the MF flux density over time.

Since GVS as well as ELF-MF both produce E-Fields, induction was thus hypothesized to trigger vestibular outcomes. Yet, compared to GVS, an ELF-MF vestibular effect still lacks evidence and data is needed.

1.4 Electric fields, currents and the vestibular systems

In the guidelines and standards, within the ELF-MF range, the main concern relates to the electrostimulation of the neural structures. Therefore, electromagnetic induction will be the focus herein. We will first consider whether the ELF-MF induced currents can easily reach the vestibular system, before considering the mechanisms through which these currents could interact with its neurophysiology.

1.4.1 High conductivity

To influence the function of a sensory system, the induced currents first need to be drawn to it. At the vestibular system level, the perilymph possesses a high conductivity value close to the one attributed to the cerebrospinal fluid (CSF), which is found at 1.79 S/m (119). The highest current densities occur for such high conductivity fluids (61,68,120) which procure a low-resistance current path to the vestibular system. The vestibular cupulas, as well as the endolymph, have the same high conductive value of 1 S/m (99). In comparison, the eye's vitreous humor is around 1.5 S/m and the retina's value is 0.7 S/m (121). The eye, easily impacted by ELF-MF induced currents, has, therefore, conductivity values lower than the ones found at the vestibular system level. This should, all the more, make the vestibular system a great candidate for "attracting" the ELF-MF induced currents to itself and revealing their potential impact.

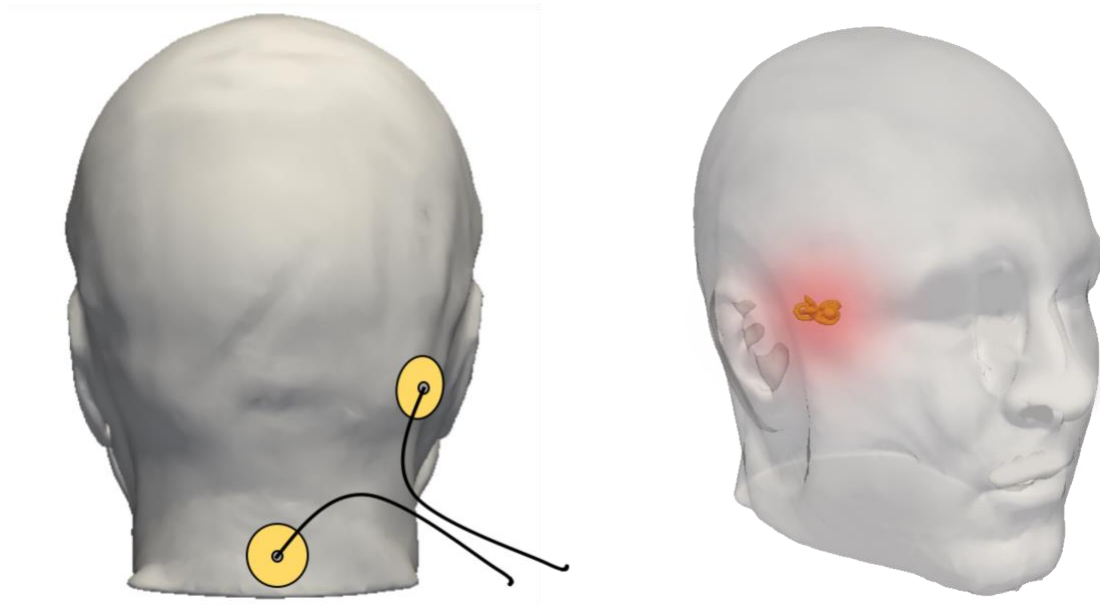


Figure I-4 Left panel shows a classical monaural GVS montages where one electrode is applied to one mastoid process while the second electrode is placed at the C7 spinous process. Right panel shows the location of the vestibular system within a human head where 60 % of the stimulation is still found. Adapted from (68).

Laakso et al. (68) analyzed different tACS montages inducing electrophosphenes. Looking at the T3-Oz montage is of particular interest since this montage is fairly close to a monaural GVS montage where the electrodes are set at the mastoid process and the base of the neck (122,123) (FIG. I-4 - Left panel). Laakso et al. (68) found that current density hotspots are mostly found at the CSF level when we apply the current to the skull. Consequently, because perilymph and CSF have close conductivity values, current density hotspots should be found at the perilymph level within the vestibular system. While the low conductivities of skin (0.10 S/m), fat (0.04 S/m) and bone (0.02 S/m) of the head obstruct the currents applied to the skull, we can still find 60 % of the stimulation in the head within 5 cm from the center of the stimulating electrode (68) (FIG. I-4 - right panel). However, no such obstruction occurs with ELF-MF, as the fields go through the anatomical structures without any hindrance, making it ideal for electrostimulation of the vestibular system bathed in high conductivity fluids.

1.4.2 Transduction mechanism

Now that we have seen that electric currents can easily be drawn to the eye and even more so to the vestibular system, we need to consider how these currents could modulate their function.

Amongst several theories explaining how the E-Fields impact human neurophysiology, the transduction hypothesis has been pushed forward as the most reliable (for review see (124)). Transduction is defined as translating one signal into another. Sensory transduction, therefore, relates to how a sensory system translate a stimulus into the electric signal transmitted by the axons to be processed in the brain. This is classically done through a modulation of the cell membranes' potential enabling neurotransmitter release in the synaptic cleft. Both the visual and the vestibular system use transduction mechanisms.

Studying phototransduction in the retina is useful for two reasons. First, because retinal photoreceptors are the best understood cells amongst all the sensory cells, they provide a great model for understanding sensory transduction in general (125). Second, as stated before, the retina is not a peripheral system but an integrative part of the CNS with which

it shares a comparable synaptic organization (125). Therefore it is considered as a good neural processing model for the brain (70).

Vestibular hair cells also use transduction mechanisms in which mechanical head movements inputs are transduced in electrical signals sent to the CNS. Physiologically when the stereocilia are deflected towards the kinocilium (FIG. I-5.1), the mechano-electric transducer (MET) channels open and potassium (K^+) enters the hair cells (FIG. I-5.2) depolarizing it (FIG. I-5.3). This results in the activation of voltage-gated calcium channels (VGCCs) (FIG. I-5.4). The more the hair cells are depolarized the more VGCCs open, the more calcium (Ca^{2+}) enters the hair cells (FIG. I-5.4), helping the quantal release of neurotransmitters (mainly glutamate) within the synaptic cleft (FIG. I-5.5). Glutamate, through quantal transmission at the vestibular hair cell ribbon synapse, mostly binds on post-synaptic AMPA and NMDA receptors. This triggers the opening of ionic channels which depolarize the membrane in the postsynaptic neuron. This finally results in triggering spikes in the afferent nerve fiber (7,89) (FIG. I-5.6). Indeed, from the postsynaptic end, the transmission of information to the brain requires that postsynaptic voltages be converted to spike trains transmitted to the CNS (5,7). This means that the spiking activity sent to the central nervous system rigorously reflects hair cell activity.

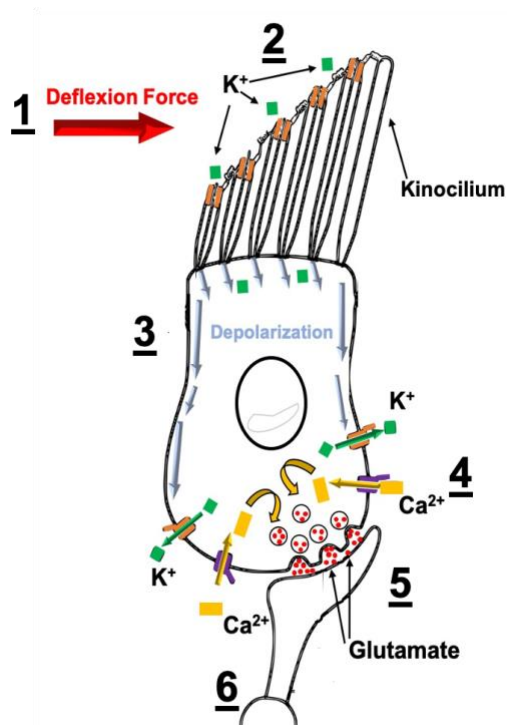


Figure I-5. Illustration of the six hair cell's transduction stages. Adapted from (92). 1) Mechanic force deflecting the stereocilia. 2) Potassium entering hair cell. 3) Hair cell basolateral current depolarizing the hair cell. 4) Inward calcium currents. 5) Glutamate release in cleft. 6) Spike encoder.

At the cortical level, electric currents (126–128) as well as ELF-MF (129) both create an induced voltage able to change the transmembrane neuronal potential modulating glutamate concentrations (130,131). This is also true for the retinal photoreceptors as evidence shows that electrophosphenes and magnetophosphenes are due to a modulation of the retinal cell's membrane electrical potential by the E-Fields (68,70,132).

However, for transduction to be a valid hypothesis for the vestibular system, it must be implied that the induced E-Fields and currents modulate the hair cells' membrane potential.

Yet, traditionally the currents are thought to bypass the hair cells to directly impact the spike trigger zone of the primary afferents (14,97,133). Indeed, direct electrical stimulation of the afferents triggers vestibular responses (134,135), even when the vestibular apparatus is completely removed (136).

Therefore, although it is thought that what is true for the visual system also applies to other sensory systems (124), further proof is needed to validate the transduction hypothesis for the vestibular system.

1.4.3 Hair cells and E-Fields

In healthy humans, the vestibulo-ocular response to GVS, known as eVOR, is phasic when a direct electrical vestibular stimulation is switched on or off, but remains tonic as long as the same stimulation is maintained (137). However, patients injected with Gentamicin have impaired phasic and tonic eVOR responses (138). Gentamicin is an aminoglycoside antibiotic drug that can infiltrate through the transduction channels. It is known for its ototoxic effect that can damage and/or kill the hair cells. Due to the known refractory periods after the generation of action potentials, Aw et al. (138) suggested that the impaired eVOR responses are due to a decreased neurotransmitter release within the synaptic cleft, therefore underlining the impact of the E-Fields on the hair cells in humans. Yet, Gentamicin also induces secondary loss of vestibular afferents which may plausibly reduce their excitability to electric stimulations.

However, Zenner et al. (139) showed that alternating E-Fields electrically evoked hair cell motility (changes in hair cell length). These changes were more prominent in type I hair cells and abolished with damaged cell membranes. Also, the precise protocols put together by Norris et al. (140) and more recently by Gensberger et al. (141) looking at the precise site of action of the E-Fields on the vestibular system demonstrated that both DC (140) and AC currents (141) also impact the hair cells.

1.4.4 Voltage gated calcium channels and E-Fields

Going against the more traditional thought relating the impact of E-Field on the spike trigger zone of the primary afferents, some evidence states that electric currents modulate the hair cells (118,138–141), pushing the transduction hypothesis further. Therefore, considering this point as true, we now need to understand which step of the transduction mechanism could be impacted by the E-Fields.

Voltage Gated Calcium Channels and more specifically the L-type (L-VGCCs), seem to be the cornerstone when it comes to electromagnetic fields stimulations as they are extremely sensitive to ELF-MF (129,142). Indeed, Pall writes in his review of the literature (142) that “most if not all electromagnetic fields-mediated responses may be produced through VGCC stimulation” and VGCCs are “essential to the responses produced by extremely low frequency (including 50/60 Hz) electromagnetic fields”. Indeed, when Verapamil, an L-type VGCCs blocker is used, most of the effects of Electromagnetic field stimulation are impaired or blocked (142).

L-VGCCs are the most common type found at the hair cell level (143). They are activated at the hair cells' resting potential. This resting firing rate is sustained by a continuous depolarizing current through the not entirely closed MET channels at rest. This enables biphasic potentials of the hair cells allowing for the preservation of the temporal information found in the stimuli. That means that sinusoidal stimuli induce an identical sinusoidal modulation of the membrane potential.

VGCCs have particularly fast activation/deactivation kinetics, in the order of microseconds (144), enabling them to respond to stimuli with frequency much higher than the powerline frequencies found at 50/60 Hz. VGCCs localization is of particular interest. Indeed, they are near the ribbon synapses where the neurotransmitter quantal release is done continuously. This is both true at the retinal (145,146) and the vestibular hair cell (143) levels. The great amount of releasable pool of vesicles within ribbon synapses enable smooth graded changes in post-synaptic membrane potentials (147) which enable both the retinal photoreceptors and the vestibular hair cells to transmit small signals very reliably (87,144). Thus, VGCCs are perfectly appropriate for quickly, precisely and continuously modulating neurotransmitter release under high-frequency conditions.

Furthermore, trying to find the exact E-Field site of action, Norris et al. (140) looked at the effect of GVS when normal perilymph was replaced with a low calcium/high magnesium perilymph. Interestingly, all afferent responses in this case were abolished pointing to the paramount role played by Ca^{2+} and the L-VGCCs when GVS is applied. By depolarizing the hair cell membrane, the E-Field would activate the L-VGCCs letting the Ca^{2+} in the

cells. In cascade this triggers glutamate release within the synaptic cleft which is linearly proportional to the number of opened VGCCs. Therefore, through glutamate release within the synaptic cleft, postsynaptic activity is linearly linked to the presynaptic Ca^{2+} current (144) and thus to the membrane polarization (92). Interestingly, at the retinal level, the same linear relationship between the presynaptic amount of Ca^{2+} , the neurotransmitter (also glutamate) release in the synaptic cleft and the encoding of small changes in light intensity, has been shown at the rod photoreceptor ribbon synapse (148), presumably responsible for phosphene generation (70). Indeed, Attwell (70) emphasized the role of VGCCs and the graded potential cells on magnetophosphenes production.

In summary, the ELF-MF stimulations could dynamically modulate the hair cells' membrane potential. Through L-VGCC activation and glutamate release, smooth graded firing rate perturbations could be induced. Interestingly, biophysical models show that ELF-MFs at 60 Hz can cause a time-varying membrane potential modulation effect which can advance or delay spike timing (80,149).

1.5 Stimulation thresholds

E-Fields and currents impact the vestibular system (for review see (14)) and growing evidence points that hair cells are implicated (118,138–141,150).

In their introduction, Fitzpatrick and Day (14), described how, in 1790, Alessandro Volta felt a spinning sensation before collapsing when he applied electric currents directly to his ears. Interestingly, this description matches d'Arsonval's ELF-MF experiment (65). Indeed, d'Arsonval reported that some participants similarly felt rotating sensations and some also collapsed. While d'Arsonval's work is mostly known for phosphene generation, the fact that participants also felt vertigo could underline similar neurophysiological mechanisms between the emergence of phosphenes and vestibular outcomes. We saw that graded potential cells with VGCCs are a potential link. However, one can experience phosphenes without experiencing vestibular outcomes (98). Both systems could therefore be triggered at different thresholds.

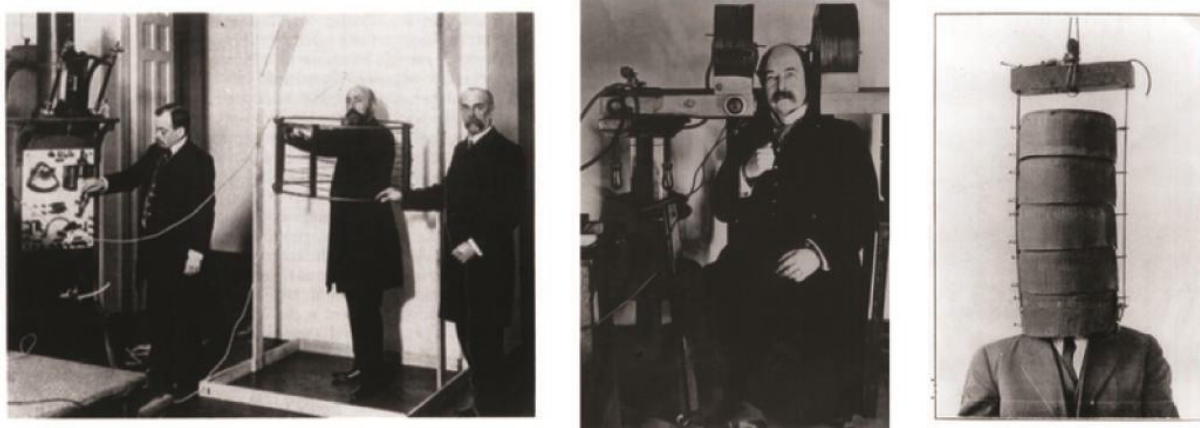


Figure I-6 D'Arsonval' s electromagnetic human stimulations. Source (<http://www.cinq.ulaval.ca/TMS>)

Unfortunately, to the best of our knowledge, unlike what has been done for phosphenes (64), no specific dosimetry study has accurately modeled the E-Fields needed to trigger vestibular outcomes. It is therefore problematic to estimate E-Field values and currents reaching precisely the vestibular system. Indeed, there is an obvious knowledge gap in the literature and accurate modeling and dosimetry studies specific to the vestibular system are needed. However, if we want to be able to compare the vestibular outcomes triggered by currents used with GVS with the potential outcomes due to the ELF-MF induced E-Fields and currents, we need to have an interpretative framework to help us. Therefore, based on existing literature one can try to establish some gross estimations.

Because of the vast GVS body of knowledge, we will start by investigating current intensity thresholds. GVS is a specific form of tDCS and/or tACS (117). Therefore, given the tDCS and tACS literature and the related growing dosimetry interest, we will look at conversions between the current intensities applied to the skull and the generated E-Fields within the head. Knowing the specific GVS effects for given current intensities, we will be able to grasp the estimated E-Field values (in V/m) needed for such effects. Finally, based on recent literature, we will try to estimate the dB/dt values needed to generate the E-Field needed to trigger vestibular outcomes.

1.5.1 Current intensity thresholds

To our knowledge, the lowest GVS intensity value triggering very small vestibular outcomes in humans is 0.1 mA (151) when applied to the mastoid processes. Such current intensity generates ocular torsion movements close to 1 deg/sec but no horizontal nor any vertical nystagmus (151). Moreover, the lowest threshold found to induce acute vestibulospinal outcomes is 0.2 mA for healthy controls and 0.1 mA for airplane pilots with the mean lowest GVS postural threshold found at 0.32 mA (152). The perceptual threshold varies greatly. For instance, Ertl et al. (153) found the lowest perception threshold at 1.76 mA without any differences between seated and supine healthy participants. However, they recommend 2 mA to generally induce reliable vestibular perceptions (153). Nonetheless, Lenggenhager et al. (154) found a perceptual threshold at 1 mA with seated participants and 1.5 mA is found for participant lying down (155,156). To our knowledge, there is no estimated specific threshold for autonomous responses. The intensity usually used to trigger such responses is 2 mA (157–162). However, Lenggenhager et al. (154) triggered autonomous responses with a 1 mA current which will be considered herein as the lowest threshold for autonomous responses. Therefore, we can consider different current intensity thresholds depending on the vestibular pathways. Note also that only a few microamperes, applied directly within the inner ear are sufficient to modulate vestibular outcomes (140,141,163). Therefore, at the vestibular level, very little E-Field (V/m) is expected to induce modulations.

1.5.2 E-Field thresholds

Up to date, with the use of tDCS/tACS stimulations, no dosimetry consensus seems to have been reached. Indeed, E-Field values depend on different parameters such as population, age, electrode size, and montages, but also the choice of conductivities taken for the different anatomical structures used within a given model. Therefore, E-Field values generated by 1 mA at the skull level can be estimated between 0.14 V/m and 1.57 V/m in the head (164,165,174–176,166–173). Even the use of the same model can procure great inter-subject variability in the E-Fields generated at the cortex level (166). Indeed, Laakso

et al. (166) found that a 1 mA tDCS generates maximum E-Fields values ranging from 0.62 V/m to 1.43 V/m at the cortex level. Indeed the currents applied to the skull with tDCS are dampened by the low conductivity of the skull (68) but also by individual anatomical features such as the thickness of the CSF and/or of the skull bone itself (166).

Direct E-Field measures seem, therefore, more reliable than dosimetry models. In implanted epileptic participants, 2 mA tDCS stimulations generate 0.4 V/m both at the cortical level and more deeper structures such as the peri-ventricular white matter (167). Given that i) the vestibular system lies between the cortex and the peri-ventricular white matter and that ii) CSF and vestibular conductivity values match (see section 1.4.1), we will grossly estimate that Huang et al. results (167) also applies to the vestibular system. We have seen that 0.1 mA is the lowest current intensity capable of triggering vestibular outcomes. Therefore, 0.02 V/m could be sufficient to trigger vestibular outcomes. Interestingly, this value fits within Attwell's magnetophosphenes threshold range (0.01-0.06 V/m) (70). Therefore, if our threshold estimates are true, the vestibular hair cells could be as sensitive as the retinal photoreceptors.

Nonetheless, as mentioned previously, one can see phosphenes without experiencing vestibular outcomes. Thus, other parameters than E-Fields strength, such as sensory specificity or integration could explain such issues.

1.5.3 DB/dt thresholds

We could estimate the dB/dt threshold following equation [2]. To date, E-Field estimations have been mostly done at cortical and/or head levels (64,98). Based on Allen et al. (177), the radius of the human cortex can be estimated at 0.06 meters. Therefore, at the cortical level, a dB/dt of 0.66 T/s could be sufficient to start triggering the vestibular system. However, for equation [2] to be used, the field (B) needs to be homogeneous and this is rarely the case when moving in MRI vicinity or in the case of live-line electric utility workers.

Therefore, here again, more realistic estimates should be preferred. To our knowledge, the best estimation to date has been proposed by Laakso et al. (64). Based on real human movement recordings and different head models, obtained through MRI imaging, peak E-Field at the cortex level generated with 1T/s was estimated between 0.09 V/m and 0.23 V/m (64). To remain conservative, only 0.09 V/m will be used herein.

Once again, given cortical and vestibular anatomical contiguities, the nearness of the CSF and perilymph conductivity values and the fact that dB/dt and E-Fields values are linearly proportional, 0.22 T/s could represent a first dB/dt threshold estimation. However, using full head 2 T/s stimulations, Glover et al. (98) did not show any postural modulation despite being much higher than the vestibulospinal threshold estimate here (Table I-2). Other parameters than strict dB/dt values could, therefore, be also of interest to stimulate the vestibular system. Indeed, field orientation for instance could play a major role since the magnetophosphenes thresholds can vary 2.5 fold depending on whether the magnetic fields are applied top-down or front-back (72).

Table I-2 Summary of the vestibular thresholds in mA, V/m and T/s depending on the vestibular pathways.

Vestibular pathway	Authors	Current intensities threshold (mA)	Estimated E-fields threshold (V/m)	Estimated dB/dt threshold at head level (Laakso et al., 2013) (T/s)
Vestibulo-ocular	Severac Cauquil et al., 2003	0.1	0.02	0.22
Vestibulo-Spinal	Yang et al., 2015	0.32	0.06	0.66
Vestibulo-cortical (Perception)	Fitzpatrick et al., 2002	1.5	0.3	3.33
	Lenggenhager et al., 2008	1	0.2	2.22
	Ertl et al .2018	1.76	0.35	3.88
Vestibulo- autonomous	Lenggenhager et al., 2008	1	0.2	2.22

1.6 ELF-MF and Galvanic vestibular stimulations: same effects?

Workers and patients moving within the vicinity of MRI scanners report transient sensory sensations such as illusions of rotating movements, vertigo, dizziness and nausea (178–180), suggesting that ELF-MF could interact with the vestibular system (98).

Following this rationale, in the vicinity of an MRI scanner, ELF-MF induced E-Fields could generate comparable GVS outcomes. For that matter, Laasko et al. (64), modeled that slow movements in a 3 T MRI environment produce current intensities in the same order of magnitude as the ones currently used in GVS studies.

To contrast outcomes, ELF-MF should be compared to AC-GVS as both stimulations are not constant in time. However, AC-GVS stimuli activate the vestibular system by the same means as their continuous counterparts (14). Thus, we will include both AC-GVS and DC-GVS studies herein. Because the vestibular system is complex, we will consider analyzing the vestibular pathways separately.

1.6.1 Vestibulo-thalamo-cortical pathway: sensory perception and cognitive functions

1.6.1.1 Subjective perception

1.6.1.1.1 Dizziness and vertigo

Patients and/or participants pushed in and out of an MRI bore tend to describe acute perceptions, which can be related to vestibular outcomes. Indeed, they often report illusions of movement as well as disorientation, vertigo, dizziness, and fatigue (74,98,186,178–185). Of all the aforementioned responses, vertigo and dizziness are the major reported ones (98,178–180,185,187). Moreover, these perceptions are more reported during movement inside the bore and less, if not, while lying still at the center of the bore or standing still besides it (178,180,183,188). Furthermore, going slower and making frequent stops, when entering and exiting the bore significantly reduces the triggering as well as the

intensity of dizziness (186,189). On the contrary, the faster one moves around the MRI scanner and/or the higher the static field strength, the higher the induced dB/dt and the greater the vestibular perceptions (74,179,182,185,190–192). This is why employees working in such an environment try to limit their speed purposefully (60,190,191).

Normal movements around a 1.5 T MRI scanners generate dB/dt values ranging from 7 to 50 T/s peak at head level (73,193). This is estimated herein up to 4.5 V/m peak which should already trigger all vestibular pathways. Therefore, the dB/dt and the E-Field levels within a 3 T or even 7 T MRI environment should be even greater.

Interestingly, the same outcomes with lower E-field values are obtained when alternating currents are applied to the vestibular system with GVS (159,161,194–196). Thus, ELF-MF could potentially be an increasing factor for dizziness, vertigo, and disorientation. However, outside of an MRI environment, Glover et al. (98) failed to trigger any feeling of movement nor any vertigo with 40 ms full-head 5 T/s ELF-MF stimuli representing 0.45 V/m. Other parameters such as field orientation (72) could be taken into consideration. Furthermore, longer stimulation periods could also be needed to trigger more noticeable outcomes.

1.6.1.2 Feeling of curving or leaning and feelings of unreality or strangeness

Very few studies report feelings of curving or leaning (98,186). Nonetheless, this sensation is the most reported subjective sensation in Uwano et al. (186), in which about 10 % of the participants felt it, especially when the bed was moving inside the MRI bore. Sensations of unreality, studied with questionnaires, are also, though rarely, be reported in the same conditions (178,186,188,197).

Patients with vestibular dysfunctions and diseases often report feelings of unreality or strangeness, which can also be induced in healthy subjects with vestibular stimulations including GVS (40,198,199). Although, Heilmaier et al. (178) did not find any statistical differences between the ELF-MF and SMF conditions, both Uwano et al. (186) and

Theysohn et al. (188) found that these reports were more acknowledged when movement occurred in the SMF. However, considering the few data available, definitely attributing these effects to induction would be a hasty conclusion. Nonetheless, the fact that such sensation is more important with movement is interesting and future research should further investigate the induction hypothesis for such outcomes.

1.6.1.3 A vestibular link to metallic taste perception (dysgeusia)

When people are in MRI vicinity, they often report metallic taste alongside vertigo (74,178,185,187,188,200–203). As found in Patel et al. (74), this sensation can be ranked third amongst the commonly reported sensations. Fast movers within the MRI's SMF gradient experience these effects more than the people moving at a slower pace (185) matching other findings attributing this sensation to induction (188). Heilmaier et al. (178), on the other hand, did not find any significant differences between the moving sequence in the MRI's SMF gradient and staying still at the isocenter of the bore. Cavin et al. (203) found people reporting metallic taste at 1.3 T/s and sensations increases with faster nodding head movements within the SMF, inducing higher dB/dt values ranging up to 4.1 T/s. Therefore, E-Fields between 0.11 and 0.36 V/m could be needed to start inducing a metallic taste. Moreover, as seen before, these values can largely and easily be exceeded in a normal MRI setting (73,193).

Several mechanisms could explain metallic taste in an MRI setting. Weintraub et al. (187) explain it could come from an electrolysis phenomenon due to an induced battery effect between two types of dental metal feelings. However, this hypothesis does not stand given Cavin et al. (203) results showing that participants, without dental feelings, experience it. A second hypothesis is a direct cranial nerve stimulation by the induced currents. Indeed, the facial nerve (CN VII), the glossopharyngeal nerve (CN IX), the vagal nerve (CN X), as well as the trigeminal nerve (CN V), all carry taste information to the CNS (204). However, this is very unlikely since the threshold for nerve activation is estimated at 6.2 V/m (205) which is rarely reached in such conditions.

Direct electrical tongue stimulation is a very probable hypothesis, as electrogustometry using currents intensities below 10 μ A trigger such response (206).

However, interestingly, the metallic taste can also be linked to vestibular dysfunctions. Indeed, it is found in vestibular pathologies such as schwannomas (207) and could be used as an early diagnostic symptom in such pathologies (208). Furthermore, GVS also induces metallic taste (156,159,209–214). To our knowledge, no study has formalized an intensity threshold. However, looking at the existing literature a minimum of 0.2 V/m seems to be needed. Therefore, one cannot neglect the hypothesis that ELF-MF induced currents triggering the vestibular system could induce dysgeusia, granted the fact that metallic taste can be induced by a vestibular electrical stimulation as specific as GVS.

1.6.1.4 Spatial attention

The vestibular system is highly implicated in spatial orientation (215) as it plays an important role in space perception (26,27,216,217) and distance evaluation (218). GVS impacts cognitive functions since the vestibular system is implicated in such processes (28,39,154,215,219–222).

The line bisection task is a widely used test to evaluate spatial cognition. During this test, participants draw a vertical line, aligned with their perceived trunk midline, pointing at the middle of a horizontal segment. Thus, the role of the task is to divide the segment into two halves.

The line bisection test is a spatial attention task closely linked to right parietal dominance in right-handed individuals (117,223–225). Indeed, with this test, clinicians assess right hemisphere stroke patients presenting spatial neglect syndromes (217,226). Interestingly, spatial neglect shares common brain areas also involved in vestibular cortical integration (227,228). Indeed, the vestibulo-thalamocortical pathways are asymmetric (9,216,228,229) and right parietal areas, including the right parieto-temporal junction, largely integrate vestibular inputs (9,224,227,229–231). Right cathodal GVS, mainly integrated within the

right hemisphere (225), improves the performance of the bisection test in neglect patients (232) and the test is biased in healthy participants depending on GVS polarity (225,228).

Through the line bisection task, studies investigated spatial attention in participants when submitted to ELF-MF in MRI environments (179,185,233,234). However, the results of the line bisection tasks in ELF-MF conditions within MRI environments are inconclusive. Heinrich et al. (179) found no spatial accuracy changes in the ELF-MF condition, while Van Nierop et al. (233) found a nonsignificant spatial bias to the left. On the other hand, De Vocht et al. (234) found the time to complete the test was greater after participants moved their heads in the SMF. However, GVS biases the test spatially and, to our knowledge, no reference mentions a GVS-impact on time during this test. Yet, the generated E-Fields, in the ELF-MF studies, are estimated at 0.21 V/m which is just at our estimated perceptual threshold. This could therefore explain the lack of results and greater E-Fields could be needed.

1.6.2 Vestibulo-ocular pathway: Visual acuity and Visual tracking

Visual acuity refers to vision clarity. Clear vision necessitates a stabilized image on the central foveal region of the retina. Image instability on the retina procures blurry vision as well as oscillopsia described as a movement of the visual scene. On the other hand, visual tracking necessitates being able to shift the fovea toward a target and stabilize gaze. Thus, this process needs to coordinate both saccadic and smooth pursuit eye movements to maintain a clear image on the retina during the task (235).

Visual tracking and visual acuity can both be related to the vestibular system, as it is responsible for controlling gaze and stabilizing the image on the retina (21–23,92,236–238). Indeed, visuo-ocular control tests (6,239) and dynamic visual acuity tests (240–245) are clinically used to assess vestibular dysfunction and provide excellent outcomes for VOR impairment. Undeniably, visual acuity declines with vestibular gain abnormality due to impaired VOR.

Visual tracking and visual acuity were both studied within MRI environments (73,179,185,246). Magnetic fields affect the visual sensory domain (233,247) and people working in the vicinity of 9.4 T MRI scanners develop smooth pursuit and spontaneous nystagmus abnormalities (74). The dB/dt values reported by Heinrich et al. (179,185) and by Van Nierop et al. (233) range from 0.8 T/s to 2.4T/s generating E-Fields between 0.07 V/m and 0.21 V/m. The level of the generated E-Fields could, therefore, impact the vestibulo-ocular pathways and thus the visual sensory domain. Indeed, they are strong enough to start inducing ocular outcomes (151). GVS impacts eye motor control (151,248–252) and participants report blurry vision with GVS when 0.2 V/m is applied (154). Although GVS-induced nystagmus can be suppressed when vision is present (253) due to fixation based inhibitory mechanisms, GVS still impacts vision (254).

1.6.3 Vestibulo-autonomous pathway

The vestibular system is closely linked to the autonomous system (10,45). Connections between the viscera and the vestibular nuclei exist (255) with a clear vestibular pathway for nausea and vomiting (256). Motion sickness symptoms such as nausea, pallor, and sweating are often related to the vestibular system via vestibulo-sympathetic reflexes (10,159,161).

When workers, participants or patients are in ELF-MF conditions within an MRI environment, nausea is one of the most reported effects (75,98,178,181,188,190,197). Yet, such perceptions can either be statistically different (188) or not (178) between stationary versus moving conditions.

Although scarcely mentioned, sweat attacks, tachycardia and vomiting can also occur while in MRI settings (178,184,188,197). However, whether such sensations are related to induction is hard to establish since it's either not related to movement (178) or the information relative to movement is simply not provided (184,188,197).

In an MRI environment, these sensations have been investigated while patients or participants are lying down on the MRI bed. In such conditions the average dB/dt value is

estimated at 0.8 T/s (98,100,257), estimated herein at 0.07 V/m. I found 0.2 V/m to be the lower E-Field value inducing such sensations (Table I-2). Yet, to the best of our knowledge, there is no study formally investigating the threshold at which such sensations start being perceived. Therefore, our threshold estimation could be overestimated.

AC-GVS triggers nausea (157–161) sweating (10,154,162,196) tachycardia (154,158) and vomiting sensations (154,161,209,258). Nonetheless, although GVS triggers the vestibulo-autonomous pathways, very little consistent information is found to date enabling to link the reported sensations with induction and future investigations are thus needed.

1.6.4 Vestibulo-spinal pathway: postural control

Van Nierop et al. (259), analyzed postural control after the participants moved their heads with their eyes closed in a 7 T MRI environment. They recorded postural sway using an accelerometer worn around the waist. Depending on the distance between the participants and the bore, the head movements generated dB/dt values estimated between 1.20 and 2.40 T/s at the head level. This represents 0.1 V/m and 0.21 V/m E-Fields, already sufficient for postural perturbations (Table I-2). All sway variables increased in ELF-MF conditions. Yet, interestingly, with the same level of induction, Glover et al. (98) did not show any postural modulations when applying exclusive 2 T/s ELF-MF full-head stimulations.

1.6.5 Summary and caveat

Most of the studies we have covered occur in MRI settings. This is problematic since the Lorentz Force and the movement induced ELF-MF physically coexist. Furthermore, the Lorentz Force as proved to greatly and specifically impact the vestibulo-ocular reflex which is a direct assessment of vestibular function. In opposition, although the outcomes reviewed here can theoretically be triggered by both the ELF-MF and GVS stimulations, the evidence is weaker. Therefore, although some authors argue that induced E-Fields impact the vestibular system in MRI settings (64,182,259,260), considering the Lorentz Force effects, doubts remain concerning the induction hypothesis.

However, given Antunes et al. computational model, the Lorentz force is thought to start being strong enough to act on the cupula at 0.43 T (99).

Yet, Van Nierop et al. (259) measured 0.37 T and 0.24 T respectively at 90 cm and 130 cm from a 7 T MRI bore. Indeed, following equation [3] we know that the strength of the flux density (B) proportionally decreases with increased distance from the source. This obviously means lower flux density measures in the vicinity of 1.5 and 3 T MRI scanners. Considering such flux density values, we can only presume that, in these cases, the Lorentz Force would not be strong enough to trigger vestibular outcomes.

Nevertheless, movements outside the bore are swifter and more complex than those inside the bore when lying on the bed. According to Fuentes et al. (193), the intensity and the spatial distribution of the induced currents within the head rely on workers' occupation. Indeed, the E-Fields depend on i) the direction of head movements, ii) the head position and distance relative to the bore, and iii) the speed at which the head travels through space. This explains why moving outside the bore generates stronger dB/dt values than the ones obtained within the bore (191,193,261). Indeed, in a 1.5 T MRI scanner environment, where the flux density values were measured under 0.7 T, De Vocht et al. (73) obtained dB/dt levels up to 50 T/s at head level (4.5 V/m). Therefore, in such conditions where the Lorentz force impact is low or even non-existent, the vestibular outcomes could be attributed to induction.

1.7 Electromagnetic induction and the vestibular system: a need for new research

1.7.1 Going beyond MRIs

As we have seen so far, most of the research looking at the impact of ELF-MFs on the vestibular system occurs in MRI environments. Although still debated, ELF-MF in this context could have an impact on the vestibular system (64,98,182). However, remarkably, exposure to such magnitude of static magnetic fields gradient is mostly confined to medical and/or research contexts while ELF-MF stimulations are ubiquitous wherever electricity is

produced, transported, and used. This makes ELF-MF from domestic electricity as well as commonly used electrical household appliances much more prevalent in our daily lives. However, to date, data is scarce and inconclusive, revealing a research gap and a need for more specific vestibular ELF-MF stimulations studies which is the core of this thesis.

1.7.2 Investigating higher frequencies

Nowadays, 50 Hz or 60 Hz ELF-MF are ubiquitous in modern societies. Exposure levels with household appliances, such as hair dryers or electric hair clippers, reach up to 2 mT (61,62). In this case, at 50 and/or 60 Hz, the dB/dt values reach respectively 0.8 T/s and 1T/s, equivalent to 0.07 V/m and 0.09 V/m. This is theoretically enough to produce small vestibulo-ocular and vestibulospinal responses. Furthermore, higher ELF-MF exposures occur during very specific tasks. For instance, “live cable” workers are subjected to high fields up to 10 mT (53), generating 4.44 T/s at 50 Hz and 5.33 T/s at 60 Hz. With respective E-Field values of 0.39 V/m and 0.47 V/m, this is theoretically enough to trigger all vestibular pathways.

Given that vestibular hair cells phase lock with frequencies up to thousands of hertz (262,263) the ubiquitous ELF-MF fluctuating either at 50 or 60 Hz could potentially impact the vestibular system and it is, therefore, paramount to acquire such knowledge for security and safety purposes.

1.7.3 Power-line frequency exclusive ELF-MF postural modulations

Interestingly, non-MRI exclusive ELF-MF studies at 60 Hz have shown postural control modulations (264–266). In these studies, the authors used full-body ELF-MF stimuli centered at head level with a dB/dt value of 0.7 T/s (0.06 V/m). Postural modulation was investigated using center of pressure (COP) analysis with force plates. Prato et al. (264) and Thomas et al. (265) showed less motion in the anteroposterior plane, interpreted as improved stability, when they applied the ELF-MF stimuli. They reproduced the same protocol with healthy participants compared to rheumatoid arthritis or fibromyalgia

patients (266), and reported similar improved stability results in all three groups. Legros et al. (267), also using 60 Hz ELF-MF stimuli only, similarly measured postural control using COP analysis on a force platform. The E-Fields generated in this case were 0.08 V/m. As in Prato et al. (264) and Thomas et al. (266,268), they showed a reduction in sway oscillations in the anteroposterior plane. In this case, sway velocity was the impacted variable. These low E-Field values are close to the vestibulospinal threshold (Table I-2). Given that postural control is multisensory in nature, with vestibular, visual, and proprioceptive inputs integrated to manage balance (20), it was suggested that exclusive ELF-MF could impact the vestibular system. However, the results should be interpreted with caution. Indeed, in all of the three reported studies, the fields were applied to the entire body. Therefore, other mechanisms, besides a vestibular impact, could also explain the results.

To our knowledge, our study is the only one targeting the vestibular system with exclusive ELF-MF stimulations (269). Yet, with dB/dt values ranging up to 142 T/s, we did not record postural control modulations. However, we pointed out important methodological limitations including the use of a stimulation device providing the participants with positional cues which could have biased the postural outcomes.

1.8 Thesis direction and aims – Electric and magnetically induced vestibular-driven effects

The data reviewed here have important implications. The fact that both the eye and the vestibular system share : 1) high conductivity 2) transduction mechanism 3) important neurophysiological similarities with L-VGCC, ribbon synapsis and glutamate found in both systems 4) sensitivity to E-Fields and 5) some ELF-MF studies show postural control modulations is not trifling and makes the vestibular system a great candidate to be impacted by the ELF-MFs. Thus, the induction hypothesis needs to be investigated further. However, although theory seems in favor of such a mechanism, data confirming it, is clearly lacking.

This opens new research avenues in which more specific ELF-MF vestibular stimulations should be considered. This is of great interest for the safety of workers and for everyone

subjected to such fields which are encountered daily in our modern societies. Also, such research would also be beneficial for better understanding the vestibular system and deepen our understanding of its function.

This is the background in which this thesis falls, and this work is a modest attempt to push such investigations further.

The aims of this thesis are threefold:

- 1) the main goal is to investigate whether the vestibular system is sensitive to ELF-MF exposures at powerline frequencies. If so, this would push forward the rational stating that different neurological and/or neurosensory systems, sharing neurophysiological similarities, could equivalently be impacted by ELF-MF.
- 2) a second goal is also to try to deepen the knowledge related to the interaction mechanisms between the ELF-MF and human neurophysiology helping to fill the actual knowledge gap (86).
- 3) finally, more broadly, our work also aims at providing more data needed within the international guideline's scope (86), to help set acute ELF-MF thresholds and, thus, try to better protect the public as well as the workers worldwide.

Given i) that the research topic of this thesis is fairly new ii) that postural modulations have been reported at power-line frequencies iii) that the dB/dt levels in those studies match the vestibulospinal threshold and iv) an explicit role of the vestibular system has not been clearly established, our first experimental study (chapter 3) follows on from this postural lineage. Furthermore, postural control is an important behavioral outcome reflecting real-life concerns within high ELF-MF work environments. Indeed, impaired balance while live-line working could be greatly detrimental to the workers.

Consecutive to the seminal work done by Glover et al. (98), we will show postural control analysis of healthy participants while exposed to full head ELF-MF stimulations above Glover's vestibular threshold (98). The conclusions of this first study will give rise to the importance of more specific asymmetrical vestibular stimulations and field orientation

relative to the vestibular system which we implemented in the second postural experiment (chapter 3). This study will further underline two distinct important points. The first is a potentially greater implication of our ELF-MF stimulations on specific vestibular structures that secondly pushes forward the fact that new vestibular outcomes need to be investigated. Therefore, in the third experiment (chapter 4), we will consider inspecting the subjective visual vertical while healthy participants are once again subjected to asymmetrical vestibular specific ELF-MF stimulations.

Finally, a general discussion gathering the main findings of the studies within a broader context will enable us to provide future perspectives and conclude (chapter 5).

1.9 References

1. Wiest G. The origins of vestibular science. *Ann N Y Acad Sci.* 2015;1343(1):1–9.
2. Jamon M. The development of vestibular system and related functions in mammals: Impact of gravity. *Front Integr Neurosci.* 2014;8(FEB):1–13.
3. Mast FW, Preuss N, Hartmann M, Grabherr L. Spatial cognition, body representation and affective processes: the role of vestibular information beyond ocular reflexes and control of posture. *Front Integr Neurosci [Internet].* 2014;8(July):44.
4. Cullen KE. The vestibular system: Multimodal integration and encoding of self-motion for motor control. *Trends Neurosci [Internet].* 2012;35(3):185–96.
5. Khan S, Chang R. Anatomy of the vestibular system: A review. *NeuroRehabilitation.* 2013;32(3):437–43.
6. Baloh RW, Honrubia V, Kerber A. Clinical neurophysiology of the vestibular system. 4th Edition. Contemporary neurology series. New York: Oxford University Press, Inc; 2011. 1–455 p.
7. Goldberg JM, Wilson VJ, Cullen KE, Angelaki DE, Broussard DM, Buttner-

- Ennever J, et al. *The Vestibular System: A Sixth Sense*. The Vestibular System: A Sixth Sense. 2012. 1–560 p.
8. Purves D, Augustine G, Fitzpatrick D, Hall W, LaMantia A, McNamara J, et al. *Neuroscience* 4th edition. 4th edition. 2008.
 9. Lopez C, Blanke O. The thalamocortical vestibular system in animals and humans. *Brain Res Rev* [Internet]. 2011;67(1–2):119–46.
 10. Yates BJ, Bolton PS, Macefield VG. Vestibulo-Sympathetic Responses. *Compr Physiol*. 2015;4(2):851–87.
 11. Hlavacka F, Njiokiktjien C. Postural Responses Evoked by Sinusoidal Galvanic Stimulation of the Labyrinth. *Acta Otolaryngol*. 1985;99(January):107–12.
 12. Dakin CJ, Luu BL, van den Doel K, Inglis JT, Blouin J-S. Frequency-specific modulation of vestibular-evoked sway responses in humans. *J Neurophysiol* [Internet]. 2010;103(2):1048–56.
 13. Takakusaki K. *Functional Neuroanatomy for Posture and Gait Control*. *J Mov Disord*. 2017;10(1):1–17.
 14. Fitzpatrick RC, Day BL. Probing the human vestibular system with galvanic stimulation. *J Appl Physiol* [Internet]. 2004;96(6):2301–16.
 15. Fitzpatrick RC, Wardman DL, Taylor JL. Effects of galvanic vestibular stimulation during human walking. *J Physiol* [Internet]. 1999;517 (Pt 3):931–9.
 16. Blouin J-S, Dakin CJ, van den Doel K, Chua R, McFadyen BJ, Inglis JT. Extracting phase-dependent human vestibular reflexes during locomotion using both time and frequency correlation approaches. *J Appl Physiol*. 2011;111(5):1484–90.
 17. Bresciani J-P, Blouin J, Popov K, Sarlegna F, Bourdin C, Vercher J-L, et al. Vestibular signals contribute to the online control of goal-directed arm movements. *Curr Psychol Cogn*. 2002;21:263–80.

18. Guerraz M, Blouin J, Vercher J-L. From head orientation to hand control: evidence of both neck and vestibular involvement in hand drawing. *Exp Brain Res* [Internet]. 2003;150(1):40–9.
19. Mars F, Archambault PS, Feldman AG. Vestibular contribution to combined arm and trunk motion. *Exp Brain Res*. 2003;150(4):515–9.
20. Smith CP, Reynolds RF. Vestibular feedback maintains reaching accuracy during body movement. *J Physiol*. 2017;595(4):1339–49.
21. MacDougall HG, Weber KP, McGarvie LA, Halmagyi GM, Curthoys IS. The video head impulse test: Diagnostic accuracy in peripheral vestibulopathy. *Neurology*. 2009;73(14):1134–41.
22. Halmagyi GM, Curthoys IS. A clinical sign of canal paresis. *Arch Neurol* [Internet]. 1988;45(7):737–9.
23. Iwasaki S, Smulders YE, Burgess AM, McGarvie LA, MacDougall HG, Halmagyi GM, et al. Ocular vestibular evoked myogenic potentials to bone conducted vibration of the midline forehead at Fz in healthy subjects. *Clin Neurophysiol*. 2008;119(9):2135–47.
24. Cullen KE. Vestibular processing during natural self-motion: implications for perception and action. *Nat Rev Neurosci* [Internet]. 2019.
25. Brandt T, Schautzer F, Hamilton DA, Brüning R, Markowitsch HJ, Kalla R, et al. Vestibular loss causes hippocampal atrophy and impaired spatial memory in humans. *Brain*. 2005;128(11):2732–41.
26. Borel L, Lopez C, Péruch P, Lacour M. Vestibular syndrome: A change in internal spatial representation. *Neurophysiol Clin*. 2008;38(6):375–89.
27. Borel L, Redon-Zouiteni C, Cauvin P, Dumitrescu M, Devèze A, Magnan J, et al. Unilateral vestibular loss impairs external space representation. *PLoS One*. 2014;9(2):1–10.

28. Hanes DA, Mccollum G. Cognitive-vestibular interactions: A review of patient difficulties and possible mechanisms. *J Vestib Res.* 2006;16:75–91.
29. Rajagopalan A, Jinu K, Sailesh K, Mishra S, Reddy U, Mukkadan J. Understanding the links between vestibular and limbic systems regulating emotions. *J Nat Sci Biol Med [Internet].* 2017 [cited 2017 Mar 6];8(1):11.
30. Balaban CD, Thayer JF. Neurological bases for balance - anxiety links. *J Anxiety Disord.* 2001;15:53–79.
31. Winter L, Kruger THC, Laurens J, Engler H, Schedlowski M, Straumann D, et al. Vestibular stimulation on a motion-simulator impacts on mood states. *Front Psychol.* 2012;3(NOV):1–7.
32. Winter L, Wollmer M a, Laurens J, Straumann D, Kruger TH. Cox’s Chair Revisited: Can Spinning Alter Mood States? *Front Psychiatry [Internet].* 2013;4(October):132.
33. McGeoch PD, Ramachandran VS. Vestibular stimulation can relieve central pain of spinal origin. *Spinal cord Off J Int Med Soc Paraplegia.* 2008;46(11):756–7.
34. Gargano F, Hing W, Cross C. Vestibular influence on cranio-cervical pain: a case report. *New Zeal J Physiother.* 2012;40(2):51–8.
35. Spitoni GF, Pireddu G, Galati G, Sulpizio V, Paolucci S, Pizzamiglio L. Caloric vestibular stimulation reduces pain and somatoparaphrenia in a severe chronic central post-stroke pain patient: A case study. *PLoS One.* 2016;11(3):1–14.
36. Ferrè ER, Haggard P, Bottini G, Iannetti GD. Caloric vestibular stimulation modulates nociceptive evoked potentials. *Exp Brain Res.* 2015;233(12):3393–401.
37. Blanke O. Multisensory brain mechanisms of bodily self-consciousness. *Nat Rev Neurosci [Internet].* 2012;13(8):556–71.
38. Lenggenhager, B. & Lopez C. vestibular contributions of sence of body self and

- others. 2015;1–38.
39. Lopez C, Lenggenhager B, Blanke O. How vestibular stimulation interacts with illusory hand ownership. *Conscious Cogn [Internet]*. 2010;19(1):33–47.
 40. Lopez C. A neuroscientific account of how vestibular disorders impair bodily self-consciousness. *Front Integr Neurosci [Internet]*. 2013;7(December):91.
 41. Lopez C. The vestibular system: balancing more than just the body. *Curr Opin Neurobiol [Internet]*. 2016;29(1):74–88.
 42. Peiffer, Christian Serino A, Blanke O. The vestibular system: a spatial reference for bodily self-consciousness. *Front Integr Neurosci [Internet]*. 2014;8(April):31.
 43. Schwabe L, Blanke O. Out-of-body experiences: False climbs in a supine position? *Proc Int Jt Conf Neural Networks*. 2008;3704–10.
 44. Fuller PM, Jones TA, Jones SM, Fuller CA. Neurovestibular modulation of circadian and homeostatic regulation: Vestibulohypothalamic connection? *Proc Natl Acad Sci U S A*. 2002;99(24):15723–8.
 45. Yates BJ, Bronstein AM. The effects of vestibular system lesions on autonomic regulation: Observations, mechanisms, and clinical implications. *J Vestib Res*. 2005;15:119–29.
 46. Samoudi G, Nissbrandt H, Dutia MB, Bergquist F. Noisy galvanic vestibular stimulation promotes GABA release in the substantia nigra and improves locomotion in Hemiparkinsonian rats. *PLoS One*. 2012;7(1).
 47. Cohen B, Martinelli GP, Raphan T, Schaffner A, Xiang Y, Holstein GR, et al. The vasovagal response of the rat: Its relation to the vestibulosympathetic reflex and to Mayer waves. *FASEB J*. 2013;27(7):2564–72.
 48. Yamamoto Y, Struzik ZR, Soma R, Ohashi K, Kwak S. Noisy vestibular stimulation improves autonomic and motor responsiveness in central neurodegenerative

- disorders. *Ann Neurol*. 2005;58(2):175–81.
49. Yakushin SB, Martinelli GP, Raphan T, Xiang Y, Holstein GR, Cohen B. Vasovagal oscillations and vasovagal responses produced by the vestibulo-sympathetic reflex in the rat. *Front Neurol*. 2014;5 APR(April):1–11.
 50. Mezei G, Kheifets LI, Nelson LM, Mills KM, Iriye R, L. KJ. Household appliance use and residential exposure to 60-Hz magnetic fields. *J Expo Anal Environ Epidemiol*. 2001;11(1):41–9.
 51. Lambrozo J, Souques M. Electromagnetic Fields, Environment and Health. In: (ID1) AP, (ID2) MS, editors. *Electromagnetic Fields, Environment and Health* [Internet]. Paris: Springer Paris; 2012. p. 35–50.
 52. Gauger J. Household appliance magnetic field survey. *IEEE Transactions on Power apparatus and systems*. PAS. 1985;104(9):2436–44.
 53. WHO. Extremely Low Frequency Fields Environmental Health Criteria Monograph No.238. [Internet]. WHO,. Geneva; 2007.
 54. Perrin A, Souques M. Champs électromagnétiques, environnement et santé. September. Les Ulys: Edp Sciences; 2018.
 55. Cason AM, Kwon B, Smith JC, Houpt TA. Labyrinthectomy abolishes the behavioral and neural response of rats to a high-strength static magnetic field. *Physiol Behav* [Internet]. 2009;97(1):36–43.
 56. Duyn JH. The future of ultra-high field MRI and fMRI for study of the human brain. *Neuroimage*. 2012;62(2):1241–8.
 57. IEEE. IEEE Standard for Safety Levels With Respect to Human Exposure to Electric, Magnetic, and Electromagnetic Fields, 0 Hz to 300 GHz. Vol. 2005, IEEE Std C95.1-2005 (Revision of IEEE Std C95.1-1991). 2019. 0_1-238.
 58. IEEE. IEEE Standard for Safety Levels with Respect to Human Exposure to

Electromagnetic Fields, 0–3 kHz. Technology. 2002.

59. ICNIRP. Guidelines for limiting exposure to time-varying electric and magnetic fields (1 Hz to 100 kHz). *Health Phys* [Internet]. 2010;99(6):818–36.
60. ICNIRP. Guidelines for Limiting Exposure to Electric Fields Induced by Movement of the Human Body in a Static Magnetic Field and by Time-Varying Magnetic Fields below 1 Hz. *Health Phys* [Internet]. 2014;106(3):418–25.
61. Gandhi OP, Kang G, Wu D, Lazzi G. Currents induced in anatomic models of the human for uniform and nonuniform power frequency magnetic fields. *Bioelectromagnetics*. 2001;22(2):112–21.
62. Gauger J. Household Appliance Magnetic Field Survey. *IEEE Trans Power Appar Syst*. 1985 Sep;PAS-104(9):2435–44.
63. IEEE. C95.6. IEEE standard for safety levels with respect to human exposure to electromagnetic fields, 0-3kHz. IEEE: New York. New York: The institute of Electrical and Electronics Engineers, Inc.; 2002.
64. Laakso I, Kännälä S, Jokela K. Computational dosimetry of induced electric fields during realistic movements in the vicinity of a 3 T MRI scanner. *Phys Med Biol* [Internet]. 2013;58(8):2625–40.
65. D'Arsonval A. Dispositifs pour la mesure des courants alternatifs de toutes fréquences. *Compt Rend Soc Biol*. 1896;3,(May 2):450–451.
66. Lövsund P, Öberg PÅ, Nilsson SEG, Reuter T. Magnetophosphenes: a quantitative analysis of thresholds. *Med Biol Eng Comput*. 1980;18(3):326–34.
67. Kavet R, Bailey WH, Bracken TD, Patterson RM. Recent advances in research relevant to electric and magnetic field exposure guidelines. *Bioelectromagnetics*. 2008;29(7):499–526.
68. Laakso I, Hirata A. Computational analysis shows why transcranial alternating

- current stimulation induces retinal phosphenes. *J Neural Eng.* 2013;10(2008):046009.
69. Taki M, Suzuki Y, Wake K. Dosimetry considerations in the head and retina for extremely low frequency electric fields. *Radiat Prot Dosimetry.* 2003;106(4):349–56.
 70. Attwell D. Interaction of low frequency electric fields with the nervous system: the retina as a model system. *Radiat Prot Dosimetry [Internet].* 2003;106(4):341–8.
 71. Laakso I, Hirata A. Computational analysis of thresholds for magnetophosphenes. *Phys Med Biol.* 2012;57(19):6147–65.
 72. Hirata A, Takano Y, Fujiwara O, Dovan T, Kavet R. An electric field induced in the retina and brain at threshold magnetic flux density causing magnetophosphenes. *Phys Med Biol.* 2011;56(13):4091–101.
 73. Vocht F De, Engels H, Kromhout H. Neurobehavioral Effects Among Subjects Exposed to High Static and Gradient Magnetic Fields From a 1.5 Tesla Magnetic Resonance Imaging System — A Case-Crossover Pilot Study. *Magn Reson Med.* 2003;674(April):670–4.
 74. Patel M, Williamsom R a, Dorevitch S, Buchanan S. Pilot study investigating the effect of the static magnetic field from a 9.4-T MRI on the vestibular system. *J Occup Environ Med [Internet].* 2008;50(5):576–83.
 75. Schenck JF. Safety of Strong , Static Magnetic Fields. *J Magn Reson Imaging.* 2000;12:2–19.
 76. Lövsund P, Öberg PÅ, Nilsson SEG. Magneto- and electrophosphenes: A comparative study. *Med Biol Eng Comput.* 1980;18(6):758–64.
 77. Lövsund P, Öberg PÅ, Nilsson SEG, Reuter T. Magnetophosphenes: a quantitative analysis of thresholds. *Med Biol Eng Comput.* 1980;18(3):326–34.

78. Iles JF. Simple models of stimulation of neurones in the brain by electric fields. *Prog Biophys Mol Biol.* 2005;87(1 SPEC. ISS.):17–31.
79. Modolo J, Thomas AW, Legros A. Neural mass modeling of power-line magnetic fields effects on brain activity. *Front Comput Neurosci [Internet].* 2013;7(April):1–15.
80. Modolo J, Thomas AW, Stodilka RZ, Prato FS, Legros A. Modulation of Neuronal Activity With Extremely Low-Frequency Magnetic Fields: Insights From Biophysical Modeling. In: 2010 IEEE Fifth International Conference on Bio-Inspired Computing: Theories and Applications (BIC-TA). 2010. p. 1356–64.
81. Ghione S, Del Seppia C, Mezzasalma L, Bonfiglio L. Effects of 50 Hz electromagnetic fields on electroencephalographic alpha activity, dental pain threshold and cardiovascular parameters in humans. *Neurosci Lett.* 2005;382(1–2):112–7.
82. Bell GB, Marino AA, Chesson AL. Frequency specific blocking in the human brain caused by electromagnetic fields. *Neuroreport.* 1994;5:510–2.
83. Bell GB, Marino AA, Chesson AL. Alterations in brain electrical activity caused by magnetic fields : detecting the detection process Andrew A . Marino a and Andrew L . Chesson b. *Electroencephalogr Clin Neurophysiol.* 1992;83:389–97.
84. Graham C, Cook MR, Cohen HD, Gerkovich MM. Dose response study of human exposure to 60 Hz electric and magnetic fields. 1994;447–83.
85. Legros A, Corbacio M, Beuter A, Modolo J, Goulet D, Prato FS, et al. Neurophysiological and behavioral effects of a 60 Hz, 1,800 μ T magnetic field in humans. *Eur J Appl Physiol.* 2012;112(5):1751–62.
86. ICNIRP. Gaps in Knowledge Relevant to the “Guidelines for Limiting Exposure to Time-Varying Electric and Magnetic Fields (1 Hz-100 kHz).” *Health Phys.* 2020;118(5):533–42.

87. Juusola M, French AS, Uusitalo RO, Weckström M. Information processing by graded-potential transmission through tonically active synapses. *Trends Neurosci.* 1996;19(7):292–7.
88. Lagnado L, Gomis A, Job C. in the Synaptic Terminal of Retinal Bipolar Cells. *Cell.* 1996;17:957–67.
89. Eatock RA, Songer JE. Vestibular hair cells and afferents: two channels for head motion signals. Vol. 34, *Annual review of neuroscience.* 2011. 501–534 p.
90. Ghosh KK, Haverkamp S, Wassle H. Glutamate receptors in the rod pathway of the mammalian retina. *J Neurosci [Internet].* 2001;21(21):8636–47.
91. Sadeghi SG, Pyott SJ, Yu Z, Glowatzki E. Glutamatergic Signaling at the Vestibular Hair Cell Calyx Synapse. 2014;34(44):14536–50.
92. Goldberg JM, Wilson VJ, Cullen KE, Angelaki DE, Broussard DM, Buttner-Ennever J, et al. The Vestibular System: A Sixth Sense. *The Vestibular System: A Sixth Sense.* Oxford University Press; 2012. 1–560 p.
93. Kremer H, van Wijk E, Märker T, Wolfrum U, Roepman R. Usher syndrome: Molecular links of pathogenesis, proteins and pathways. *Hum Mol Genet.* 2006;15(SUPPL. 2):262–70.
94. Cosgrove D, Zallocchi M. Usher protein functions in hair cells and photoreceptors. *Int J Biochem Cell Biol [Internet].* 2014 Jan;46(3):80–9.
95. Lagnado L, Schmitz F. Ribbon Synapses and Visual Processing in the Retina. *Annu Rev Vis Sci [Internet].* 2015;1(1):235–62.
96. Evans ID, Palmisano S, Loughran SP, Legros A, Croft RJ. Frequency-dependent and montage-based differences in phosphene perception thresholds via transcranial alternating current stimulation. *Bioelectromagnetics.* 2019;
97. Goldberg JM, Smith CE, Fernández C. Relation between discharge regularity and

- responses to externally applied galvanic currents in vestibular nerve afferents of the squirrel monkey. *J Neurophysiol* [Internet]. 1984;51(6):1236–56.
98. Glover PM, Cavin I, Qian W, Bowtell R, Gowland PA. Magnetic-field-induced vertigo: A theoretical and experimental investigation. *Bioelectromagnetics*. 2007;28(5):349–61.
 99. Antunes a, Glover PM, Li Y, Mian OS, Day BL. Magnetic field effects on the vestibular system: calculation of the pressure on the cupula due to ionic current-induced Lorentz force. *Phys Med Biol* [Internet]. 2012;57(14):4477–87.
 100. Ward BK, Roberts DC, Della Santina CC, Carey JP, Zee DS. Vestibular stimulation by magnetic fields. *Ann N Y Acad Sci*. 2015;1343(1):69–79.
 101. Kangarlu A, Robitaille PML. Biological effects and health implications in magnetic resonance imaging. *Concepts Magn Reson*. 2000;12(5):321–59.
 102. Oman CM, Young LR. The physiological range of pressure difference and cupula deflections in the human semicircular canal: Theoretical considerations. *Acta Otolaryngol*. 1972;
 103. Otero-Millan J, Zee DS, Schubert MC, Roberts DC, Ward BK. Three-dimensional eye movement recordings during magnetic vestibular stimulation. *J Neurol* [Internet]. 2017;1–6.
 104. Ward BK, Roberts DC, Della Santina CC, Carey JP, Zee DS. Magnetic vestibular stimulation in subjects with unilateral labyrinthine disorders. *Front Neurol*. 2014;5 MAR(March):1–8.
 105. Jareonsettasin P, Otero-Millan J, Ward BK, Roberts DC, Schubert MC, Zee DS. Multiple time courses of vestibular set-point adaptation revealed by sustained magnetic field stimulation of the labyrinth. *Curr Biol* [Internet]. 2016;26(10):1359–66
 106. Shaikh AG. A trail of artificial vestibular stimulation: electricity, heat, and magnet.

- J Neurophysiol. 2012;108(1):1–4.
107. Glover PM, Li Y, Antunes A, Mian OS, Day BL. A dynamic model of the eye nystagmus response to high magnetic fields. *Phys Med Biol* [Internet]. 2014;59(3):631–45
 108. Roberts DC, Marcelli V, Gillen JS, Carey JP, Della Santina CC, Zee DS. MRI magnetic field stimulates rotational sensors of the brain. *Curr Biol* [Internet]. 2011;21(19):1635–40.
 109. Ward BK, Roberts DC, Della Santina CC, Carey JP, Zee DS. Vestibular stimulation by magnetic fields. *Ann N Y Acad Sci*. 2015;1343(1):69–79.
 110. Houpt TA, Carella L, Gonzalez D, Janowitz I, Mueller A, Mueller K, et al. Behavioral effects on rats of motion within a high static magnetic field. *Physiol Behav* [Internet]. 2011;102(3–4):338–46.
 111. Houpt TA, Kwon B, Houpt CE, Neth B, Smith JC. Orientation within a high magnetic field determines swimming direction and laterality of c-Fos induction in mice. *Am J Physiol Regul Integr Comp Physiol* [Internet]. 2013;305(7):R793-803.
 112. Houpt TA, Cassell JA, Hood A, DenBleyker M, Janowitz I, Mueller K, et al. Repeated exposure attenuates the behavioral response of rats to static high magnetic fields. *Physiol Behav* [Internet]. 2010;99(4):500–8.
 113. Houpt TA, Houpt CE. Circular swimming in mice after exposure to a high magnetic field. *Physiol Behav* [Internet]. 2010;100(4):284–90.
 114. Ward BK, Lee YH, Roberts DC, Naylor E, Migliaccio AA, Della Santina CC. Mouse Magnetic-field Nystagmus in Strong Static Magnetic Fields Is Dependent on the Presence of Nox3. *Otol Neurotol* [Internet]. 2018;39(10):e1150–9.
 115. Ward BK, Tan GXJ, Roberts DC, Della Santina CC, Zee DS, Carey JP. Strong static magnetic fields elicit swimming behaviors consistent with direct vestibular stimulation in adult zebrafish. *PLoS One*. 2014;9(3).

116. Marcelli V, Esposito F, Aragri A, Furia T, Riccardi P, Tosetti M, et al. Spatio-temporal pattern of vestibular information processing after brief caloric stimulation. 2009;70:312–6.
117. Utz KS, Dimova V, Oppenländer K, Kerkhoff G. Electrified minds: Transcranial direct current stimulation (tDCS) and Galvanic Vestibular Stimulation (GVS) as methods of non-invasive brain stimulation in neuropsychology-A review of current data and future implications. *Neuropsychologia*. 2010;48(10):2789–810.
118. Długaiczek J, Gensberger KD, Straka H. Galvanic vestibular stimulation: from basic concepts to clinical applications. *J Neurophysiol*. 2019;121(6):2237–55.
119. Baumann SB, Wozny DR, Kelly SK, Meno FM. The electrical conductivity of human cerebrospinal fluid at body temperature. *IEEE Trans Biomed Eng*. 1997;44(3):220–3.
120. Bohnert J, Dossel O. Effects of time varying currents and magnetic fields in the frequency range of 1 kHz to 1 MHz to the human body-a simulation study. ... *Med Biol Soc* ... [Internet]. 2010;2010:6805–8.
121. Lindenblatt G, Silny J. A model of the electrical volume conductor in the region of the eye in the ELF range. *Phys Med Biol* [Internet]. 2001 Nov 1;46(11):3051–9
122. Welgampola MS, Ramsay E, Gleeson MJ, Day BL. Asymmetry of balance responses to monaural galvanic vestibular stimulation in subjects with vestibular schwannoma. *Clin Neurophysiol* [Internet]. 2013;124(9):1835–9
123. Mackenzie SW, Irving R, Monksfield P, Kumar R, Dezso A, Reynolds RF. Ocular torsion responses to electrical vestibular stimulation in vestibular schwannoma. *J Neurosci Methods* [Internet]. 2018;129:2350–60
124. Sonnier H, Marino AA. Sensory transduction as a proposed model for biological detection of electromagnetic fields. *Electro- and Magnetobiology*. 2001;20(2):153–75.

125. Kandel ER, Schwartz JH, Jessell TM. Principles of Neural Science [Internet]. Vol. 4, Neurology. 2000. 1414 p.
126. Miranda PC, Lomarev M, Hallett M. Modeling the current distribution during transcranial direct current stimulation. *Clin Neurophysiol*. 2006;117(7):1623–9.
127. Ruffini G, Wendling F, Merlet I, Molaee-Ardekani B, Mekkonen A, Salvador R, et al. Transcranial Current Brain Stimulation (tCS): Models and Technologies. *IEEE Trans neural Syst Rehabil Eng [Internet]*. 2013;21(3):333–45.
128. Durand DM. Electric field effects in hyperexcitable neural tissue: a review. *Radiat Prot Dosimetry*. 2003;106(4):325–31.
129. Mathie A, E. Kennard L, L. Veale E. Neuronal ion channels and their sensitivity to extremely low frequency weak electric field effects. *Radiat Prot Dosimetry [Internet]*. 2003;106(4):311–5.
130. Stagg CJ, Best JG, Stephenson MC, O’Shea J, Wylezinska M, Kincses ZT, et al. Polarity-Sensitive Modulation of Cortical Neurotransmitters by Transcranial Stimulation. *J Neurosci [Internet]*. 2009;29(16):5202–6.
131. Zaghi S, Acar M, Hultgren B, Boggio PS, Fregni F. Noninvasive Brain Stimulation with Low-Intensity Electrical Currents: Putative Mechanisms of Action for Direct and Alternating Current Stimulation. *Neurosci [Internet]*. 2010;16(3):285–307.
132. Hirata A, Takano Y, Fujiwara O, Dovan T, Kavet R. An electric field induced in the retina and brain at threshold magnetic flux density causing magnetophosphenes. *Phys Med Biol*. 2011;
133. Goldberg JM, Fernández C, Smith CE. Responses of vestibular-nerve afferents in the squirrel monkey to externally applied galvanic currents. *Brain Res*. 1982;252(1):156–60.
134. Precht W, Shimazu H. Functional Connections of Tonic and Kinetic Neurons With Primary Vestibular Afferents. *J Neurophysiol*. 1965;28(6):1014–28.

135. Shimazu H, Precht W. Tonic and Kinetic Responses of Cat'S Vestibular Neurons To Horizontal Angular Acceleration. *J Neurophysiol* [Internet]. 1965;28(6):991–1013.
136. Spiegel EA, Scala NP. Response of the labyrinthine apparatus to electrical stimulation. *Arch Otolaryngol*. 1943;38(2):131–8.
137. Aw ST, Todd MJ, Halmagyi GM. Latency and initiation of the human vestibuloocular reflex to pulsed galvanic stimulation. *J Neurophysiol* [Internet]. 2006;96(2):925–30.
138. Aw ST, Todd MJ, Aw GE, Weber KP, Halmagyi GM. Gentamicin vestibulotoxicity impairs human electrically evoked vestibulo-ocular reflex. *Neurology*. 2008;71(22):1776–82.
139. Zenner HP, Reuter G, Hong S, Zimmermann U, Gitter AH. Electrically evoked motile responses of mammalian type I vestibular hair cells. *J Vestib Res*. 1992;2(3):181–91.
140. Norris CH, Miller AJ, Perin P, Holt JC, Guth PS. Mechanisms and effects of transepithelial polarization in the isolated semicircular canal. *Hear Res*. 1998;123(1–2):31–40.
141. Gensberger KD, Kaufmann A-K, Dietrich H, Branoner F, Banchi R, Chagnaud BP, et al. Galvanic Vestibular Stimulation: Cellular Substrates and Response Patterns of Neurons in the Vestibulo-Ocular Network. *J Neurosci* [Internet]. 2016;36(35):9097–110.
142. Pall ML. Electromagnetic fields act via activation of voltage-gated calcium channels to produce beneficial or adverse effects. *J Cell Mol Med*. 2013;17(8):958–65.
143. Rodríguez-Contreras A, Yamoah EN. Effects of permeant ion concentrations on the gating of L-type Ca²⁺ channels in hair cells. *Biophys J*. 2003;84(5):3457–69.
144. Keen EC, Hudspeth AJ. Transfer characteristics of the hair cell ' s afferent synapse.

- PNAS. 2006;103(14):5537–42.
145. Nouvian R, Beutner D, Parsons TD, Moser T. Structure and function of the hair cell ribbon synapse. *J Membr Biol*. 2006;209(2–3):153–65.
 146. Heidelberger R, Thoreson WB, Witkovsky P. Synaptic transmission at retinal ribbon synapses. *Prog Retin Eye Res*. 2005;24(6):682–720.
 147. LoGiudice L, Matthews G. The Role of Ribbons at Sensory Synapses. *Neurosci [Internet]*. 2009;15(4):380–91.
 148. Thoreson WB, Rabl K, Townes-Anderson E, Heidelberger R. A highly Ca²⁺-sensitive pool of vesicles contributes to linearity at the rod photoreceptor ribbon synapse. *Neuron*. 2004;42(4):595–605.
 149. Modolo J, Thomas AW, Legros A. Possible mechanisms of synaptic plasticity modulation by extremely low-frequency magnetic fields. *Electromagn Biol Med*. 2013;32(November 2012):137–44.
 150. Kwan A, Forbes PA, Mitchell DE, Blouin J-S, Cullen KE. Neural substrates, dynamics and thresholds of galvanic vestibular stimulation in the behaving primate. *Nat Commun [Internet]*. 2019;10(1):1904.
 151. Severac Cauquil A, Faldon M, Popov K, Day BL, Bronstein AM. Short-latency eye movements evoked by near-threshold galvanic vestibular stimulation. *Exp Brain Res*. 2003;148:414–8.
 152. Yang Y, Pu F, Lv X, Li S, Li J, Li D, et al. Comparison of Postural Responses to Galvanic Vestibular Stimulation between Pilots and the General Populace. *Biomed Res Int [Internet]*. 2015;2015:1–6.
 153. Ertl M, Boegle MKR, Stephan T, Dieterich M. Vestibular perception thresholds tested by galvanic vestibular stimulation. *J Neurol [Internet]*. 2018;(0123456789):9–11.

154. Lenggenhager B, Lopez C, Blanke O. Influence of galvanic vestibular stimulation on egocentric and object-based mental transformations. *Exp Brain Res.* 2008;184(2):211–21.
155. Fitzpatrick RC, Marsden J, Lord SR, Day BL. Galvanic vestibular stimulation evokes sensations of body rotation. *Neuroreport.* 2002;13(18):2379–83.
156. Lobel E, Kleine JF, Bihan DL, Leroy-Willig a, Berthoz a. Functional MRI of galvanic vestibular stimulation. *J Neurophysiol.* 1998;80(5):2699–709.
157. Bent LR, Bolton PS, Macefield VG. Modulation of muscle sympathetic bursts by sinusoidal galvanic vestibular stimulation in human subjects. *Exp Brain Res.* 2006;174(4):701–11.
158. Grewal T, James C, MacEfield VG. Frequency-dependent modulation of muscle sympathetic nerve activity by sinusoidal galvanic vestibular stimulation in human subjects. *Exp Brain Res.* 2009;197(4):379–86.
159. Hammam E, Dawood T, Macefield VG. Low-frequency galvanic vestibular stimulation evokes two peaks of modulation in skin sympathetic nerve activity. *Exp Brain Res.* 2012;219(4):441–6.
160. James C, Stathis A, MacEfield VG. Vestibular and pulse-related modulation of skin sympathetic nerve activity during sinusoidal galvanic vestibular stimulation in human subjects. *Exp Brain Res.* 2010;202(2):291–8.
161. Klingberg D, Hammam E, Macefield VG. Motion sickness is associated with an increase in vestibular modulation of skin but not muscle sympathetic nerve activity. *Exp Brain Res.* 2015;233(8):2433–40.
162. Bolton PS, Wardman DL, Macefield VG. Absence of short-term vestibular modulation of muscle sympathetic outflow, assessed by brief galvanic vestibular stimulation in awake human subjects. *Exp Brain Res.* 2004;154(1):39–43.
163. Kim J. Head movements suggest canal and otolith projections are activated during

- galvanic vestibular stimulation. *Neuroscience* [Internet]. 2013;253:416–25.
164. Bikson M, Grossman P, Thomas C, Zannou AL, Jiang J, Adnan T, et al. Safety of Transcranial Direct Current Stimulation: Evidence Based Update 2016. *Brain Stimul* [Internet]. 2016;9(5):641–61.
 165. Laakso I, Tanaka S, Koyama S, Santis V De, Hirata A. Brain Stimulation Inter-subject Variability in Electric Fields of Motor Cortical tDCS. *Brain Stimul* [Internet]. 2015;8(5):906–13.
 166. Laakso I, Tanaka S, Koyama S, De Santis V, Hirata A. Inter-subject variability in electric fields of motor cortical tDCS. *Brain Stimul* [Internet]. 2015;8(5):906–13.
 167. Huang Y, Liu AA, Lafon B, Friedman D, Dayan M, Wang X, et al. Measurements and models of electric fields in the in vivo human brain during transcranial electric stimulation. *Elife*. 2017;6:1–27.
 168. Truong DQ, Magerowski G, Blackburn GL, Bikson M, Alonso-Alonso M. Computational modeling of transcranial direct current stimulation (tDCS) in obesity: Impact of head fat and dose guidelines. *NeuroImage Clin* [Internet]. 2013;2(1):759–66.
 169. Miranda PC, Mekonnen A, Salvador R, Ruffini G. The electric field in the cortex during transcranial current stimulation. *Neuroimage*. 2013;70:48–58.
 170. Minhas P, Member MB, Woods IAJ, Rosen AR, Kessler SK. Transcranial Direct Current Stimulation in Pediatric Brain: A computational modeling study. In: *Annual International Conference of the IEEE Engineering in Medicine and Biology Society IEEE Engineering in Medicine and Biology Society*. 2012. p. 859–62.
 171. Alam M, Truong DQ, Khadka N, Bikson M. Spatial and polarity precision of concentric high-definition transcranial direct current stimulation (HD-tDCS). *Phys Med Biol*. 2016;61(12):4506–21.
 172. Dmochowski JP, Datta A, Bikson M, Su Y, Parra LC. Optimized multi-electrode

- stimulation increases focality and intensity at target. *J Neural Eng.* 2011;8(4).
173. Datta A, Zhou X, Su Y, Parra LC, Bikson M. Validation of finite element model of transcranial electrical stimulation using scalp potentials: Implications for clinical dose. *J Neural Eng.* 2013;10(3).
 174. Datta A, Bansal V, Diaz J, Patel J, Reato D, Bikson M. Gyri-precise head model of transcranial direct current stimulation: Improved spatial focality using a ring electrode versus conventional rectangular pad. *Brain Stimul [Internet].* 2009;2(4):201-207.e1.
 175. Datta A, Bikson M, Fregni F. Transcranial direct current stimulation in patients with skull defects and skull plates: High-resolution computational FEM study of factors altering cortical current flow. *Neuroimage [Internet].* 2010;52(4):1268–78.
 176. Parazzini M, Fiocchi S, Rossi E, Paglialonga A, Ravazzani P. Transcranial Direct Current Stimulation: Estimation of the Electric Field and of the Current Density in an Anatomical Human Head Model. *IEEE Trans Biomed Eng.* 2011;58(6):1773–80.
 177. Allen JS, Damasio H, Grabowski TJ. Normal neuroanatomical variation in the human brain: An MRI-volumetric study. *Am J Phys Anthropol.* 2002;118(4):341–58.
 178. Heilmaier C, Theysohn JM, Maderwald S, Kraff O, Ladd ME, Ladd SC. A large-scale study on subjective perception of discomfort during 7 and 1.5T MRI examinations. *Bioelectromagnetics.* 2011;32(8):610–9.
 179. Heinrich A, Szostek A, Meyer P, Nees F, Rauschenberg J, Gröbner J, et al. Cognition and Sensation in Very High Static Magnetic Fields: A Randomized Case-Crossover Study with Different Field Strengths. *Radiology.* 2013;266(1):236–45.
 180. Rauschenberg J, Nagel AM, Ladd SC, Theysohn JM, Ladd ME, Möller HE, et al. Multicenter study of subjective acceptance during magnetic resonance imaging at 7 and 9.4 T. *Invest Radiol [Internet].* 2014;49(5):249–59.

181. Versluis MJ, Teeuwisse WM, Kan HE, Van Buchem MA, Webb AG, Van Osch MJ. Subject tolerance of 7 T MRI examinations. *J Magn Reson Imaging*. 2013;38(3):722–5.
182. Schaap K, Portengen L, Kromhout H. Exposure to MRI-related magnetic fields and vertigo in MRI workers. *Occup Environ Med*. 2015;161–6.
183. Atkinson IC, Sonstegaard R, Pliskin NH, Thulborn KR. Vital signs and cognitive function are not affected by 23-sodium and 17-oxygen magnetic resonance imaging of the human brain at 9.4 T. *J Magn Reson Imaging*. 2010;32(1):82–7.
184. Chakeres DW, De Vocht F. Static magnetic field effects on human subjects related to magnetic resonance imaging systems. *Prog Biophys Mol Biol*. 2005;87(2-3 SPEC. ISS.):255–65.
185. Heinrich A, Szostek A, Nees F, Meyer P, Semmler W, Flor H. Effects of static magnetic fields on cognition, vital signs, and sensory perception: A meta-analysis. *J Magn Reson Imaging*. 2011;34(4):758–63.
186. Uwano I, Metoki T, Sendai F, Yoshida R, Kudo K, Yamashita F, et al. Assessment of Sensations Experienced by Subjects during MR Imaging Examination at 7T. *Magn Reson Med Sci*. 2015;14(1):35–41.
187. Weintraub MI, Khoury A, Cole SP. Biologic effects of 3 Tesla (T) MR imaging comparing traditional 1.5 T and 0.6 T in 1023 consecutive outpatients. *J Neuroimaging*. 2007;17(3):241–5.
188. Theysohn JM, Maderwald S, Kraff O, Moenninghoff C, Ladd ME, Ladd SC. Subjective acceptance of 7 Tesla MRI for human imaging. *Magn Reson Mater Physics, Biol Med*. 2008;21(1–2):63–72.
189. Chakeres DW, Kangarlu A, Boudoulas H, Young DC. Effect of static magnetic field exposure of up to 8 Tesla on sequential human vital sign measurements. *J Magn Reson Imaging*. 2003;18(3):346–52.

190. De Vocht F, Van Drooge H, Engels H, Kromhout H. Exposure, health complaints and cognitive performance among employees of an MRI scanners manufacturing department. *J Magn Reson Imaging*. 2006;23(2):197–204.
191. De Vocht F, Wilén J, Mild KH, Van Nierop LE, Slottje P, Kromhout H. Health effects and safety of magnetic resonance imaging. *J Med Syst*. 2012;36(3):1779–80.
192. Gorlin A, Hoxworth JM, Pavlicek W, Thunberg CA, Seamans D. Acute vertigo in an anesthesia provider during exposure to a 3T MRI scanner. *Med Devices (Auckl)*. 2015;8:161–6.
193. Fuentes MA, Trakic A, Wilson SJ, Crozier S. Analysis and Measurements of Magnetic Field Exposures for Healthcare Workers in Selected MR Environments. *IEEE Trans Biomed Eng*. 2008;55(4):1355–64.
194. Dzendolet E. Sinusoidal Electrical Stimulation of the Human Vestibular Apparatus. *Percept Mot Skills* [Internet]. 1963;17(5):171–85.
195. El Sayed K, Dawood T, Hammam E, Macefield VG. Evidence from bilateral recordings of sympathetic nerve activity for lateralisation of vestibular contributions to cardiovascular control. *Exp Brain Res*. 2012;221(4):427–36.
196. MacDougall HG, Moore ST, Curthoys IS, Black FO. Modeling postural instability with Galvanic vestibular stimulation. *Exp Brain Res*. 2006;172(2):208–20.
197. van Osch MJP, Webb AG. Safety of Ultra-High Field MRI: What are the Specific Risks? *Curr Radiol Rep* [Internet]. 2014;2(8):61.
198. Lopez C, Halje P, Blanke O. Body ownership and embodiment: Vestibular and multisensory mechanisms. *Neurophysiol Clin*. 2008;38(3):149–61.
199. Lopez C, Schreyer HM, Preuss N, Mast FW. Vestibular stimulation modifies the body schema. *Neuropsychologia* [Internet]. 2012;50(8):1830–7.
200. ICNIRP. Guidelines on limits of exposure to static magnetic fields. International

- Commission on Non-Ionizing Radiation Protection. *Health Phys.* 2009;66(1):504–14.
201. Kangarlu A, Burgess RE, Zhu H, Nakayama T, Hamlin RL, Abduljalil AM, et al. Cognitive, cardiac, and physiological safety studies in ultra high field magnetic resonance imaging. *Magn Reson Imaging.* 1999;17(10):1407–16.
 202. Jokela K, Saunders RD. Physiologic and Dosimetric Considerations for Limiting Electric Fields Induced in the Body By Movement in a Static Magnetic Field. *Health Phys [Internet].* 2011;100(6):641–53.
 203. Cavin I., Glover PM, Bowtell R., Gowland P. Threshold for perceiving a metallic taste at large magnetic field. *J Magn Reson Imaging.* 2007;(26):1357–1361.
 204. Heckmann JG, Heckmann SM, Lang CJG, Hummel T. Neurological aspects of taste disorders. *Arch Neurol.* 2003;60(5):667–71.
 205. Reilly JP. Magnetic field excitation of peripheral nerves and the heart: a comparison of thresholds. *Biomed Eng (NY).* 1991;29(November):571–9.
 206. Stillman JA, Morton RP, Goldsmith D. Automated electrogustometry: A new paradigm for the estimation of taste detection thresholds. *Clin Otolaryngol Allied Sci.* 2000;25(2):120–5.
 207. Sahu RN, Behari S, Agarwal VK, Giri PJ, Jain VK. Taste dysfunction in vestibular schwannomas. *2008;56(1):42–6.*
 208. Brown E, Staines K, Dental B, Street LM, Bs B, Presentation C. Case Report Vestibular Schwannoma Presenting as Oral Dysgeusia: An Easily Missed Diagnosis. *Case Rep Dent.* 2016;2016:1–6.
 209. Dilda V, MacDougall HG, Curthoys IS, Moore ST. Effects of Galvanic vestibular stimulation on cognitive function. *Exp Brain Res.* 2012;216(2):275–85.
 210. Bense S, Stephan T, Yousry TA, Brandt T, Dieterich M. Multisensory cortical signal

- increases and decreases during vestibular galvanic stimulation (fMRI). *J Neurophysiol* [Internet]. 2001;85(2):886–99.
211. Latt D. THE POSTURAL SWAY RESPONSE TO GALVANIC VESTIBULAR STIMULATION IN HUMANS. North. University of Pittsburg; 1997.
 212. Hanson J. Galvanic Vestibular Stimulation Applied to flight Training. California Polytechnic State University; 2009.
 213. Tax CMW, Bom AP, Taylor RL, Todd N, Cho KKJ, Fitzpatrick RC, et al. The galvanic whole-body sway response in health and disease. *Clin Neurophysiol* [Internet]. 2013;124(10):2036–45.
 214. Goel R, Kofman I, Jeevarajan J, De Dios Y, Cohen HS, Bloomberg JJ, et al. Using low levels of stochastic vestibular stimulation to improve balance function. *PLoS One*. 2015;10(8):1–25.
 215. Hitier M, Besnard S, Smith PF. Vestibular pathways involved in cognition. *Front Integr Neurosci* [Internet].
 216. Eickhoff SB, Weiss PH, Amunts K, Fink GR, Zilles K. Identifying human parieto-insular vestibular cortex using fMRI and cytoarchitectonic mapping. *Hum Brain Mapp*. 2006;27(7):611–21.
 217. Patel M, Roberts RE, Arshad Q, Ahmed M, Riyaz MU, Bronstein AM. Galvanic Vestibular Stimulation Induces a Spatial Bias in Whole-body Position Estimates. *Brain Stimul* [Internet]. 2015;8(5):981–3.
 218. Torok E, Ferrè ER, Kokkinara E, Csepe V, Swapp D, Haggard P. Up, down, near, far: An online vestibular contribution to distance judgement. *PLoS One*. 2017;12(1):1–12.
 219. Reichenbach A, Bresciani JP, B?lthoff HH, Thielscher A. Reaching with the sixth sense: Vestibular contributions to voluntary motor control in the human right parietal cortex. *Neuroimage* [Internet]. 2016;124:869–75.

220. Preuss N, Kalla R, Mori R, Mast FW. Framing susceptibility in a risky choice game is altered by galvanic vestibular stimulation. *Sci Rep* [Internet]. 2017;7(1):2947.
221. Smith PF, Zheng Y. From ear to uncertainty: vestibular contributions to cognitive function. *Front Integr Neurosci* [Internet]. 2013;7(November):84.
222. Palla A, Lenggenhager B. Ways to investigate vestibular contributions to cognitive processes. *Front Integr Neurosci* [Internet]. 2014;8(May):40.
223. Arshad Q, Siddiqui S, Ramachandran S, Goga U, Bonsu A, Patel M, et al. Right hemisphere dominance directly predicts both baseline V1 cortical excitability and the degree of top-down modulation exerted over low-level brain structures. *Neuroscience*. 2015;311(October):484–9.
224. Lopez C, Blanke O, Mast FW. The human vestibular cortex revealed by coordinate-based activation likelihood estimation meta-analysis. *Neuroscience* [Internet]. 2012;212:159–79.
225. Fink GR, Marshall JC, Weiss PH, Stephan T, Grefkes C, Shah NJ, et al. Performing allocentric visuospatial judgments with induced distortion of the egocentric reference frame: An fMRI study with clinical implications. *Neuroimage*. 2003;20(3):1505–17.
226. Committeri G, Pitzalis S, Galati G, Patria F, Pelle G, Sabatini U, et al. Neural bases of personal and extrapersonal neglect in humans. *Brain*. 2007;130(2):431–41.
227. Karnath HO, Dieterich M. Spatial neglect - A vestibular disorder? *Brain*. 2006;129(2):293–305.
228. Ferrè ER, Bottini G, Haggard P. Vestibular modulation of somatosensory perception. *Eur J Neurosci*. 2011;34(8):1337–44.
229. Dieterich M, Brandt T. The bilateral central vestibular system: Its pathways, functions, and disorders. *Ann N Y Acad Sci*. 2015;1343(1):10–26.

230. Dieterich M, Kirsch V, Brandt T. Right-sided dominance of the bilateral vestibular system in the upper brainstem and thalamus. *J Neurol* [Internet]. 2017.
231. Philbeck JW, Behrmann M, Biega T, Levy L. Asymmetrical perception of body rotation after unilateral injury to human vestibular cortex. *Neuropsychologia*. 2006;44(10):1878–90.
232. Wilkinson D, Zubko O, Sakel M, Coulton S, Higgins T, Pullicino P. Galvanic vestibular stimulation in hemi-spatial neglect. *Front Integr Neurosci* [Internet]. 2014;8(January):4.
233. Van Nierop LE, Slotje P, Van Zandvoort M, Kromhout H. Simultaneous exposure to MRI-related static and low-frequency movement-induced time-varying magnetic fields affects neurocognitive performance: A double-blind randomized crossover study. *Magn Reson Med*. 2015;74(3):840–9.
234. de Vocht F De, Stevens T, Glover P, Sunderland A, Gowland P, Kromhout H. Cognitive Effects of Head-Movements in Stray Fields Generated by a 7 Tesla Whole-Body MRI Magnet. *Bioelectromagnetics*. 2007;255(28):247–55.
235. Grossberg S, Srihasam K, Bullock D. Neural dynamics of saccadic and smooth pursuit eye movement coordination during visual tracking of unpredictably moving targets. *Neural Networks* [Internet]. 2012;27:1–20.
236. Leigh JR, Zee DS. *The Neurology of Eye Movements* [Internet]. 5th editio. New York: Oxford University Press; 2015.
237. Straube A. Pharmacology of vertigo/nystagmus/oscillopsia. *Curr Opin Neurol*. 2005;18(1):11–4.
238. Von Hofsten C. Action in development. *Dev Sci*. 2007;10(1):54–60.
239. Brandt T, Strupp M. General vestibular testing. *Clin Neurophysiol*. 2005;116(2):406–26.

240. Roberts R, Gans R, Johnson E, Chisolm T. Computerized dynamic visual acuity with volitional head movement in patients with vestibular dysfunction. *Ann Otol Rhinol Laryngol* [Internet]. 2006;115(9):658–66.
241. Schubert MC, Herdman SJ, Tusa RJ. Vertical Dynamic Visual Acuity in Normal Subjects and Patients with Vestibular Hypofunction. 2002;372–7.
242. Herdman SJ. Computerized dynamic visual acuity test in the assessment of vestibular deficits. Vol. 9, *Handbook of Clinical Neurophysiology*. 2010. p. 181–90.
243. Herdman SJ, Schubert MC, Das VE, Tusa RJ. Recovery of Dynamic Visual Acuity in Unilateral Vestibular Hypofunction. *Arch Otolaryngol Head Neck Surg*. 2003;129:819–24.
244. Dannenbaum E, Paquet N, Chilingaryan G, Fung J. Clinical evaluation of dynamic visual acuity in subjects with unilateral vestibular hypofunction. *Otol Neurotol*. 2009;30(3):368–72.
245. Schubert MC, Migliaccio AA, Clendaniel RA. Mechanism of Dynamic Visual Acuity Recovery With Vestibular Rehabilitation. *Arch Phys Med Rehabil*. 2010;89(3):500–7.
246. De Vocht F, Glover P, Engels H, Kromhout H. Pooled analyses of effects on visual and visuomotor performance from exposure to magnetic stray fields from MRI scanners: Application of the Bayesian framework. *J Magn Reson Imaging*. 2007;26(5):1255–60.
247. De Vocht F, Stevens T, Glover P, Sunderland A, Gowland P, Kromhout H. Cognitive effects of head-movements in stray fields generated by a 7 tesla whole-body MRI magnet. *Bioelectromagnetics*. 2007;28(4):247–55.
248. Schneider E, Glasauer S, Dieterich M. Central processing of human ocular torsion analyzed by galvanic vestibular stimulation. *Neuroreport* [Internet]. 2000;11(7):1559–63.

249. MacDougall HG, Brizuela AE, Burgess AM, Curthoys IS. Between-subject variability and within-subject reliability of the human eye-movement response to bilateral galvanic (DC) vestibular stimulation. *Exp Brain Res*. 2002;144(1):69–78.
250. Schlosser HG, Unterberg A, Clarke A. Using video-oculography for galvanic evoked vestibulo-ocular monitoring in comatose patients. *J Neurosci Methods*. 2005;145(1–2):127–31.
251. Schneider E, Glasauer S, Dieterich M. Comparison of Human Ocular Torsion Patterns During Natural and Galvanic Vestibular Stimulation. *J Neurophysiol*. 2002;87:2064–73.
252. Kleine JF, Guldin WO, Clarke AH. Variable otolith contribution to the galvanically induced vestibulo-ocular reflex. *Neuroreport*. 1999;10(5):1143–8.
253. Curthoys IS, MacDougall HG. What galvanic vestibular stimulation actually activates. *Front Neurol*. 2012;JUL(July):1–5.
254. Utz KS, Korluss K, Schmidt L, Rosenthal A, Oppenländer K, Keller I, et al. Minor adverse effects of galvanic vestibular stimulation in persons with stroke and healthy individuals. *Brain Inj*. 2011;25(11):1058–69.
255. Jian B, Shintani T, Emanuel B, Yates B. Convergence of limb, visceral, and vertical semicircular canal or otolith inputs onto vestibular nucleus neurons. *Exp Brain Res*. 2002;144(2):247–57.
256. Horn CC. Why is the neurobiology of nausea and vomiting so important? *Appetite*. 2008;50(2–3):430–4.
257. Mian OS, Li Y, Antunes a, Glover PM, Day BL. On the vertigo due to static magnetic fields. *PLoS One [Internet]*. 2013;8(10):e78748.
258. Grabherr L, Macaudo G, Lenggenhager B. The Moving History of Vestibular Stimulation as a Therapeutic Intervention. *Multisens Res [Internet]*. 2015;28(5–6):653–87.

259. Van Nierop LE, Slottje P, Kingma H, Kromhout H. MRI-related static magnetic stray fields and postural body sway: A double-blind randomized crossover study. *Magn Reson Med*. 2013;70(1):232–40.
260. Van Nierop LE. *The Magnetized brain*. Universiteit Utrecht; 2015.
261. Kännälä S, Toivo T, Alanko T, Jokela K. Occupational exposure measurements of static and pulsed gradient magnetic fields in the vicinity of MRI scanners. *Phys Med Biol*. 2009;54(7):2243–57.
262. Grant W, Curthoys I. Otoliths - Accelerometer and seismometer; Implications in Vestibular Evoked Myogenic Potential (VEMP). *Hear Res*. 2017;353:26–35.
263. Curthoys IS, Grant JW, Burgess AM, Pastras CJ, Brown DJ, Manzari L. Otolithic receptor mechanisms for vestibular-evoked myogenic potentials: A review. *Front Neurol*. 2018;9(MAY):z.
264. Prato FS, Thomas a W, Cook CM. Human standing balance is affected by exposure to pulsed ELF magnetic fields: light intensity-dependent effects. *Neuroreport* [Internet]. 2001;12(7):1501–5.
265. Thomas AW, Drost DJ, Prato FS. Human subjects exposed to a specific pulsed (200 μ T) magnetic field: Effects on normal standing balance. *Neurosci Lett*. 2001;297(2):121–4.
266. Thomas AW, White KP, Drost DJ, Cook CM, Prato FS. A comparison of rheumatoid arthritis and fibromyalgia patients and healthy controls exposed to a pulsed (200 μ T) magnetic field: effects on normal standing balance. *Neurosci Lett*. 2001;309(1):17–20.
267. Legros A, Corbacio M, Beuter A, Modolo J, Goulet D, Prato FS, et al. Neurophysiological and behavioral effects of a 60 Hz, 1,800 IT magnetic field in humans. *Eur J Appl Physiol*. 2012;112(5):1751–62.
268. Thomas AW, White KP, Drost DJ, Cook CM, Prato FS. Human subjects exposed to

a specific pulsed (200 uT) magnetic field : effects on normal standing balance. 2001;309:17–20.

269. Villard S, Allen A, Bouisset N, Corbacio M, Thomas A, Guerraz M, et al. Impact of extremely low-frequency magnetic fields on human postural control. *Exp Brain Res* [Internet]. 2018;0(0):0.

2 Human Postural Control Under High Levels of Extremely Low Frequency Magnetic Fields

(Published in IEEE-Access)

2.1 Introduction

Extremely Low-Frequency Magnetic Field (ELF-MF < 300 Hz) at powerline frequencies (i.e 60 Hz in North America) are ubiquitous in modern societies due to the generation, distribution and use of alternating current (AC). From a health and safety perspective, agencies such as the International Commission for Non-Ionizing Radiation Protection (ICNIRP) and the International Committee on Electromagnetic Safety from the Institute of Electrical and Electronics Engineers (IEEE-ICES) depend on reliable scientific data to set guidelines and recommendations (1,2), to protect workers and the general public against electrostimulation induced adverse health effects.

In this regard, the latest IEEE-ICES standards state the necessity to investigate established acute mechanisms capable of synaptic activity alterations (2). The most reliable effect of synaptic polarization is the acute perception of magnetophosphenes. Magnetophosphenes are flickering visual manifestations perceived when exposed to a sufficiently strong ELF-MF (3). Therefore, the ICNIRP and the IEEE-ICES report synaptic activity alterations thresholds based on Saunders and Jefferys (4) and Lövsund et al. (5) magnetophosphenes studies.

Magnetophosphenes are reported to result from the modulation of the retinal cells (4–6). Since the retina is recognized as an integrative part of the Central Nervous System (CNS), magnetophosphenes are considered as a good conservative model to be generalized to the entire CNS (6).

In the vestibular system, the mechanical information of head movements is transduced into an electric signal via sensory cells called hair cells. Compellingly, both the vestibular

system and the retina use graded potential sensory cells (7) known for their high sensitivity mainly due to the continuous release of glutamate through ribbon synapses (8–11). Moreover, as retinal cells (6,12), vestibular hair cells are known to be easily impacted by weak electrical currents (13–17). Therefore, vestibular hair cells also appear as perfect targets for interaction with ELF-MF induced currents.

Consequently, from the perspective of the guidelines, the investigation of ELF-MF on the vestibular system is legitimate, as it would broaden the understanding of the underlining mechanisms enabling to better understand how phosphenes could be generalized to the entire CNS. Individuals around Magnetic Resonance Imaging (MRI) scanners often report illusions of rotating, vertigo, dizziness, and nausea, suggesting an interaction between MF and the vestibular system (18–20). In 2007, Glover et al. (21), published a seminal study on the interactions between static and time-varying MF and the vestibular system. They identified three different mechanisms possibly responsible for vestibular responses to MF exposure: i) the Diamagnetic Susceptibility (DS), ii) the Magneto-HydroDynamic (MHD) forces and iii) the Electromagnetic Induction (referred as induction herein). The DS hypothesis has been consistently dismissed as negligible, in both theoretical and experimental works (21–24). Conversely, MHD forces have been reported to modulate the vestibular system in a strong static magnetic field (SMF) environment. Indeed, a strong oriented SMF generates a Lorentz force that triggers nystagmus through activation of the Vestibulo-Ocular Reflex (22–25). However, MHD does not apply in an SMF-free environment. The third hypothesis of interaction is the induction mechanism based on Faraday's law of induction, stating that changing magnetic flux density over time (dB/dt in T/s) induces Electric Fields (E-Fields) and currents within conductors such as the human body. Indeed, besides magnetophosphenes, effects resulting from magnetic induction in humans have been reported on the central nervous system (4,26–31), the autonomous nervous system (32–34), and the peripheral nervous system (35).

In their “static subject changing field” experiment, Glover et al. (21) proposed a formal attempt to test if ELF-MF induction modulates vestibular performance. They showed no effect of a 2 T/s ELF-MF on human postural control, but they still hypothesized that stimulation over 4 T/s should be able to trigger a vestibular response (21).

Consequently, our work furthers the investigation of postural responses using full head homogeneous ELF-MF stimulations with high dB/dt, up to 40 T/s with the main objective to study vestibular outcomes at power frequency (60 Hz). Since the magnitude of vestibular outcomes increases linearly with current intensity (36–38), we expected to observe an increase in postural modulations with higher dB/dt values.

2.2 Methods

2.2.1 Participants

Twenty healthy participants (6 females - 14 males, 23.5 ± 3.68 years old) were tested. We excluded volunteers with a history of any vestibular-related dysfunction, chronic illnesses, neurological diseases, and participants having permanent metal devices above the neck. Participants had to refrain from exercise and alcohol, caffeine or nicotine intake 24 hours before the study.

2.2.2 Experimental devices

ELF-MF stimulations were delivered to the subjects' head via a customized head coil exposure system (FIG. 2.-1 left panel) consisting of a pair of 99-turn coils (11 layers of 9 turns each, 35.6 cm inner diameter and 50.1 cm outer diameter) made of hollow square copper wire cooled by circulating water. The two coils were assembled into a Helmholtz-like configuration, spaced 20.6 cm from center to center. The system was controlled and data was collected using a custom LabVIEW™ script (LabVIEW 2014 version 14.0.1 (32 bit)) through a 16-bit National Instruments A/D Card output channel (National Instruments, Austin, TX), driving two MRI gradient amplifiers capable of delivering up to 200 A at ± 345 V (MTS Automation Model No. 0105870, Horsham, PA, USA). A Biot-Savart model of our custom coil system was computed using a customized Matlab program (MatLab version 9.3 – The MathWorks Inc., USA) considering two systems of 11 solenoids of 9 turns stacked on each other following the geometrical characteristics presented above. This model presented in FIG. 2-2 shows the homogeneity of the magnetic field at the location of the participant's head. MF flux densities measurements were recorded every centimeter

from the center of the coil in both the Antero-Posterior (AP) and Medio-Lateral (ML) axes (FIG. 2-2 right panel) with a single axis MF Hall transducer probe (± 200 mT range with 0.1% accuracy, Senis AG Model No. 0YA05F-C.2T2K5J, Baar, Switzerland). These measurements showed great agreement with our model (FIG. 2-2 right panel). During the experiment, the probe was located 16 cm from the center of the coils, and data were recorded and used to synchronize all measurements with MF expositions. A force plate (OR6-7-1000, AMTI, USA) was used to collect participant's body sway at 1 kHz according to 6 degrees of freedom: forces and moments data each in the 3 dimensions. The Center of Pressure (COP) trajectory was calculated post-recording using a calibration matrix provided by the manufacturer. No hardware filtering was applied. A motorized non-magnetic lift enabled vertical movement of the coil system, such that it could raise and lower, centering the participants' ears between the coils (FIG. 2-1 left panel). A Direct Current (DC) stimulation was delivered using a transcranial current stimulation device (StarStim, Neuroelectrics, Spain), controlled with the NIC software (Neuroelectrics Instrument Controller, version 1.4.1 Rev.2014-12-01) via Bluetooth.



Figure 2-1 Stimulation apparatus. Volunteers stood in complete darkness, feet together, arms by their side and eye closed on a 1.5 cm foam pad covering the force plate. Their head was fully stimulated by Helmholtz-like coils centered on their ears, with ELF-MF stimulations at 8.89 T/s, 26.66 T/s and 39.98 T/s (left panel). The binaural bipolar DC montage stimulating both vestibular systems at 2 mA. The cathode is behind the right mastoid process and the anode is behind the left mastoid process (right panel).

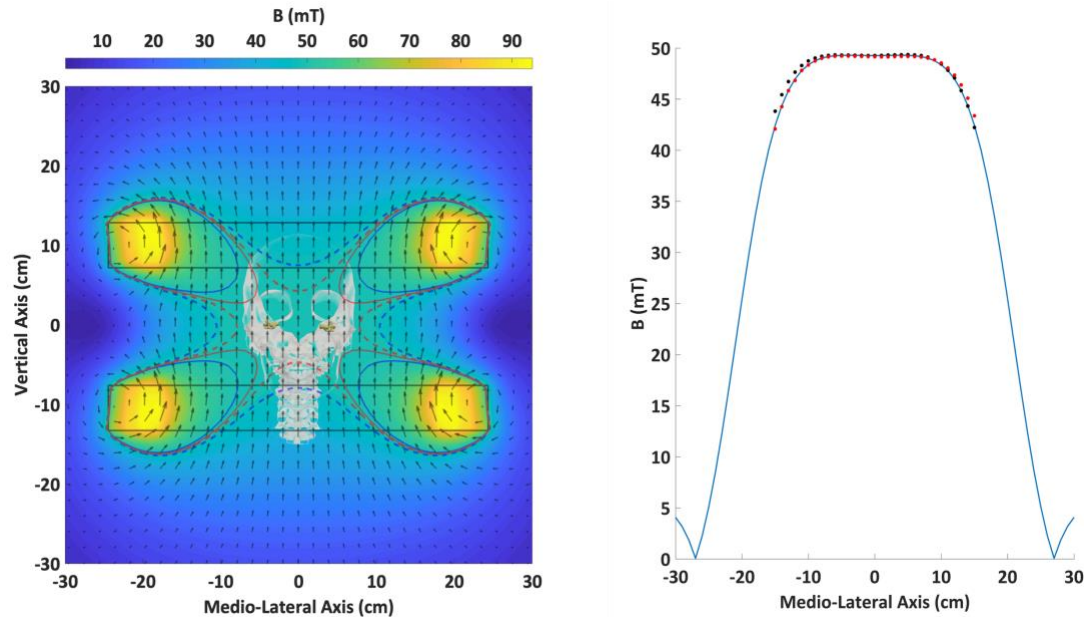


Figure 2-2 Two-dimensional spatial illustration of the MF level distribution around the exposure system computed according to the Bio-Savart law (Left panel). The thick black rectangles represent the outer boundaries of both coils. Small black arrows represent the magnetic vector field. Red and blue lines represent respectively the boundaries of a 1% and 5% flux density variation limit area from the center. Dashed lines represent the lower boundary while solid lines represent the upper boundary. Participants' vestibular systems, illustrated by the yellow structures in the head, lie within a 50 mT ($\pm 0.5\%$) vertically- oriented homogeneous field . Flux density values for full head homogeneous ELF-MF stimulations targeted at 50 mT (right panel). The blue line represents the expected flux density values given by the model along the mediolateral axis. Red and black dots are actual flux density measurements along the mediolateral and anteroposterior axes respectively

2.2.3 Protocol

After giving written informed consent, participants were equipped with the Starstim device. A DC stimulation was used as a positive control condition to validate the choice of our dependent variables. Positive control is defined herein as a condition in which specific known effects are expected (39). Indeed, based on the scientific literature, DC is known to

increase the postural sway, specifically oriented towards the anodal side of the stimulation (for review see (40)). In this regard, a classical binaural bipolar montage was used (FIG. 2-1 right panel). Both mastoid processes were previously rubbed with alcohol wipes (Mooremedical, USA) to improve impedance. Circular 25 cm² Ag/AgCl electrodes (StarStim, Neuroelectronics, Spain) were saturated with 8 mL of saline solution to provide proper conduction. Electrodes were secured using the StarStim neoprene cap and tape. To ensure appropriate stimulations, electrode impedances were maintained below 10 k Ω throughout the experiment as recommended by the manufacturer. The cathode was placed behind the right ear. Before starting the testing, the participants were exposed to a 5 seconds 2 mA DC exposure as a familiarization sample and to make sure they all swayed towards the anodal side (40). Participants were then asked to stand still, in complete darkness, during 20 seconds on a 1.5 cm thick foam surface arranged over the force plate with their eyes closed, arms along the sides and feet together to sensitize the vestibular system (40). Participants heads' stayed within the ELF-MF stimulation system at all times during the trials (FIG. 2-1 Left panel). A second investigator, blinded to the type of stimulation, was present to prevent potential loss of balance.

Following a repeated measure plan, we presented four type of stimulations in a random order to all our participants. One DC (2 mA) and three MF (50 mT) exposures were all delivered for 5 seconds. To reach high levels of dB/dt, we chose to modulate the exposure frequencies instead of exposure flux density. In the ELF range, the highest synaptic sensitivity occurs at 20 Hz (2), a frequency also known to induce vestibular modulations (41). Moreover, since vestibular electrical stimulations up to 100 Hz have shown to impact the vestibulospinal pathways (42), we decided to stay within these boundaries and investigated 90 Hz. Therefore, 20, 60, and, 90 Hz respectively produced 8.89 T/s, 26.66 T/s, and 39.98 T/s, two to tenfold higher than the 4 T/s threshold. Two control trials (CTRL) without stimulation were also done for each participant. All trials were randomly distributed. Thirty-second rest periods were taken between each trial. A timeline of our experiment is presented in FIG. 2-3. To prevent postural outcomes bias due to cerebrovascular alterations participants could not sit during rest (43). To conceal the noise generated by the coils, subjects wore earplugs throughout the experiment. This protocol

was approved by the Health Sciences Research Ethics Board (#106122) at Western University.

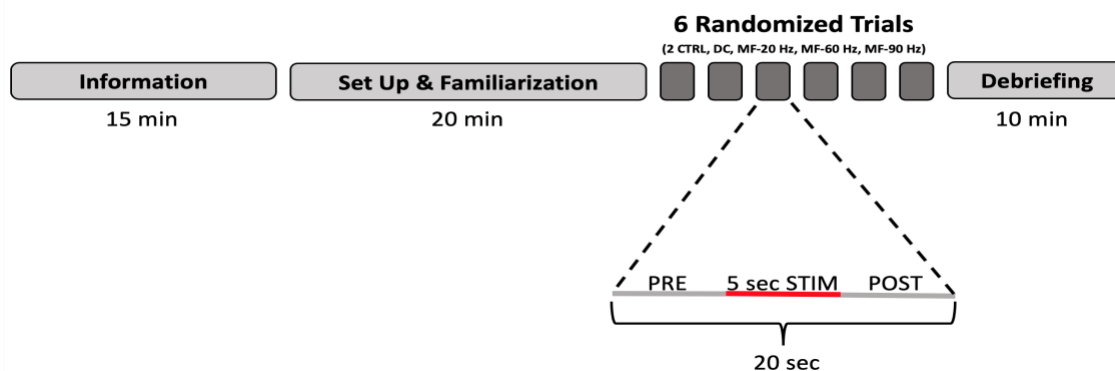


Figure 2-3 Schematic representation of the postural control protocol

2.2.4 Data analysis

The COP time-series were filtered with a low pass bidirectional 4th order Butterworth zero-phase digital filter with a cutoff frequency of 5 Hz. Cutoff frequency was determined after a residual analysis using a customized Matlab program. Sway characteristics were also computed using a customized MatLab program. Classically sway variables are analyzed on orthogonal AP and ML axes independently. However, our participants were put in unconventional conditions to sensitize vestibular function and AP-ML analyzes are known to be biased by biomechanical factors (36–38). Secondly, AP and ML data are not independent as balance is controlled by coordinating the body in space in both dimensions simultaneously (46). Finally, anatomical (47) and/or physiological (48) asymmetries between the two vestibular systems could induce subtle angular deviations not purely found along the classical AP-ML axis. Therefore planar sway analyzes were favored over one-dimensional analyses.

Among classical sway variables, the pathlength (the total length of COP excursion) has proved to be the more sensitive and reliable outcome (41–42). Pathlength was computed as the total sum of the distances between each point in the AP-ML plane. However, because pathlength varies with recording data time it is often hard to compare results from one study to another. Therefore, mean velocity (pathlength over time) was retained.

A Principal Component Analysis (PCA) was conducted on COP datasets to find the main direction of sway (51) (FIG. 2-3). The main direction of sway is described by the first principal component (PC1) which accounts for the largest part of the COP time-series' variance. θ , the angle between the ML axis and the PC1 axis was computed to describe the main direction of sway (FIG. 2-4A). θ was always presented within 0° and 180° , regardless of the direction of the movement towards the right or the left: 0° being aligned with the ML axis toward the right side of the participant. The second principal component (PC2) represents the axis orthogonal to PC1. PC1 and PC2 can be used to compute the 95% confidence interval ellipse of the sway for each trial (51) (FIG. 2-4B and 2-4C). Each PC expresses a certain percentage of the total variance of the data. The percentage of variance explained (VE) by PC1 was used to analyze how the sway was dispersed in space. Indeed, as VE of PC1 approaches 100 %, the ellipse merges closer to PC1 itself, thus expressing less spatial dispersion (FIG. 2-4C). Likewise, VE closer to 50 % would indicate that the total variance is gradually equally shared by PC1 and PC2 indicating a dispersed sway bounded by a circle (FIG. 2-4 B).

To investigate the acute effects of DC and MF, the sway responses were all analyzed during the first 2 seconds after stimulation onset within which the peak postural response for DC was found and reported in previous work (52).

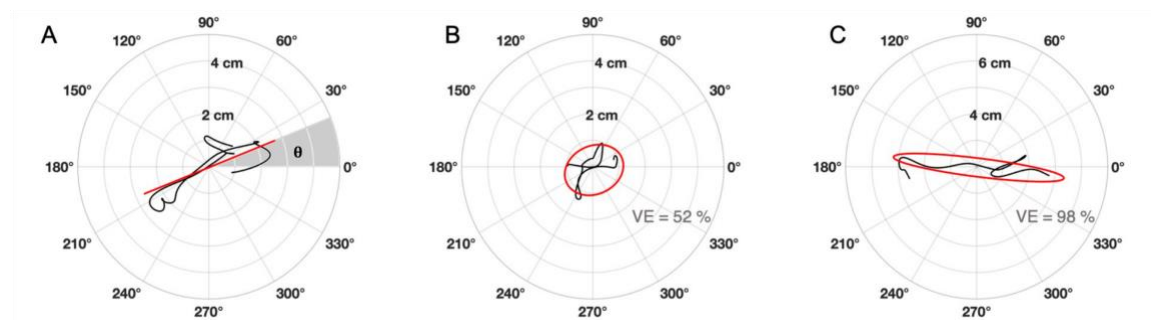


Figure 2-4 Graphical representation of dependent variables found with Principal Component Analysis. In all panels, the movement of COP is represented by the black line. In A, the red line represents the main direction of sway at an angle θ symbolized by the grey shaded area. A direction of sway at 90 degrees angle would indicate a pure

AP sway. In B and C red ellipses are examples of dispersion of the orientation of sway in space. In B, 52 % of the variance explained is expressed along the first PC whereas, in C, 98 % of the variance explained is expressed along the first PC.

2.2.5 Statistical analysis

All statistical analyses were performed using R version 3.3.2 (53). A level of significance of $\alpha = 0.05$ was adopted throughout data analysis. Percentages were not normally distributed, therefore, a logarithmic transform was used for VE.

One set of control data was randomly chosen and used to compare the effect of DC while the other set was used in contrast to MF stimulations. To investigate the effect of DC stimulations (DC vs CTRL), paired t-tests were used to analyze mean velocity as well as VE. To explore the effect of frequency on mean velocity as well as on VE, the data were analyzed by one-way repeated-measures ANOVAs with frequency (CTRL + the 3 frequencies modalities) as the within-subject variable.

For θ analyses, circular statistics were used using the circular library in R. Using Rayleigh's test for uniformity of the distributions, we first ensured that θ data samples were not distributed uniformly. Mean θ and Angular Deviation (\pm AD) were used to describe the main direction of sway. A Watson-Williams two-sample test was used to investigate the effect of DC on the direction of the sway. A Watson-Williams multi-sample test was used to investigate the effect of frequency on the direction of the sway (54).

2.3 Results

2.3.1 DC Stimulations.

The effect was unambiguous and reflected previous findings. Systematic loss of balance towards the anodal side was observed. Table 2-1 shows that both velocities ($t(19) = 5.1398$, $p < 0.001$, $r^2 = 0.58$) and VE ($t(19) = 2.91$, $p < 0.05$, $r^2 = 0.30$) were significantly greater

during DC than without. However, θ did not change with DC ($F(1,38) = 0.48, p = 0.49$) and stayed generally aligned along ML.

Table 2-1 Descriptive statistics for the DC results (CTRL vs DC). Mean and standard errors (\pm SE) values for Velocities and Variance Explained as well as mean angles and angular deviations (\pm AD) for Theta.

	CTRL	DC
Velocity (cm/s) ***	2.5 \pm 0.3	5.3 \pm 0.6
Variance Explained (%) *	82.3 \pm 2.6	91.6 \pm 2.1
Theta ($^{\circ}$)	- 8.7 \pm 39.5	- 0.3 \pm 31.2

CTRL : Control Condition ; DC: Direct Current condition

* $p < 0.05$ for paired t-test comparing CTRL and DC

*** $p < 0.001$ for paired t-test comparing CTRL and DC

2.3.2 ELF-MF stimulations

No significant differences between frequency of MF stimulation were found on Velocity ($F(3,57) = 1.26, p = 0.29$, FIG. 2-5A) nor on VE ($F(3,57) = 0.42, p = 0.73$, FIG. 2-5B). Similarly, no significant differences were found for θ ($F(3,76) = 1.52, p = 0.21$) between the frequency conditions. The FIG. 2-6 shows participants majorly swayed along the ML axis with a circular mean of -0.77° for all conditions.

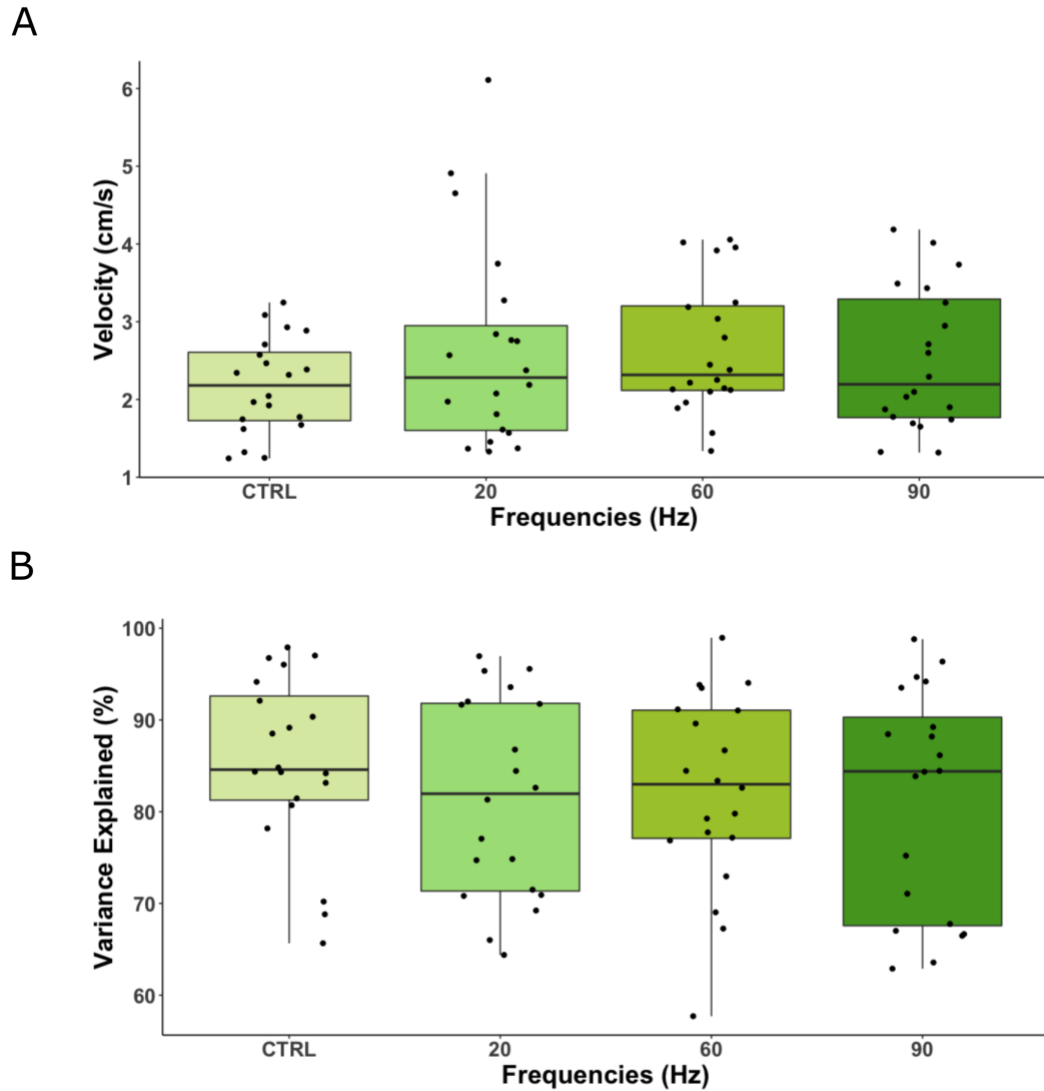


Figure 2-5 Mean velocities (A) and Variance explained (B) for CTRL vs all MF experimental conditions. Error bars represent 95% confidence intervals

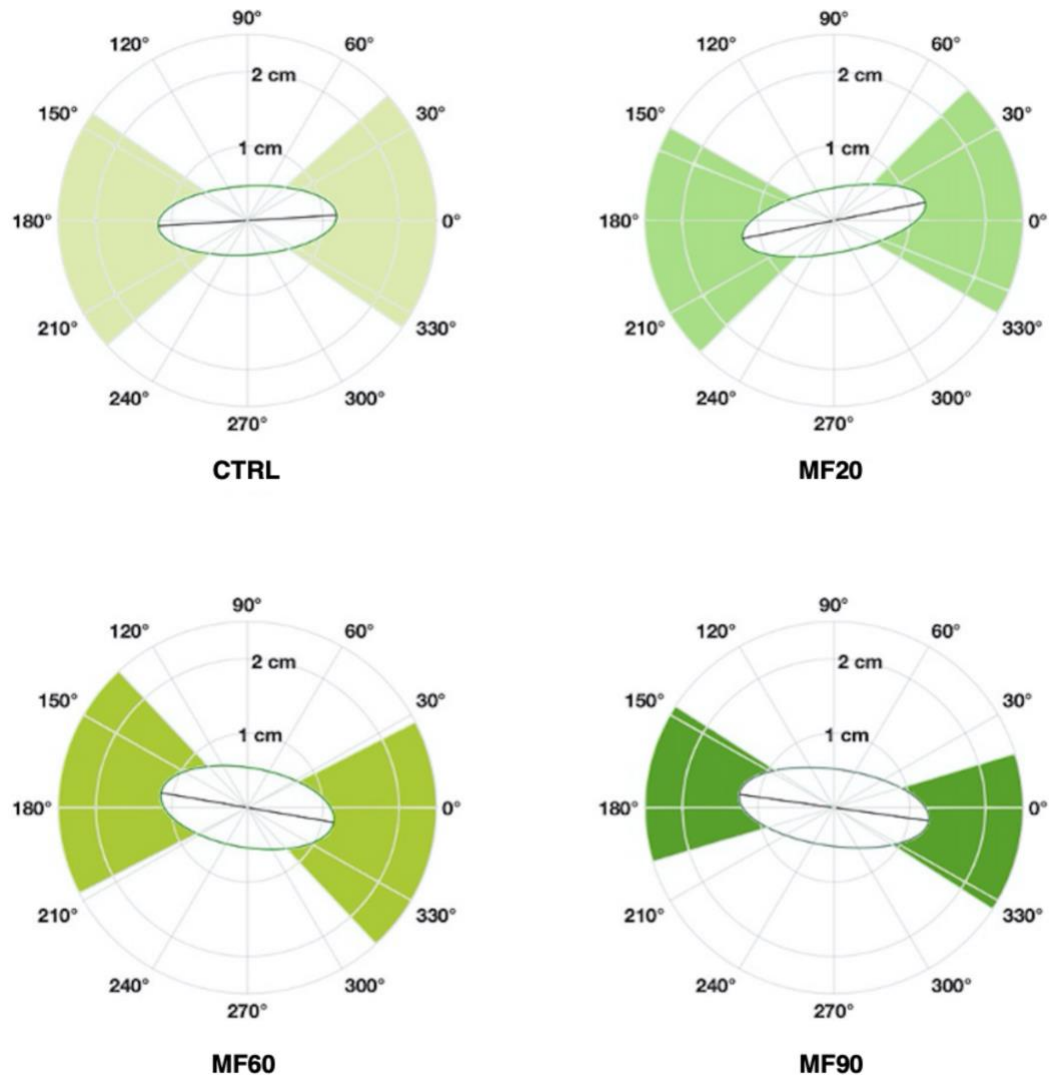


Figure 2-6 Average sway orientation for CTRL vs all MF experimental conditions. The black lines represent the main direction of sway (PC1) at the angle θ . The length of each black line is proportional to the mean quantity of movement expressed by the participants. Ellipses are a representation of the mean area of COP displacement. Shaded areas from light green (CTRL) to dark green (90 Hz) represent the angular deviation as frequency increases

2.3.3 Phosphene perceptions

Out of the 20 participants, 13 (65 %) declared seeing phosphenes at least once during the entire experiment.

2.4 Discussion

Given the very important neurophysiological similarities between the retinal and the vestibular sensory cells and the fact that electromagnetic induction produces magnetophosphenes, this study aimed to investigate the impact of full head 50 mT homogeneous ELF-MF stimulations at 20 Hz, 60 Hz and 90 Hz on human postural control in which the vestibular system plays a major role.

We replicated the “Static Subject Changing Field” experiment from Glover et al. (21) with a greater number of participants, more sensitive postural outcomes measures at higher dB/dt values than their 4 T/s vestibular threshold.

First, the use of a DC stimulation enabled us to validate the postural variables chosen in this work. As predicted, DC increased the quantity of movement. Indeed, greater velocity values characterized the loss of balance experienced by all participants. Similarly, increased sway alignment shown by greater VE values and the direction angles along the mediolateral axis portrayed the well-known DC-induced movements directed towards the anodal side in the frontal plane (for review see (40)).

Contrary to our hypothesis, our findings showed no postural response to ELF-MF stimulations despite being up to tenfold above Glover’s 4 T/s threshold. Indeed, in our study, peak dB/dt levels reached 8.89 T/s, 26.66 T/s, and 39.98 T/s at 20 Hz, 60 Hz, and 90 Hz respectively.

For their international guidelines and standards, ICNIRP and IEEE-ICES need *in-situ* E-Field threshold assessments to which uncertainty and safety factors are applied to fully protect the public as well as the workers (1,2). These publications estimate *in-situ* E-Fields using Maxwell equations applied to an ellipsoid model (55), but have acknowledged later

that anatomical models could also be used (2). Nonetheless, it is acknowledged that good estimations of *in-situ* E-Fields are also obtained with analytical spherical models (56). Therefore, we estimated the *in situ* induced E-Field generated by our stimulations, with the following equation derived from Maxwell's third law:

$$E = \frac{r}{2} \frac{\partial B}{\partial t} = \pi r f B$$

where E represents the induced E-Field and r the radius of the Faraday's loop within a homogeneous alternating flux density B of frequency f. Given a 5 cm radius loop encompassing both vestibular systems (FIG. 2-7), the 4 T/s threshold presented by Glover et al. (21) would produce 0.1 V/m tangentially to that loop. Following the same reckoning, our stimulation would produce peak E-Field at 0.225 V/m, 0.65 V/m, and 1 V/m for our respective frequencies at the level of the vestibular systems. Despite having E-Field values twice to ten times higher than the theoretical threshold estimated by Glover et al. (21), no differences in the quantity of movement, spatial dispersion nor on the direction of sway were observed.

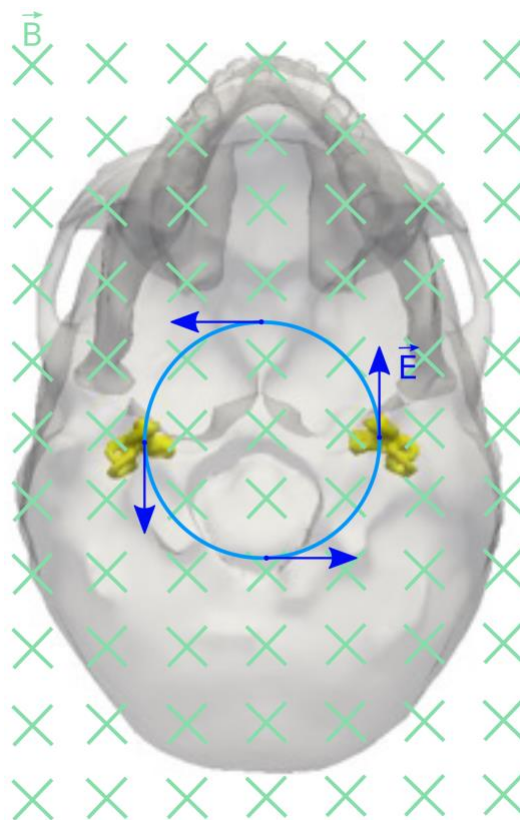


Figure 2-7 Bottom view of field orientation within a head representation. Both yellow structures are the vestibular systems. The green crosses represent the homogeneous MF increasing towards the top of the head. The light blue circle symbolizes a 5 cm radius Faraday's loop encompassing both vestibular systems. The dark blue arrows represent the tangential induced E-Fields generated at selected points of the loop.

In this light, several key points should be addressed to understand the absence of postural response: i) the role of the frequencies of stimulation used to reach high dB/dt values, ii) the role of the orientation of the MF, and finally iii) the anatomy and physiology of the vestibular structures impacted.

First, stimulation frequencies of 20 Hz, 60 Hz, and 90 Hz were chosen to generate dB/dt levels theoretically capable of triggering vestibular responses.

Importantly, in the case of electrical stimulation of the vestibular system, it is considered that postural outcomes are mostly due to semicircular canal activation (for review see (57)). Moreover, with alternating signals, as stimulation frequency increases, the weight of the

otolithic input increases while the weight of the canalithic input decreases (58). As a consequence, the high frequencies used in our study may have mainly impacted the otoliths, potentially yielding to weaker postural modulations.

Second, since the otoliths were the most likely impacted targets of our magnetic stimulations, their relative orientation to the induced fields must be considered. The otolithic subsystem is composed of the utricle and the saccule, which are responsible for detecting head horizontal and vertical linear accelerations respectively. The utricle is mostly planar, lying in the horizontal plane, whereas the saccule is mostly planar, lying orthogonally in the vertical plane. Given the orientation of both utricles and saccules in space, their respective vestibular hair cells would predominately be crossed perpendicularly by the induced E-Fields. Considering that only E-Fields colinear to the body of the neuronal cells have a maximum impact (59), only a fraction of the induced E-Fields could have influenced the otolithic hair cells. Therefore, considering that the induced E-Field threshold to modulate vestibular function was indeed met, its alignment relative to sensitive target cells (hair cells) may not have been optimal to allow a functional response.

Finally, anatomically both saccules' and utricles' maculae are divided by a striola. On each side of the striola, the vestibular hair cells are oppositely disposed, such that for any imposed head acceleration, one side will be excited while the other side will be inhibited (40,60). Considering such cross-striolar inhibition mechanisms (61), any impact of induced E-Fields and currents on oppositely oriented hair cells would be reduced within each otolithic sub-systems, on each side of the head (40). Consequently, little net vestibular signals would only be generated and integrated.

In summary, i) the use of high frequencies limited the postural responses by favorizing the otolithic over the canalithic system ii), only a fraction of induced E-Field influenced the otolithic hair cells, and iii), this remaining fraction of induced E-Field was subjected to the cross-striolar inhibition mechanism in both utricular and saccular maculae which further limited the effect on postural control.

Interestingly, studies using 0.7 T/s 60 Hz ELF-MF stimulations orthogonal to ours, have observed an impact on human postural control (62–65). However, these results should be

interpreted with caution. First, the dB/dt value was far below the theoretical 4T/s threshold. Second, the whole body was exposed and, therefore, the effects could have resulted from other sensory and/or motor modulations. Nonetheless, the suggestion of the crucial effect of the orientation of the field can also be found in the magnetophosphenes literature. Indeed, magnetophosphenes thresholds can vary 2.5 fold depending on field orientation (56). Considering Lövsund et al. (66,67), in which the fields exposed the participants' head laterally, the 2019 IEEE ICES standards (2) report a magnetophosphenes threshold at 20 Hz to be at 0.075 V/m peak. Yet considering Hirata et al. (56), this threshold could be lowered to 0.04 V/m peak when the field is orientated vertically. While vertical magnetic fields are well suited to impact retinal cells, lowering the magnetophosphenes thresholds (56), the same field orientation is, as seen in our results, ineffective on the vestibular hair cells

Furthermore, the vestibular systems, being more deeply nestled within the skull than the eyes, the Faraday's loop encompassing both vestibular apparatuses, is smaller than the loop enclosing both eyes. Therefore, the E-Fields at the vestibular system level are smaller than at the retinal level. However, with our MF at 20 Hz, an E-Field of 0.225 V/m is induced at the vestibular system level, which is more than 5 times stronger than the 0.04 V/m peak phosphene threshold calculated by Hirata et al. (56) with the same field orientation. It is also 3 times stronger than the 0.075 V/m peak estimated head exposures threshold of the guidelines (2). This indicates that with the dB/dt values reaching 40 T/s in the current study, the induced E-Fields for the retina and/or the CNS were above the threshold values used as bases in the guidelines and recommendations. Despite induced E-Fields exceeding the electrostimulation threshold values from the guidelines, no sensorimotor effects, besides phosphenes, were found in our study. Therefore, given the close neurophysiological similarities between vestibular hair cells and retinal cells, the absence of postural modulation showed by our results could challenge the idea of generalizing the threshold from retinal effects to the entire CNS. Indeed, our results suggest that the generalization based on neurophysiological similarities may not be appropriate. It is important to keep in mind that field orientation and structure localization in the CNS are also important parameters playing a role in the ability of an external MF to induce effective

neurostimulation. Yet, such considerations would greatly benefit from specific dosimetry work concerning the vestibular system, which is still lacking to date.

It is also important to keep in mind that the main objective of this work was to study the potential effect of a whole head exposure to a power-frequency MF on postural outcomes. In these specific conditions, it was hard to control for magnetophosphenes' perception, which has to be acknowledged as a possible confounding factor. This is however unlikely since body sway recordings during flickering light perceptions with frequencies above 16 Hz do not significantly differ from recordings with uniform room illumination (68), suggesting that magnetophosphenes perception would not have modulated postural outcomes. Yet full adaptation to darkness could reduce phosphene perception and help to better control such factors (69).

2.5 Conclusion

Our study suggests that before a formal investigation of the level for an acute postural response to ELF-MF, further research should address the difficulty of specifically targeting the vestibular system. Furthermore, more parameters such as MF orientation and frequency as well as vestibular anatomical and neurophysiological specificities need to be taken into consideration. Complementarily, more specific and potentially more responsive vestibular outcomes such as vestibular related eye movements or neck muscle activation should be thoroughly studied (42,70–72) to conclude on the significance and importance to study the impact of induction on the vestibular system within the frame of the guidelines.

Nonetheless, given the favored anatomical location of the retina, the fact that there is no inhibition mechanism at its level compared with the vestibular system, and the sensitivity of the retinal receptors, phosphenes remain to date the most sensitive response to ELF-MF stimulations. Therefore, to protect against potential adverse reactions associated with induced electrostimulation and to stay conservative, phosphenes should remain the basis of the international guideline.

2.6 References

1. ICNIRP. Guidelines for limiting exposure to time-varying electric and magnetic fields (1 Hz to 100 kHz). *Health Phys* [Internet]. 2010;99(6):818–36.
2. IEEE. IEEE Standard for Safety Levels With Respect to Human Exposure to Electric, Magnetic, and Electromagnetic Fields, 0 Hz to 300 GHz. Vol. 2005, IEEE Std C95.1-2005 (Revision of IEEE Std C95.1-1991). 2019. 0_1-238.
3. D'Arsonval A. Dispositifs pour la mesure des courants alternatifs de toutes fréquences. *Compt Rend Soc Biol*. 1896;3,(May 2):450–451.
4. Saunders RD, Jefferys JGR. A neurobiological basis for ELF guidelines. *Health Phys*. 2007;92(6):596–603.
5. Lövsund P, Öberg P, Nilsson SEG. Influence on vision of extremely low frequency electromagnetic fields : Industrial measurements, magnetophosphene studies in volunteers and intraretinal studies in animals. *Acta Ophthalmol*. 1979;57(5):812–21.
6. Attwell D. Interaction of low frequency electric fields with the nervous system: the retina as a model system. *Radiat Prot Dosimetry* [Internet]. 2003;106(4):341–8.
7. Juusola M, French AS, Uusitalo RO, Weckström M. Information processing by graded-potential transmission through tonically active synapses. *Trends Neurosci*. 1996;19(7):292–7.
8. Eatock RA, Songer JE. Vestibular Hair Cells and Afferents: Two Channels for Head Motion Signals [Internet]. Vol. 34, *Annual Review of Neuroscience*. 2011. 501–534 p.
9. Ghosh KK, Haverkamp S, Wässle H. Glutamate receptors in the rod pathway of the mammalian retina. *J Neurosci* [Internet]. 2001;21(21):8636–47.
10. Lagnado L, Gomis A, Job C. in the Synaptic Terminal of Retinal Bipolar Cells. *Cell*.

1996;17:957–67.

11. Sadeghi SG, Pyott SJ, Yu Z, Glowatzki E. Glutamatergic Signaling at the Vestibular Hair Cell Calyx Synapse. 2014;34(44):14536–50.
12. Laakso I, Hirata A. Computational analysis shows why transcranial alternating current stimulation induces retinal phosphenes. *J Neural Eng.* 2013;10(2008):046009.
13. Zenner HP, Reuter G, Hong S, Zimmermann U, Gitter AH. Electrically evoked motile responses of mammalian type I vestibular hair cells. *J Vestib Res.* 1992;2(3):181–91.
14. Norris CH, Miller AJ, Perin P, Holt JC, Guth PS. Mechanisms and effects of transepithelial polarization in the isolated semicircular canal. *Hear Res.* 1998;123(1–2):31–40.
15. Długaiczek J, Gensberger KD, Straka H. Galvanic vestibular stimulation: from basic concepts to clinical applications. *J Neurophysiol.* 2019;121(6):2237–55.
16. Gensberger KD, Kaufmann A-K, Dietrich H, Branoner F, Banchi R, Chagnaud BP, et al. Galvanic Vestibular Stimulation: Cellular Substrates and Response Patterns of Neurons in the Vestibulo-Ocular Network. *J Neurosci [Internet].* 2016;36(35):9097–110.
17. Aw ST, Todd MJ, Aw GE, Weber KP, Halmagyi GM. Gentamicin vestibulotoxicity impairs human electrically evoked vestibulo-ocular reflex. *Neurology.* 2008;71(22):1776–82.
18. Theysohn JM, Kraff O, Eilers K, Andrade D, Gerwig M, Timmann D, et al. Vestibular effects of a 7 tesla MRI examination compared to 1.5 T and 0 T in healthy volunteers. *PLoS One.* 2014;9(3):3–10.
19. Glover P. Magnetic Field-Induced Vertigo in the MRI Environment. *Curr Radiol Rep.* 2015;3(8):1–7.

20. Schaap K, Portengen L, Kromhout H. Exposure to MRI-related magnetic fields and vertigo in MRI workers. *Occup Environ Med.* 2015;161–6.
21. Glover PM, Cavin I, Qian W, Bowtell R, Gowland PA. Magnetic-field-induced vertigo: A theoretical and experimental investigation. *Bioelectromagnetics.* 2007;28(5):349–61.
22. Ward BK, Roberts DC, Della Santina CC, Carey JP, Zee DS. Vestibular stimulation by magnetic fields. *Ann N Y Acad Sci.* 2015;1343(1):69–79.
23. Roberts DC, Marcelli V, Gillen JS, Carey JP, Della Santina CC, Zee DS. MRI magnetic field stimulates rotational sensors of the brain. *Curr Biol [Internet].* 2011;21(19):1635–40.
24. Antunes a, Glover PM, Li Y, Mian OS, Day BL. Magnetic field effects on the vestibular system: calculation of the pressure on the cupula due to ionic current-induced Lorentz force. *Phys Med Biol [Internet].* 2012;57(14):4477–87.
25. Glover PM, Li Y, Antunes A, Mian OS, Day BL. A dynamic model of the eye nystagmus response to high magnetic fields. *Phys Med Biol [Internet].* 2014;59(3):631–45.
26. Bell GB, Marino AA, Chesson AL. Alterations in brain electrical activity caused by magnetic fields : detecting the detection process Andrew A . Marino a and Andrew L . Chesson b. *Electroencephalogr Clin Neurophysiol.* 1992;83:389–97.
27. Bell GB, Marino AA, Chesson AL. Frequency specific blocking in the human brain caused by electromagnetic fields. *Neuroreport.* 1994;5:510–2.
28. Ghione S, Del Seppia C, Mezzasalma L, Bonfiglio L. Effects of 50 Hz electromagnetic fields on electroencephalographic alpha activity, dental pain threshold and cardiovascular parameters in humans. *Neurosci Lett.* 2005;382(1–2):112–7.
29. Graham C, Cook MR, Cohen HD, Gerkovich MM. Dose response study of human

- exposure to 60 Hz electric and magnetic fields. 1994;447–83.
30. Iles JF. Simple models of stimulation of neurones in the brain by electric fields. *Prog Biophys Mol Biol*. 2005;87(1 SPEC. ISS.):17–31.
 31. Jefferys JGR, Deans J, Bikson M, Fox J. Effects of weak electric fields on the activity of neurons and neuronal networks. *Radiat Prot Dosim*. 2003;106(4):321–3.
 32. Tabor Z, Michalski J, Rokita E. Influence of 50 Hz magnetic field on human heart rate variability: linear and nonlinear analysis. *Bioelectromagnetics* [Internet]. 2004;25(6):474–80.
 33. Bortkiewicz A, Gadzicka E, Zmysłony M, Szymczak W. Neurovegetative disturbances in workers exposed to 50 Hz electromagnetic fields. *Int J Occup Med Environ Health* [Internet]. 2006;19(1):53–60.
 34. Jeong JH, Kim JS, Lee BC, Min YS, Kim DS, Ryu JS, et al. Influence of exposure to electromagnetic field on the cardiovascular system. *Auton Autacoid Pharmacol*. 2005;25(1):17–23.
 35. Comlekci S, Coskun O. Influence of 50 Hz-1 mT magnetic field on human median nerve. *Electromagn Biol Med*. 2012;31(4):285–92.
 36. Aw ST, Todd MJ, Halmagyi GM. Latency and initiation of the human vestibuloocular reflex to pulsed galvanic stimulation. *J Neurophysiol* [Internet]. 2006;96(2):925–30.
 37. Severac Cauquil A, Faldon M, Popov K, Day BL, Bronstein AM. Short-latency eye movements evoked by near-threshold galvanic vestibular stimulation. *Exp Brain Res*. 2003;148:414–8.
 38. Séverac Cauquil A, Gervet MFT, Ouaknine M. Body response to binaural monopolar galvanic vestibular stimulation in humans. *Neurosci Lett*. 1998;245(1):37–40.

39. Johnson P, Besselsen D. Practical Aspects of Experimental Design in Animal Research Experimental Design : Initial Steps. *Inst Lab Anim Res* [Internet]. 2002;43(4):203–6.
40. Fitzpatrick RC, Day BL. Probing the human vestibular system with galvanic stimulation. *J Appl Physiol* [Internet]. 2004;96(6):2301–16.
41. Mackenzie SW, Reynolds RF. Ocular torsion responses to sinusoidal electrical vestibular stimulation. *J Neurosci Methods*. 2018;294:116–21.
42. Forbes PA, Fice JB, Siegmund GP, Blouin J-S. Electrical Vestibular Stimuli Evoke Robust Muscle Activity in Deep and Superficial Neck Muscles in Humans. *Front Neurol* [Internet]. 2018;9(July):1–8.
43. Wilson TD, Serrador JM, Shoemaker JK. Head position modifies cerebrovascular response to orthostatic stress. *Brain Res*. 2003;961(2):261–8.
44. Chiari L, Rocchi L, Cappello A. Stabilometric parameters are affected by anthropometry and foot placement. *Clin Biomech*. 2002;17(9–10):666–77.
45. Rocchi L, Chiari L, Cappello a. Feature selection of stabilometric parameters based on principal component analysis. *Med Biol Eng Comput*. 2004;42(1):71–9.
46. Rhea CK, Kiefer AW, Haran FJ, Glass SM, Warren WH. A new measure of the CoP trajectory in postural sway: Dynamics of heading change. *Med Eng Phys*. 2014;36(11):1473–9.
47. Chacko LJ, Schmidbauer DT, Handschuh S, Reka A, Fritscher KD, Raudaschl P, et al. Analysis of Vestibular Labyrinthine Geometry and Variation in the Human Temporal Bone. *Front Neurosci*. 2018;12(February):1–13.
48. Hatzilazaridis I, Hatzitaki V, Antoniadou N, Samoladas E. Postural and muscle responses to galvanic vestibular stimulation reveal a vestibular deficit in adolescents with idiopathic scoliosis. *Eur J Neurosci*. 2019;(May):1–13.

49. Fitzgerald JE, Murray A, Elliott C, Birchall JP. Comparison of Body Sway Analysis Techniques: Assessment with Subjects Standing on a Stable Surface. *Acta Otolaryngol* [Internet]. 1994 Jan 8;114(2):115–9.
50. Nagymáté G, Orlovits Z, Kiss RM. Reliability analysis of a sensitive and independent stabilometry parameter set. *PLoS One*. 2018;13(4):1–14.
51. Oliveira LF, Simpson DM, Nadal J. Calculation of area of stabilometric signals using principal component analysis. 1996;17:305–12.
52. Mian OS, Day BL. Violation of the craniocentricity principle for vestibularly evoked balance responses under conditions of anisotropic stability. *J Neurosci* [Internet]. 2014;34(22):7696–703.
53. R Core Team. *R: A Language and Environment for Statistical Computing*. Vol. 0, R Foundation for Statistical Computing Vienna Austria. Vienna, Austria; 2016. p. {ISBN} 3-900051-07-0.
54. Berens P. *CircStat: A MATLAB Toolbox for Circular Statistics*. *J Stat Softw* [Internet]. 2009;31(10):1–21.
55. Reilly JP. Magnetic field excitation of peripheral nerves and the heart: a comparison of thresholds. *Biomed Eng (NY)*. 1991;29(November):571–9.
56. Hirata A, Takano Y, Fujiwara O, Dovan T, Kavet R. An electric field induced in the retina and brain at threshold magnetic flux density causing magnetophosphenes. *Phys Med Biol*. 2011;56(13):4091–101.
57. Reynolds RF, Osler CJ. Galvanic vestibular stimulation produces sensations of rotation consistent with activation of semicircular canal afferents. *Front Neurol*. 2012;JUN(June):1–2.
58. Carriot J, Jamali M, Brooks JX, Cullen KE. Integration of Canal and Otolith Inputs by Central Vestibular Neurons Is Subadditive for Both Active and Passive Self-Motion: Implication for Perception. *J Neurosci* [Internet]. 2015;35(8):3555–65.

59. Radman T, Ramos RL, Brumberg JC, Bikson M. Role of cortical cell type and morphology in subthreshold and suprathreshold uniform electric field stimulation in vitro. *Brain Stimul* [Internet]. 2009;2(4):215-228.e3.
60. Tascioglu AB. Brief Review of Vestibular Anatomy and Its Higher Order Projections. *Neuroanatomy*. 2005;4(4):24–7.
61. Uchino Y, Sato H, Kushiro K, Zakir M, Imagawa M, Ogawa Y, et al. Cross-Striolar and Commissural Inhibition in the Otolith System. *Ann Otol Rhinol Laryngol*. 1999;87(1):162–72.
62. Legros A, Corbacio M, Beuter A, Modolo J, Goulet D, Prato FS, et al. Neurophysiological and behavioral effects of a 60 Hz, 1,800 μ T magnetic field in humans. *Eur J Appl Physiol*. 2012;112(5):1751–62.
63. Thomas AW, Drost DJ, Prato FS. Human subjects exposed to a specific pulsed (200 μ T) magnetic field: Effects on normal standing balance. *Neurosci Lett*. 2001;297(2):121–4.
64. Thomas AW, White KP, Drost DJ, Cook CM, Prato FS. A comparison of rheumatoid arthritis and fibromyalgia patients and healthy controls exposed to a pulsed (200 μ T) magnetic field: effects on normal standing balance. *Neurosci Lett*. 2001;309(1):17–20.
65. Prato FS, Thomas AW, Cook CM. Human standing balance is affected by exposure to pulsed ELF magnetic fields: light intensity-dependent effects. *Neuroreport* [Internet]. 2001;12(7):1501–5.
66. Lövsund P, Öberg PÅ, Nilsson SEG, Reuter T. Magnetophosphenes: a quantitative analysis of thresholds. *Med Biol Eng Comput*. 1980;18(3):326–34.
67. Lövsund P, Öberg PÅ, Nilsson SEG. Magneto- and electrophosphenes: A comparative study. *Med Biol Eng Comput*. 1980;18(6):758–64.
68. Paulus WM, Straube A, Brandt TH. Visual stabilization of posture: Physiological

- stimulus characteristics and clinical aspects. *Brain*. 1984 Dec;107(4):1143–63.
69. Lövsund P, Öberg P, Nilsson SEG. Quantitative determination of thresholds of magnetophosphenes. *Radio Sci*. 1979;14(6 S):199–200.
 70. Dumas G, Curthoys IS, Lion A, Perrin P, Schmerber S. The skull vibration-induced nystagmus test of vestibular function—A review. *Front Neurol*. 2017;8(MAR).
 71. Curthoys IS, Grant JW, Burgess AM, Pastras CJ, Brown DJ, Manzari L. Otolithic receptor mechanisms for vestibular-evoked myogenic potentials: A review. *Front Neurol*. 2018;9(MAY):z.
 72. Curthoys IS. The new vestibular stimuli: sound and vibration—anatomical, physiological and clinical evidence. *Exp Brain Res [Internet]*. 2017;235(4):957–972.

3 Human Postural Responses to High Vestibular Specific Extremely Low-Frequency Magnetic Stimulations

(Published in IEEE-Access)

3.1 Introduction

The generation, distribution, and use of alternating current (AC) are ubiquitous in modern societies, exposing the public to 50/60 Hz Extremely Low-Frequency Magnetic Fields (ELF-MF < 300 Hz). According to Faraday's law of induction, changing magnetic flux density over time (dB/dt , measured in T/s) induces Electric Fields (E-Fields) and currents within conductors such as the human body. In this context, answering health and safety concerns to protect workers and the public is crucial. In that regard, international agencies such as the International Commission for Non-Ionizing Radiation Protection (ICNIRP) and the International Committee on Electromagnetic Safety from the Institute of Electrical and Electronics Engineers (IEEE-ICES) review scientific data to establish guidelines and standards enacted at national levels (1–3).

The main experimental paradigm to investigate the acute consequences of electrostimulation emerging from induction in humans is the perception of magnetophosphenes. Magnetophosphenes are flickering visual manifestations perceived when exposed to sufficiently strong time-varying MF (4). The main hypothesis regarding magnetophosphenes is that they result from membrane potential modulations of graded potential retinal cells, impacting in cascade the continuous release of neurotransmitters through their ribbon synapses (5). Interestingly, the retinal cells share common neurophysiological properties with the vestibular hair cells. Indeed, both types of cells use graded potential for signal processing (6) both releasing glutamate gradually from ribbon synapses (7–11).

Vestibular hair cells are found in both canals and otoliths (composed of the utricle and the saccule), responsible for detecting head rotational and linear accelerations respectively.

Vestibular hair cells transduce mechanical information (i.e. head movements) into an electric signal treated by the central nervous system (CNS) (12). Compellingly, as for the retinal cells (13), small intensity currents stimulations easily trigger the vestibular hair cells (14–18) making them likely susceptible to ELF-MF induced currents.

Since vestibular, visual, and proprioceptive inputs (19), are integrated to manage balance through postural control (20) it was suggested that ELF-MF could impact postural sway. However, our previous investigations of vestibular ELF-MF stimulations did not show acute postural outcomes (21,22), questioning the assumption that similar neurophysiological systems should respond equivalently to ELF-MF stimulations. We previously argued that the top-down orientation of our fields in regards to hair cells' orientation was not optimal for their modulation and that lateral field orientation could be better (22). The impact of field orientation had also been demonstrated to be crucial in the case of magnetophosphenes perception (23) which prompted further investigation of postural outcomes under lateral stimulation of the vestibular system. We previously attempted to address this question (21), however, clear methodological biases had to be answered to reach relevant conclusions.

Therefore, the main objective of the current work is to further investigate a potential acute vestibular impact of lateral ELF-MF stimulations at powerline frequencies (i.e 60 Hz in North America). To do so, we improved our previous study (21).

Given the close neurophysiological similarities between the retinal cells and the vestibular hair cells and the fact that both are triggered by electrical stimulations, we hypothesize that ELF-MF impact the vestibular hair cells modulating postural sway. Since greater currents cause greater vestibular outcomes (24,25), and induced currents' strength proportionally increase with dB/dt (26), we hypothesized that higher dB/dt values yield larger postural modulations.

Lövsund et al. (27), illustrated the effect of dB/dt on magnetophosphenes' perception by comparing electro- and magneto-stimulations. Indeed, in the case of an electric stimulation the current intensity delivered is not changed by an increase of the stimulation frequency, whereas the increase in frequency for an ELF-MF stimulation proportionally increases the

induced current intensity. Following the same paradigm, we compared vestibular specific ELF-MF and AC stimulations over increasing frequencies expecting to find different frequency effects in the postural responses.

3.2 Methods

3.2.1 Participants

Thirty height healthy participants (16 females-22 males, 24.3 ± 3.51 years old) were recruited for the study and tested in the Human Threshold Research Facility at St. Joseph's Hospital in London, Ontario, Canada. Were excluded volunteers with a history of any vestibular-related pathology or dysfunction, chronic illnesses, neurological diseases that affect normal body movement, and participants having permanent metal devices above the neck. Participants had to refrain from exercise and alcohol, caffeine, or nicotine intake 24 hours before the study.

3.2.2 Experimental devices

We delivered the MF vestibular specific stimulations to the subjects' right vestibular system via a customized headset coil exposure system (6.70 kg). It consisted of two 570 turn-coils of 5.9 cm of mean diameter, with a 2.5-cm diameter core of Permendur-49 (The Goodfellow Group, Coraopolis, PA, USA- see FIG. 3-1 left panel) inserted within each coil. As in our previous work (21), we used a Permendur-49 core to increase the flux density developed by the coil to reach $100 \text{ mT}_{\text{rms}}$ (141.42 mT peak) at 3 cm from the coils where the vestibular system approximately lies (28). The inductance of the coil was 26 mH. The two coils were bound together to a custom adjustable headset to better fit participants' heads (FIG. 3-1 right panel). Although we only stimulated the right vestibular system in this study, we kept both coils not to introduce any postural bias due to asymmetrical load. The whole headset was suspended by a rod system, designed to support up to 10.5 kg, tied to a vest worn around participants' chests (Atlas Camera Support, Los Angeles, Ca, USA), to unload the weight of the coils as they were maintained on the participants' head (see FIG. 3-1right panel).

We controlled the system and collected data using a custom LabVIEW™ script (LabVIEW 2014 version 14.0.1 (32 bit)) through a 16-bit National Instruments A/D Card output channel (National Instruments, Austin, TX), driving an MTS™ Magnetic Resonance Imaging gradient amplifier capable of delivering up to 200 A_{rms} at ± 345 V (MTS Automation, Horsham, PA, USA). We delivered Direct Current (DC) and AC stimulations using a transcranial current stimulation device (StarStim, Neuroelectrics, Spain) driven by the NIC software (Neuroelectrics Instrument Controller, version 1.4.1 Rev.2014-12-01) via Bluetooth. We used a force plate (OR6-7-1000, AMTI, USA) to collect participant's body sway at 1 kHz according to 6 degrees of freedom: forces and moments data each in the 3 dimensions. Data was saved in a single measurement file, along with the MTS™ amplifier's current time series, used to synchronize all measurements with MF expositions, for later analysis. The Center of Pressure (COP) trajectory was calculated post-recording using a calibration matrix provided by the manufacturer. No hardware filtering was applied.

3.2.3 Protocol

We fully equipped the participants after they gave their written informed consent. We used the same monaural montage for both DC and AC stimulations (FIG. 3-1 left panel). DC was only used as a positive control condition to validate the choice of our dependent variables. For DC stimulation, we placed the cathode behind the right mastoid process and the return electrode at the C7 spinal process (see FIG. 3-1 left panel). To improve impedance, we rubbed the right mastoid and C7 spinal processes with alcohol wipes (Mooremedical, USA). To provide proper conduction between the electrodes and the skin, we saturated the circular 25 cm² Ag/AgCl electrodes (StarStim, Neuroelectrics, Spain) with 8 mL of saline solution. We then secured the electrodes using the StarStim exposure cap and tape. To ensure appropriate stimulations, we maintained electrodes' impedances below 10 k Ω throughout the experiment, as recommended by the manufacturer. Before starting the testing, we exposed the participants to 5 seconds DC (2 mA) and AC (peak ± 2 mA at 20 Hz) trials as stimulation samples. The MF headset exposure system was then set over the StarStim exposure cap. To ensure careful headset placement, we centered the coils at

the mastoid processes level. For consistency, we kept both the StarStim cap and the MF exposure device on the head during all testing conditions.

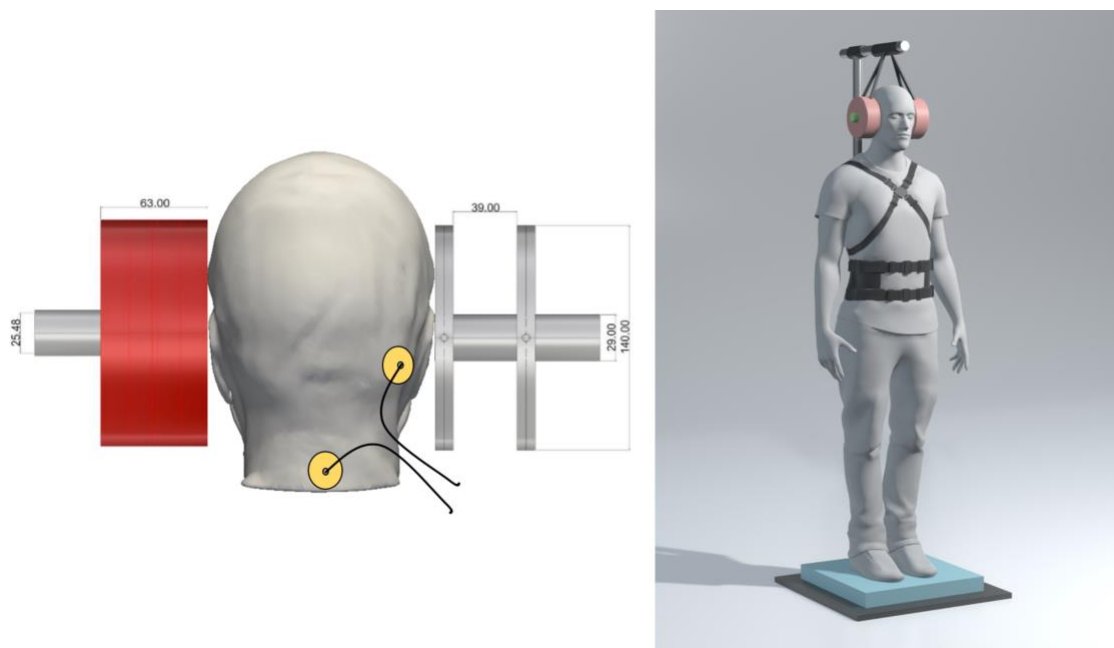


Figure 3-1 Representation of experimental exposition apparatus. The left panel shows a diagram of the custom coils system centered over the mastoid process. The electrodes (yellow circles) delivering the DC and AC currents, were placed in a monaural configuration behind the right mastoid and the C7 spinous process. The right panel shows a volunteer standing on the foam pad, wearing the vest self-sustaining the MF headset device unloading the weight of the coils.

We tested participants in periods of 20 seconds. We asked them to stand on a 6-cm thick foam pad (Airex AG, Switzerland) placed on the force plate, with the eyes closed, arms resting at their side, and feet together to maximize vestibular contribution (29). A second investigator, blinded to the type of stimulation applied to the participants, was present to prevent potential falls and for safety purposes. Exposure conditions consisted of five seconds of MF (100 mT_{rms}), DC (2mA), AC (peak \pm 2 mA), or no stimulation (CTRL). As in Villard et al. (21), we delivered MF and AC stimulations at five different frequencies (20 Hz, 60 Hz, 90 Hz, 120 Hz, and 160 Hz). All trials were randomly distributed. In a post-

experiment analysis, we randomly assigned the CTRL trials to an experimental condition and we respectively tagged them as “CTRL DC”, “CTRL AC” and “CTRL MF” for DC, AC and MF conditions. To avoid participant fatigue, dissipate the stimulation effects and allow the vestibular system to reach its normal resting firing rate between blocks, we gave 30 s of rest between trials (30). Also, to avoid cerebrovascular alterations that could bias postural outcomes after standing back up, participants could relax but could not sit during the resting periods (31).

To analyze the effects of the ELF-MF stimulation device, we recorded the participant’s postural control with and without the coils system. To keep the device and the electrodes consistently aligned with the mastoid processes throughout the experiment, these two final conditions were not randomized and were recorded at the end of the trials.

Subjects wore earplugs throughout the experiment to conceal the noise generated by the coils. The Health Sciences Research Ethics Board at Western University approved this protocol (#106122) performed following the Declaration of Helsinki.

3.2.4 Data analysis

The COP time series were filtered with a low pass bidirectional 4th order Butterworth zero-phase digital filter with a cutoff frequency of 5 Hz. The use of a residual analysis with a customized Matlab program (MatLab version 9.3 – The MathWorks Inc., USA) determined the cutoff frequency. We computed sway characteristics using a customized Matlab program. Classically, sway variables are analyzed on anteroposterior (AP) and mediolateral (ML) axes separately, but here we favored planar analyzes over one-dimensional analyses for mainly two reasons listed thereafter. First, balance is best controlled by coordinating the body in space in both dimensions simultaneously (32). Second, biomechanical factors bias AP-ML analyzes (33,34), which may be particularly impacted in a protocol sensitizing the vestibular function and involving a heavy customized headset coil exposure system. Finally, monaural electrical stimulations were used (different from the binaural bipolar montage in (21)), which induce oblique deviations in

the AP and ML plane (35). Therefore, we favored planar analyzes over one-dimensional analyses.

Electrical stimulations of the vestibular system impact both the quality (sway spatial orientation) and the quantity of movement (sway size) (29). Both were therefore considered. To investigate the acute stimulation effects, we measured the sway differences between the 5 seconds period before stimulation onset (PRE-STIM) and the 5-second stimulation period (STIM) for all our analyzes.

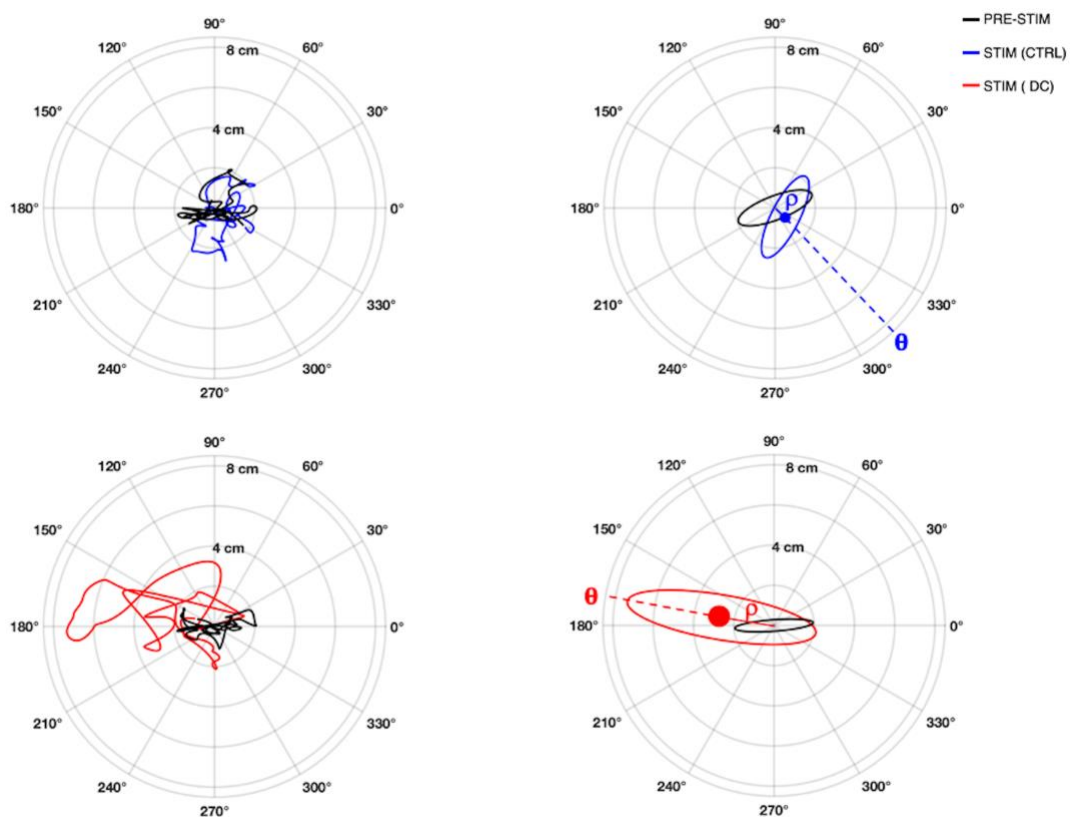


Figure 3-2 Graphical representation of postural sway for one participant. Left panels show the Center of Pressure (COP) before (black) and during the stimulation (blue in control condition, CTRL, and red in direct current condition, DC). These COP movements can be summarized on the right panels by their 95% confidence ellipses. The displacement from the ellipses' barycenter from pre-stimulation to during-stimulation provides distance ρ and the angle θ of the displacement. Finally, the size

of the dot characterizes the difference of sway movement (calculated as COP average velocity) between pre- and during stimulation.

Spatial orientation was estimated by first conducting a Principal Component Analyses (PCA) on COP datasets to compute PRE-STIM and STIM 95% confidence interval ellipses (36) for each trial (FIG. 3-2 right panels). Then the barycenter was found at the intersection of the major and minor axes of each ellipse. To facilitate the analysis, the mean of the PRE-STIM COP dataset was subtracted from both the PRE-STIM and STIM datasets, centering all the PRE-STIM barycenters on zero. To estimate the spatial direction of sway we found the angle theta (θ) between 0 degrees and STIM barycenters (FIG. 3-2 right panels).

Two analyses were done for sway size. First, we calculated the distance rho (ρ) between PRE-STIM and STIM barycenters (FIG. 3-2 right panels). Then, among classical sway variables, the pathlength (the total length of COP excursion) has proved to be the more sensitive as well as the more reliable (37,38). Therefore, we computed both PRE-STIM and STIM pathlengths as the total sum of the distances between each point in the AP-ML plane (FIG. 3-2 Left panels). However, because pathlength varies with recording time it is often hard to compare results from one study to another. For this reason, we retained mean velocity (Pathlength over time). With transcranial electrical stimulations, great E-Field variability exists between participants (39), leading to great postural outcomes variability. Therefore, we calculated the difference between the STIM and PRE-STIM mean velocities (Δ speed) for each trial in order to individualize the analysis of the stimulations' impact.

3.2.5 Statistical analysis

We performed all linear statistical analyses using R version 3.3.2 (40) and all circular statistics using the CircStat toolbox in Matlab (41). A level of significance of $\alpha = 0.05$ was adopted throughout data analysis.

Differences in all three CTRL conditions were analyzed with a one-way repeated measure analysis of variance (ANOVA). To investigate the effect of wearing the stimulation device (ON vs OFF) as well as the effect of our positive control (DC vs CTRL), we implemented

paired t-tests to analyze ρ and Δ speed. Two-way ANOVAs (2 stimulation modalities (AC / MF) x 6 conditions (CTRL plus five frequencies)) for repeated measures were used to test the effect of frequency of the time-varying exposure types on ρ and Δ speed. Rao's spacing test for circular uniformity was used to determine whether θ was distributed uniformly. If not, the mean θ and angular deviation (\pm AD), as well as the mean resultant vector length ($|\vec{r}|$), were implemented to describe the main direction of sways from PRE-STIM to STIM barycenters. $|\vec{r}|$ is a measure of angular dispersion around the mean ranging from 0 to 1. The closer $|\vec{r}|$ gets to 1, the more the angles are concentrated around the angular mean thus describing one specific direction (41)

3.3 Results

3.3.1 Differences in CTRL conditions

As seen in FIG. 3-3 and F FIG. 3-4, all CTRL conditions (blue dots) were equivalent. Indeed, no differences were found for ρ ($F(2,74) = 1.58, p = 0.21$) and for Δ speed ($F(2,74) = 0.53, p = 0.5907$). Also, no specific sway directions were found in the different CTRL groups ($p > 0.05$).

3.3.2 Effect of Stimulation device

Postural sway size was not affected by wearing the headset as no significant effect was found on ρ ($t(37) = -0.77, p = 0.44$) nor on Δ speed ($t(37) = 1.19, p = 0.24$). Also, the headset did not organize sway spatially since Rao's tests in both conditions showed that θ values were uniformly distributed ($p > 0.05$).

3.3.3 Effects of positive control

Δ speed ($t(37) = 7.81, p < 0.0001, R^2 = 0.62$ - see FIG. 3-3) and ρ ($t(37) = 6.15, p < 0.001, R^2 = 0.5$ - see FIG. 3-3) were significantly greater with DC than CTRL signing more

important sway size due to DC. Also DC clearly organised sway spatially. Indeed, as confirmed by the second experimenter, DC induced an important obvious left forward oblique postural sway (Mean $\theta = 157.4^\circ \pm 13^\circ$, $\|\vec{r}\| = 0.82$, $p = 0.001$), whereas no significant mean sway was found for CTRL ($p > 0.05$), see FIG. 3-3).

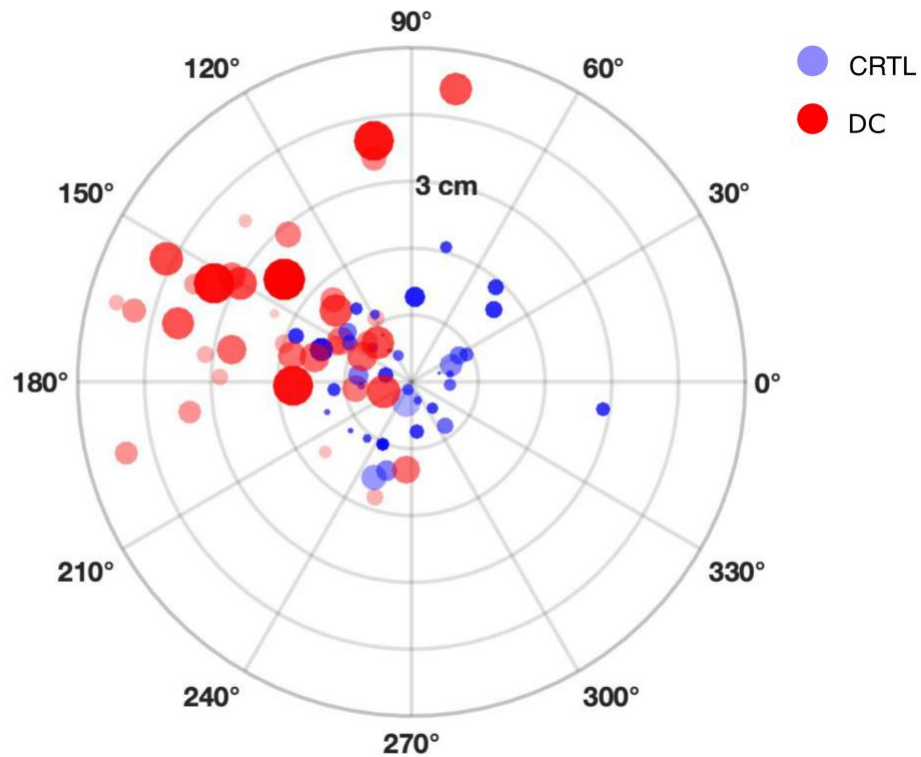


Figure 3-3 Postural shift of COP barycenters from pre- to during exposure. Pre-exposure barycenters are centered at the origin. Each dot location represents the displacement due to exposure. The dot size shows the absolute difference in Δ speed (amplitude only) while transparency shows actual Δ speed (amplitude and sign: most transparent express higher speed in pre-exposure).

3.3.4 Effects of AC and MF stimulations

FIG. 4-4 depicts θ , ρ and Δ speed data for both stimulation types (MF and AC) at 60 Hz. Indeed, results at 60 Hz are representative of all frequency conditions (see Table 3-1). Two-way ANOVAs (2 stimulation modalities (AC/MF) x 6 conditions (CTRL plus 5

frequencies)) for repeated measures indicated no significant main effects of stimulation condition for ρ ($F(1,37) = 2.8$, $p = 0.1$) nor on Δ speed ($F(1,37) = 0.80$, $p = 0.37$).

Table 3-1 Descriptive statistics for both stimulation groups (MF and AC) across all frequencies (20, 60, 90,120 and 160 Hz). Mean and standard deviation values for Δ speed and ρ . No information about θ is reported since no mean angle could be computed.

		CTRL	20 Hz	60 Hz	90 Hz	120 Hz	160 Hz
Δ speed (cm/s)	AC	-0.30 ± 2.20	0.35 ± 1.81	-0.31 ± 1.69	0.42 ± 1.67	-0.13 ± 1.71	0.17 ± 1.45
	MF	0.19 ± 1.72	0.45 ± 1.91	0.17 ± 1.85	-0.43 ± 1.59	-0.66 ± 1.32	0.07 ± 1.80
ρ (cm)	AC	0.94 ± 0.59	0.99 ± 0.55	0.95 ± 0.60	1.13 ± 0.47	1.13 ± 0.47	1.06 ± 0.64
	MF	0.96 ± 0.56	1.03 ± 0.70	0.83 ± 0.44	0.88 ± 0.50	0.93 ± 0.58	0.99 ± 0.60

Equally, no significant main effects of frequency were found for ρ : ($F(5,185) = 0.70$, $p = 0.62$) and for Δ speed ($F(5,185) = 1.83$, $p = 0.1$). Also, no interaction effects were found for ρ : ($F(5,185) = 0.88$, $p = 0.49$) and for Δ speed: ($F(5,185) = 1.64$, $p = 0.15$). Rao's test results concerning θ for all MF and AC experimental conditions as well as for CTRL groups, consistently showed that all angles in each condition were uniformly distributed ($p > 0.05$) underlining that neither MF nor AC stimulations oriented postural control in any given specific direction.

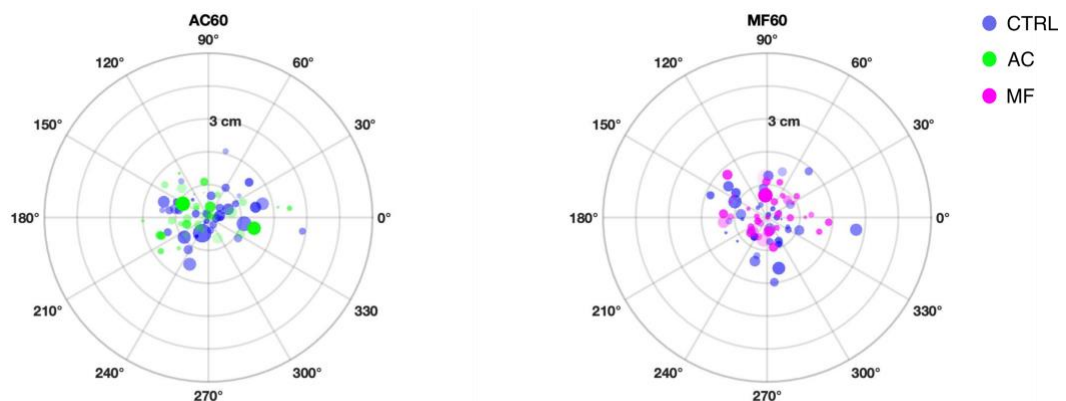


Figure 3-4 Postural modulations for AC (left) and MF (right) at 60 Hz compared to control conditions (blue dots). Results at 60 Hz are representative of all experimental conditions. Pre-exposure barycenters are centered at the origin. Each dot location represents the displacement due to exposure. The dot size shows the absolute

difference in Δ speed (amplitude only) while transparency shows actual Δ speed (amplitude and sign: most transparent express higher speed in pre-exposure).

3.4 Discussion

This work was a follow up of a previous study from our group (21), from which the methodology and analysis have been improved to account for now known biases and planar modification of the COP.

The aim here was to study the potential acute effect of vestibular exposure to a power-frequency MF on postural outcomes. We hypothesized that MF-induced E-Fields would trigger vestibular hair cells and modulate the postural sway in the same way they trigger magnetophosphenes perception when applied to retinal cells. AC stimulation is known to impact postural control in humans (29,42), and was thus used in comparison with the ELF-MF outcomes. However, since induction laws make an E-Field's strength proportional to ELF-MF frequency but not with AC, we did not expect similar frequency modulations in the outcomes.

The use of a DC stimulation as a positive control validated the postural variables chosen in this work. The mean lowest DC threshold reported in the literature to induce postural responses in healthy controls is 0.32 mA (43). Therefore, as expected, our 2 mA DC stimulation resulted in an instantaneous effect on human balance. With higher Δ speed and greater ρ , we observed a greater postural sway in DC than in the CTRL condition. As predicted, participants swayed towards the opposite side of the stimulated ear with a mean direction angle of $157.4^\circ \pm 13^\circ$, describing a left-oriented oblique forward sway expected for a right monaural cathodal DC stimulation (29). However, we did not observe differences in sway size and spatial orientation neither with ELF-MF nor AC stimulations.

Since our 2 mA AC stimulation was over 6-fold higher than the reported postural threshold, and since our DC stimulation at the same intensity triggered a postural response, the absence of AC results must, therefore, lay in the time-varying characteristics of that stimulation.

However, for the ELF-MF, we still need to consider the intensity. Indeed, the *in-situ* induced E-Field strength is intimately tethered to the stimulation's frequency. ICNIRP and IEEE-ICES suggest estimating the intensity of ELF-MF with the in-situ E-Field based on an ellipsoid model implementing Maxwell equations (44). Nonetheless, it is acknowledged that good estimates of in-situ E-Fields can be computed with analytical spherical models (23). Therefore, as previously done in our own work (21,22), we estimated the in-situ E-Field using the following equation derived from Maxwell's third law

$$E = \frac{r}{2} \frac{\partial B}{\partial t} = \pi r f B$$

where E represents the induced E-Field and r the radius of the Faraday's loop within a homogeneous alternating flux density B of frequency f. For a constant value of B at a given value of r, E will depend on the frequency f of stimulation. Following this strategy, with a flux density measured at 141.42 mT peak at the vestibular system, and frequencies ranging from 20 to 160 Hz, we obtain peak dB/dt between 18 T/s and 142 T/s. Considering a radius of 6 mm encompassing the entire vestibular system (45) (FIG. 3-5), peak E-Fields could be estimated between 0.054 V/m and 0.426 V/m. The entire E-Fields values for the respective frequencies can be found in Table 3-2.

To date, we did not find specific dosimetry work concerning the vestibular system published in the literature. However, in implanted epileptic participants, Huang et al. (46) found that 2 mA sinusoidal transcranial electrical stimulation generates 0.4 V/m at the cortical level. More interestingly, they also found such E-Fields values at deep brain structures like the anterior cingulate and the periventricular white matter (46), underlining that 2 mA at the skull, could translate to 0.4 V/m globally to the CNS. Furthermore, given the high conductivity values of the perilymph (47), the endolymph and the vestibular structures (48), the currents are easily drawn to the vestibular system. Hence, it is reasonable to estimate that our DC and AC 2 mA stimulations can also generate 0.4 V/m at the vestibular level (Table 2-2).

Table 3-2 ELF-MF and AC stimulations estimated peak E-Field values across all frequencies.

		20 Hz	60 Hz	90 Hz	120 Hz	160 Hz
Estimated E-Field (V/m)	MF	0.054	0.159	0.24	0.321	0.426
	AC	0.4	0.4	0.4	0.4	0.4

Considering the linear relationship between the applied current's intensity and the E-Field presented in Huang et al. (46), 0.32 mA translates to 0.064 V/m at the vestibular system, suggesting that the ELF-MF level at 20 Hz was the only condition below the postural threshold.

Yet, we must also consider the MF orientation and more especially the relevant E-Field fraction relative to the vestibular sensors, as it would lower the impact on the structures. Indeed, phosphene literature provides evidence that fields' orientation is of paramount importance. Hirata et al. (23) found close to a 2.5-fold difference in magnetophosphene threshold values depending on whether fields were oriented top-down or front-back relative to the retina. It has been shown that only E-Fields colinear to the body of the neuronal cells have a maximum impact (49). Therefore, we need to consider field orientation relative to the anatomical structures.

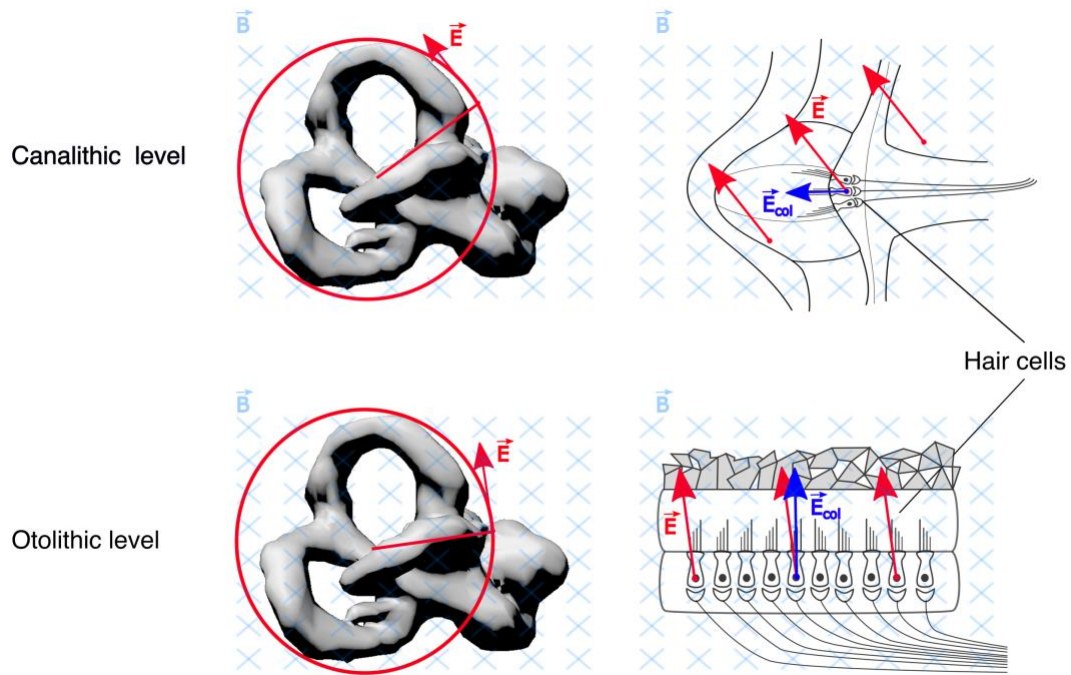


FIG. 3-5 Representation of a lateral view of E-Fields impacting the right vestibular system (3D grey structures). The upper panels consider a canalithic level while the lower panels represent an otolith level. The light blue crosses represent the homogeneous MF increasing from the right to the left side of the head. The red circles symbolize the Faraday's loops encapsulating the entire human vestibular system. The red \vec{E} arrows represent the tangential induced E-Fields generated either at the anterior canal ampulla (upper right panel) or at the utricle (lower right panel). The dark blue \vec{E}_{col} arrows represent the fractional component of \vec{E} aligned with the hair cells showing little impact at the canalithic level and greater impact at the utricular level.

ELF-MF go through the anatomical structures without any hindrance and the induced E-Fields are orthogonal to the MF, constraining the currents in specific directions. Using high-resolution X-ray microtomography imaging techniques, Chacko et al. (50) showed important inter-variability in the orientation of the canalithic membranous labyrinths. Thus, it is hard to consider how the canalithic hair cells were oriented relative to the induced E-Fields. However, utricle and saccule are reported to be mostly planar and lying in the

horizontal and vertical plane respectively (51). It seems reasonable to consider that only a small component of the E-Field orientation was colinear with canalithic hair cells (FIG. 3-5, top panels), whereas most of the E-Field would be aligned with the utricular hair cells (FIG. 3-5, bottom panels). The saccule being mostly considered orthogonal to the utricle, the fraction of the E-Field colinear to the hair cells would be almost null.

The orientation of the ELF-MF presented in this work was intended to target the right vestibular system, which by design limited the canalithic impact and favored utricular stimulation. It is also important to emphasize that only a fraction of the peak ELF-MF generated E-Fields was delivered at the vestibular sensor level, reinforcing the fact that the stimulation's strength at 20 Hz was below the postural threshold. While it is difficult to precisely assess the *in-situ* E-Fields levels generated at the other frequencies for both AC and ELF-MF, the important fact is that there is no record of postural modulations for both stimulation modalities. Once again, this steers to the time-varying characteristics of these stimulations.

The vestibular information involved in postural control is integrated into the vestibular nuclei within specific vestibular-only neurons projecting to the spinal cord, the vestibulo-cerebellum, the thalamus, and the cortex (52). This is through this integrative process that a potential stimulation frequency effect should be considered.

Although a given E-Field strength indifferently impacts canals and otoliths (29,53,54) the information coming from both subsystems does not seem to be equally integrated within these specific vestibular-only neurons. Indeed, as stimulation frequency increases, the weight of the otolithic input raises, whereas the weight of canalithic input decreases (55). Hence, our high stimulation frequencies would increase otolithic weight and decrease canalithic contribution. Since postural behavioral responses due to vestibular electrical stimulations are thought to mainly result from canalithic activations (for review see (56)), this integrative weighting mechanism could be a reason for the absence of postural modulations with both our ELF-MF and AC stimulations.

As mentioned earlier, for our ELF-MF stimulations, the utricle was potentially the most modulated structure due to E-Field orientation. Interestingly, the utricle is divided mostly

in half by a striola, on each side of which the vestibular hair cells are symmetrically polarized such that electrical stimulations excite one half while inhibiting the other (29,57). Consequently, for a homogenous E-Field stimulation over the entire utricle, little net vestibular signals would be generated and integrated, possibly leading to lower utricular effects (58).

Finally, it is hypothesized that for the biomechanical system to work efficiently, only frequencies required to control task-specific muscle physiology are used (59). Data show that leg muscles only respond to frequencies below 20 Hz, indicating that vestibular inputs above this frequency could be biomechanically low pass filtered at the muscle level (59–61). In the context of our study, this would imply that the biomechanical low pass filtering could have lowered the impact of vestibular stimulations on postural sway.

In summary within the postural control context, the use of high frequencies in both ELF-MF and AC stimulations limited sway responses by i) promoting otolithic activation over the canalithic system, dampening if not inhibiting the emergence of a net oriented head acceleration signal due to cross-striolar inhibition mechanisms and ii) being low pass filtered by the neuromuscular system.

The absence of postural response would therefore not reflect an absence of effect on the vestibular system but rather an absence of functional translation to postural control outcomes.

In that regard, we are proposing to discuss the sensitivity of the vestibular system through a look at pathways mediating quick three neurons arc reflexes such as the vestibulo-ocular and vestibulospinal reflexes (20). In this perspective, mean DC stimulations as low as 0.1 mA have been reported to trigger reflexive eye movement in healthy participants (25). Once again, considering the linear relationship between the current's intensity and the E-Field (46), 0.1 mA translates to 0.02 V/m at the vestibular system.

In this case, all ELF-MF generated E-Fields (Table 3-2) are now all above the reflexive vestibular threshold. Furthermore, Forbes et al. (62), recording human neck motoneuron activity, showed that 300 Hz AC stimulations modulate canalithic activity. This not only

highlights their sensitivity to such high frequencies but also that their activation translates into myogenic reflexive activity through less integrated vestibulospinal pathways (62). Moreover, otolithic hair cells phase lock with frequencies above 2000 Hz (63). Therefore, from a vestibulo-reflexive pathway standpoint, our stimulations' intensities were high enough to modulate vestibular activity and our stimulations' frequencies were not a limiting parameter.

Altogether, our stimulations' frequencies stand out as the main limiting postural factor in our study. Taken together with our previous studies (21,22), this work suggests that powerline-frequency vestibular specific ELF-MF stimulations cannot have functional effects on postural outcomes. Yet, vestibular reflexes are sensitive to both higher stimulation frequencies and lower stimulation intensities. Consequently, further protocols should implement eye-tracking methods (64,65) to study the ELF-MF impact on the vestibulo-ocular reflex. Furthermore, given the field orientation, and the implication of the otolithic activity at higher frequencies, the focus of further investigations could also point to specific otolithic tests such as ocular and cervical vestibular evoked myogenic potentials, both sensitive to E-Fields (66,67).

3.5 Conclusion

We did not find postural modulations with our lateral vestibular ELF-MF stimulations, which is consistent with the finding from our strong entire head top-down ELF-MF stimulation study (22). Based on Lövsund et al. (11), the synaptic threshold is 0.075 V/m peak in the ELF-MF range (3). This threshold is reported to trigger synaptic modulations, potentially leading to adverse effects in the brain (3). However, using *in-situ* E-Fields up to 0.426 V/m at the vestibular level, this study also subjected the CNS structures under the coils to fields well above this synaptic threshold and no sensorimotor effects were found (in line with our previous results (22)). Therefore, these results challenge the idea assuming that neurophysiological similarities between sensory systems would trigger equivalent responses and the possibility to generalize local effects to other parts of the CNS. It also raises the questions of the functional scale at which the E-Fields are to be estimated as well as fields' orientations relative to the structure of concern. Finally, our study highlights the

importance of understanding the mechanisms of neuronal integration. These are critical questions to be addressed to fill the actual knowledge gaps (68) which will surely be useful in the future writing of both ICNIRP guidelines and IEEE-ICES standards.

3.6 References

1. IEEE. IEEE Standard for Safety Levels with Respect to Human Exposure to Electromagnetic Fields, 0–3 kHz. Technology. 2002.
2. ICNIRP. Guidelines for limiting exposure to time-varying electric and magnetic fields (1 Hz to 100 kHz). *Health Phys* [Internet]. 2010;99(6):818–36.
3. IEEE. IEEE Standard for Safety Levels With Respect to Human Exposure to Electric, Magnetic, and Electromagnetic Fields, 0 Hz to 300 GHz. Vol. 2005, IEEE Std C95.1-2005 (Revision of IEEE Std C95.1-1991). 2019. 0_1-238.
4. D'Arsonval A. Dispositifs pour la mesure des courants alternatifs de toutes fréquences. *Compt Rend Soc Biol*. 1896;3,(May 2):450–451.
5. Attwell D. Interaction of low frequency electric fields with the nervous system: the retina as a model system. *Radiat Prot Dosimetry* [Internet]. 2003;106(4):341–8.
6. Juusola M, French AS, Uusitalo RO, Weckström M. Information processing by graded-potential transmission through tonically active synapses. *Trends Neurosci*. 1996;19(7):292–7.
7. Lagnado L, Gomis A, Job C. in the Synaptic Terminal of Retinal Bipolar Cells. *Cell*. 1996;17:957–67.
8. Eatock RA, Songer JE. Vestibular hair cells and afferents: two channels for head motion signals. Vol. 34, *Annual review of neuroscience*. 2011. 501–534 p.
9. Ghosh KK, Haverkamp S, Wassle H. Glutamate receptors in the rod pathway of the mammalian retina. *J Neurosci* [Internet]. 2001;21(21):8636–47.

10. Sadeghi SG, Pyott SJ, Yu Z, Glowatzki E. Glutamatergic Signaling at the Vestibular Hair Cell Calyx Synapse. 2014;34(44):14536–50.
11. Goldberg JM, Wilson VJ, Cullen KE, Angelaki DE, Broussard DM, Buttner-Ennever J, et al. The Vestibular System: A Sixth Sense. *The Vestibular System: A Sixth Sense*. Oxford University Press; 2012. 1–560 p.
12. Eatock RA, Fay RR, Popper AN. *Vertebrate Hair Cells*. 2006.
13. Evans ID, Palmisano S, Loughran SP, Legros A, Croft RJ. Frequency-dependent and montage-based differences in phosphene perception thresholds via transcranial alternating current stimulation. *Bioelectromagnetics*. 2019;
14. Długaiczek J, Gensberger KD, Straka H. Galvanic vestibular stimulation: from basic concepts to clinical applications. *J Neurophysiol*. 2019;121(6):2237–55.
15. Gensberger KD, Kaufmann A-K, Dietrich H, Branoner F, Banchi R, Chagnaud BP, et al. Galvanic Vestibular Stimulation: Cellular Substrates and Response Patterns of Neurons in the Vestibulo-Ocular Network. *J Neurosci [Internet]*. 2016;36(35):9097–110.
16. Aw ST, Todd MJ, Aw GE, Weber KP, Halmagyi GM. Gentamicin vestibulotoxicity impairs human electrically evoked vestibulo-ocular reflex. *Neurology*. 2008;71(22):1776–82.
17. Zenner HP, Reuter G, Hong S, Zimmermann U, Gitter AH. Electrically evoked motile responses of mammalian type I vestibular hair cells. *J Vestib Res*. 1992;2(3):181–91.
18. Norris CH, Miller AJ, Perin P, Holt JC, Guth PS. Mechanisms and effects of transepithelial polarization in the isolated semicircular canal. *Hear Res*. 1998;123(1–2):31–40.
19. Hansson EE, Beckman A, Håkansson A. Effect of vision, proprioception, and the position of the vestibular organ on postural sway. *Acta Otolaryngol*.

- 2010;130(12):1358–63.
20. Cullen KE. The vestibular system: Multimodal integration and encoding of self-motion for motor control. *Trends Neurosci* [Internet]. 2012;35(3):185–96.
 21. Villard S, Allen A, Bouisset N, Corbacio M, Thomas A, Guerraz M, et al. Impact of extremely low-frequency magnetic fields on human postural control. *Exp Brain Res* [Internet]. 2018;0(0):0.
 22. Bouisset N, Villard S, Legros A. Human Postural Control Under High Levels of Extremely Low Frequency Magnetic Fields. *IEEE-Access*. 2020;8(May):1–9.
 23. Hirata A, Takano Y, Fujiwara O, Dovan T, Kavet R. An electric field induced in the retina and brain at threshold magnetic flux density causing magnetophosphenes. *Phys Med Biol*. 2011;56(13):4091–101.
 24. Aw ST, Todd MJ, Halmagyi GM. Latency and initiation of the human vestibuloocular reflex to pulsed galvanic stimulation. *J Neurophysiol* [Internet]. 2006;96(2):925–30.
 25. Severac Cauquil A, Faldon M, Popov K, Day BL, Bronstein AM. Short-latency eye movements evoked by near-threshold galvanic vestibular stimulation. *Exp Brain Res*. 2003;148:414–8.
 26. Laakso I, Kännälä S, Jokela K. Computational dosimetry of induced electric fields during realistic movements in the vicinity of a 3 T MRI scanner. *Phys Med Biol* [Internet]. 2013;58(8):2625–40.
 27. Lövsund P, Öberg PÅ, Nilsson SEG, Reuter T. Magnetophosphenes: a quantitative analysis of thresholds. *Med Biol Eng Comput*. 1980;18(3):326–34.
 28. Yu JF, Lee KC, Wang RH, Chen YS, Fan CC, Peng YC, et al. Anthropometry of external auditory canal by non-contactable measurement. *Appl Ergon* [Internet]. 2015;50:50–5.

29. Fitzpatrick RC, Day BL. Probing the human vestibular system with galvanic stimulation. *J Appl Physiol* [Internet]. 2004;96(6):2301–16.
30. Bresciani J-P, Blouin J, Popov K, Sarlegna F, Bourdin C, Vercher J-L, et al. Vestibular signals contribute to the online control of goal-directed arm movements. *Curr Psycholgy Cogn*. 2002;21:263–80.
31. Wilson TD, Serrador JM, Shoemaker JK. Head position modifies cerebrovascular response to orthostatic stress. *Brain Res*. 2003;961(2):261–8.
32. Rhea CK, Kiefer AW, Haran FJ, Glass SM, Warren WH. A new measure of the CoP trajectory in postural sway: Dynamics of heading change. *Med Eng Phys*. 2014;36(11):1473–9.
33. Chiari L, Rocchi L, Cappello A. Stabilometric parameters are affected by anthropometry and foot placement. *Clin Biomech*. 2002;17(9–10):666–77.
34. Rocchi L, Chiari L, Cappello a. Feature selection of stabilometric parameters based on principal component analysis. *Med Biol Eng Comput*. 2004;42(1):71–9.
35. Séverac Cauquil A, Martinez P, Ouaknine M, Tardy-Gervet MF. Orientation of the body response to galvanic stimulation as a function of the inter-vestibular imbalance. *Exp Brain Res*. 2000;133(4):501–5.
36. Oliveira LF, Simpson DM, Nadal J. Calculation of area of stabilometric signals using principal component analysis. 1996;17:305–12.
37. Fitzgerald JE, Murray A, Elliott C, Birchall JP. Comparison of Body Sway Analysis Techniques: Assessment with Subjects Standing on a Stable Surface. *Acta Otolaryngol* [Internet]. 1994 Jan 8;114(2):115–9.
38. Nagymáté G, Orlovits Z, Kiss RM. Reliability analysis of a sensitive and independent stabilometry parameter set. *PLoS One*. 2018;13(4):1–14.
39. Laakso I, Tanaka S, Koyama S, De Santis V, Hirata A. Inter-subject variability in

- electric fields of motor cortical tDCS. *Brain Stimul* [Internet]. 2015;8(5):906–13.
40. R Core Team. R: A Language and Environment for Statistical Computing. Vol. 0, R Foundation for Statistical Computing Vienna Austria. Vienna, Austria; 2016. p. {ISBN} 3-900051-07-0.
 41. Berens P. CircStat: A MATLAB Toolbox for Circular Statistics. *J Stat Softw* [Internet]. 2009;31(10):1–21. Available from: <http://www.jstatsoft.org/v31/i10/>
 42. Petersen H, Magnusson M, Fransson PA, Johansson R. Vestibular stimulation perturbs human stance also at higher frequencies. *Acta Otolaryngol Suppl* [Internet]. 1995;520 Pt 2:443–6.
 43. Yang Y, Pu F, Lv X, Li S, Li J, Li D, et al. Comparison of Postural Responses to Galvanic Vestibular Stimulation between Pilots and the General Populace. *Biomed Res Int* [Internet]. 2015;2015:1–6.
 44. Reilly JP. Magnetic field excitation of peripheral nerves and the heart: a comparison of thresholds. *Biomed Eng (NY)*. 1991;29(November):571–9.
 45. Baloh RW, Honrubia V, Kerber A. Clinical neurophysiology of the vestibular system. 4th Edition. Contemporary neurology series. New York: Oxford University Press, Inc; 2011. 1–455 p.
 46. Huang Y, Liu AA, Lafon B, Friedman D, Dayan M, Wang X, et al. Measurements and models of electric fields in the in vivo human brain during transcranial electric stimulation. *Elife*. 2017;6:1–27.
 47. Baumann SB, Wozny DR, Kelly SK, Meno FM. The electrical conductivity of human cerebrospinal fluid at body temperature. *IEEE Trans Biomed Eng*. 1997;44(3):220–3.
 48. Antunes a, Glover PM, Li Y, Mian OS, Day BL. Magnetic field effects on the vestibular system: calculation of the pressure on the cupula due to ionic current-induced Lorentz force. *Phys Med Biol* [Internet]. 2012;57(14):4477–87.

49. Radman T, Ramos RL, Brumberg JC, Bikson M. Role of cortical cell type and morphology in subthreshold and suprathreshold uniform electric field stimulation in vitro. *Brain Stimul* [Internet]. 2009;2(4):215-228.e3.
50. Chacko LJ, Schmidbauer DT, Handschuh S, Reka A, Fritscher KD, Raudaschl P, et al. Analysis of Vestibular Labyrinthine Geometry and Variation in the Human Temporal Bone. *Front Neurosci*. 2018;12(February):1–13.
51. Khan S, Chang R. Anatomy of the vestibular system: A review. *NeuroRehabilitation*. 2013;32(3):437–43.
52. Cullen KE. Vestibular processing during natural self-motion: implications for perception and action. *Nat Rev Neurosci* [Internet]. 2019;
53. Curthoys IS, MacDougall HG. What galvanic vestibular stimulation actually activates. *Front Neurol*. 2012;JUL(July):1–5.
54. Day BL, Ramsay E, Welgampola MS, Fitzpatrick RC. The human semicircular canal model of galvanic vestibular stimulation. *Exp Brain Res*. 2011;210(3–4):561–8.
55. Carriot J, Jamali M, Brooks JX, Cullen KE. Integration of Canal and Otolith Inputs by Central Vestibular Neurons Is Subadditive for Both Active and Passive Self-Motion: Implication for Perception. *J Neurosci* [Internet]. 2015;35(8):3555–65.
56. Reynolds RF, Osler CJ. Galvanic vestibular stimulation produces sensations of rotation consistent with activation of semicircular canal afferents. *Front Neurol*. 2012;JUN(June):1–2.
57. Tascioglu AB. Brief Review of Vestibular Anatomy and Its Higher Order Projections. *Neuroanatomy*. 2005;4(4):24–7.
58. Uchino Y, Sato H, Kushiro K, Zakir M, Imagawa M, Ogawa Y, et al. Cross-Striolar and Commissural Inhibition in the Otolith System. *Ann Otol Rhinol Laryngol*. 1999;87(1):162–72.

59. Forbes P a, Dakin CJ, Vardy AN, Happee R, Siegmund GP, Schouten AC, et al. Frequency response of vestibular reflexes in neck, back, and lower limb muscles. *J Neurophysiol* [Internet]. 2013;110(July 2013):1869–81.
60. Dakin CJ, Luu BL, van den Doel K, Inglis JT, Blouin J-S. Frequency-specific modulation of vestibular-evoked sway responses in humans. *J Neurophysiol* [Internet]. 2010;103(2):1048–56.
61. Forbes PA, Siegmund GP, Schouten AC, Blouin J-S. Task, muscle and frequency dependent vestibular control of posture. *Front Integr Neurosci* [Internet]. 2014;8(January):94.
62. Forbes PA, Kwan A, Rasman XBG, Mitchell DE, Cullen XKE, Blouin JS. Neural mechanisms underlying high-frequency vestibulocollic reflexes in humans and monkeys. *J Neurosci*. 2020;40(9):1874–87.
63. Curthoys IS. The new vestibular stimuli: sound and vibration—anatomical, physiological and clinical evidence. *Exp Brain Res* [Internet]. 2017;235(4):957–972.
64. Mackenzie SW, Reynolds RF. Ocular torsion responses to sinusoidal electrical vestibular stimulation. *J Neurosci Methods*. 2018;294:116–21.
65. Otero-Millan J, Roberts DC, Lasker A, Zee DS, Kheradmand A. Knowing what the brain is seeing in three dimensions: A novel, noninvasive, sensitive, accurate, and low-noise technique for measuring ocular torsion. *J Vis* [Internet]. 2015;15(14):1–15.
66. Monobe H, Murofushi T. Vestibular testing by electrical stimulation in patients with unilateral vestibular deafferentation: Galvanic evoked myogenic responses testing versus galvanic body sway testing. *Clin Neurophysiol*. 2004;115(4):807–11.
67. Rosengren SM, Jombik P, Halmagyi GM, Colebatch JG. Galvanic ocular vestibular evoked myogenic potentials provide new insight into vestibulo-ocular reflexes and unilateral vestibular loss. *Clin Neurophysiol* [Internet]. 2009;120(3):569–80.

68. ICNIRP. Gaps in Knowledge Relevant to the “Guidelines for Limiting Exposure to Time-Varying Electric and Magnetic Fields (1 Hz-100 kHz).” *Health Phys.* 2020;118(5):533–42.

4 Vestibular Extremely low frequency magnetic and electric stimulation effects on human subjective visual vertical perception

(Under review in Brain Stimulation)

4.1 Introduction

Electric fields (E-Fields) applied to the human vestibular systems modulate their hair cell activity (1–4). The most well-known and reported means for such vestibular specific E-Fields modulation involves applying direct (DC) or alternating (AC) electric currents to the mastoid processes (for review, see (5)).

Since Michael Faraday's work, we know that variations in magnetic flux density over time (dB/dt measured in T/s) also generate E-Fields and currents in conductors, such as the human body, via magnetic induction. Interestingly, some evidence points that induced E-Fields from time-varying magnetic fields (MF) can modulate the vestibular system activity (6–8).

This high sensitivity of the human vestibular system to small electrical signals is critical from a general public health perspective. Indeed, international recommendations and standards regarding the general public and workers' exposure to so called extremely low-frequency magnetic fields (ELF-MF; < 300 Hz) are based on the smallest exposure levels triggering a reliable systematic neurophysiological response documented to date, which refers to magnetophosphenes perception (9,10). Magnetophosphenes are defined as the perception of flickering lights in the peripheral visual field as a consequence of an ELF-MF stimulation (11).

Magnetophosphenes perception is reported to result from the ability of the retinal graded potential cells to detect small *in-situ* E-Fields variations produced by both AC and time-varying MF and transduce them into a visual perception (12). Interestingly, graded potential cells are also found in other sensory systems such as the vestibular system (13). Indeed, the vestibular hair cells are the graded potential cells transducing the mechanical head acceleration outcomes into electric signals carried by the vestibular nerves. Vestibular hair cells are found in the semi-circular canals as well as in the otoliths (composed of

sacculle and utricle), respectively sensing linear and angular head accelerations. The extreme sensitivity of the hair cells makes the vestibular system another likely target of the ELF-MF induced E-Fields.

Previous work from our group (14,15) suggested that both application and orientation of ELF-MF might preferentially target the otolithic subsystems. Particularly, a monaural lateral ELF-MF stimulation at the mastoid level would preferentially expose the utricle (14). Furthermore, with higher frequencies the weight of the otolithic input increases while the weight of the canalithic input decreases (16). Therefore, at powerline frequencies, otolithic information is more likely to be much more predominantly integrated than canalithic inputs. Moreover, a specific utricle assessment, known as ocular vestibular evoked myogenic potentials (oVEMPS) (17,18), shows that utricles are best tuned at 100 Hz as eye muscle responses progressively decrease above and under this frequency (19–21). Interestingly, oVEMPS are still high at 50 Hz (20), indicating that E-Fields at powerline frequency could modulate otolithic function.

As shown in orbital flight research, the otoliths sense the linear-pull of gravity and, therefore, greatly contribute to the assessment of verticality (22). One of the most commonly used spatial orientation tasks is the subjective visual vertical (SVV). The SVV is the measure of the angle between the perceived vertical and the “true” (gravitational) vertical (23). The SVV is multimodal, relying on visual, proprioceptive, and cortical afferences but it is known as primarily linked to the vestibular function (24,25). In fact, the capability of perceiving verticality has been more specifically related to the vestibular otolithic function (26) and utricular activation in particular when the head is held upright (27).

The SVV is sensitive to a variety of vestibular stimulations including DC (28–31). The literature showing SVV modulations with transcranial electric stimulation applied at the mastoid processes is particularly interesting when studying ELF-MF upon the vestibular system because it suggests that induced E-Fields targeting the vestibular organs might indeed generate changes on a vestibular task.

For DC, the effect is well documented as a misperception of SVV toward the anodal electrode (28–31). A meta-analysis of Zink et al. (32) presented the relationship between SVV and ocular rotation (24). It showed that while SVV misperception increases linearly with the stimulation current, the ocular torsion, on the other hand, increases following a negative exponential curve (24). From the model provided in Dalmaijer's work, we can assess that with a 2 mA DC stimulation, about 70% of SVV measurement can be interpreted as originating from ocular torsion. It is therefore likely that an alternating ocular rotation, due to the changing polarity of the time-varying E-Fields, would modulate SVV results.

However, there could be differences in the SVV outcomes between AC and MF stimulations as electrophosphenes and magnetophosphenes differences have been acknowledged for decades (33). Indeed, the head's anatomical structures such as bone, cerebrospinal fluid, and skin could dampen the E-Fields generated by AC (34,35). However, we do not expect such a mechanism with ELF-MF penetrating all structures without impediment. Furthermore, electrical vestibular stimulations globally impact the entire system (5,36,37) whereas a monaural lateral ELF-MF could be more utricular specific (14). Therefore, we suggest that compared to AC, lateral monaural ELF-MF stimulations will more specifically affect the utricular system. Thus, we focused on the perception of verticality as a biomarker of the utricular performance and we compared the effects of both AC and ELF-MF vestibular stimulations, expecting to find greater modulation of verticality perception with the latter.

4.2 Methods

4.2.1 Participants

Thirty-three (33) participants (10 males, 24.6 ± 4 years) took part in the experiment. We excluded participants with any history of vestibular-related pathology, chronic illnesses, neurological diseases affecting normal body movements, and prone to seizures. We also ruled out people self-reporting permanent metal devices above the neck or using recreational drugs. Finally, we asked our participants to abstain from alcohol and caffeine intake for 24 hours before the experiment. This protocol was approved by Western

University's Ethics Board for Health Science Research Involving Human Subjects (protocol #109161).

4.2.2 Stimulations

We delivered ELF-MF exposures via a custom exposure system consisting of a 176-turn coil (11 turns of 16 layers over a length of 6.2 cm, 6 cm inner diameter, and 22 cm outer diameter) made of 5 mm wide hollow square copper wire cooled by circulating water and powered by an MTS™ Magnetic Resonance Imaging (MRI) gradient amplifier array capable of delivering up to 200 A_{rms} at ± 345V (MTS Automation, Horsham, PA, USA). ELF-MF exposure was delivered using a single-coil centered at the level of the left mastoid process (FIG. 4-1 upper panel).

We produced DC and AC with a transcranial current stimulation device (StarStim, Neuroelectronics, Spain) and the NIC software (Neuroelectronics Instrument Controller, version 1.4.1 Rev.2014-12-01) was used to drive the StarStim device via Bluetooth. In both electrical stimulations, a binaural bipolar montage (Anode-Left, Cathode-Right for DC) delivered electric stimulations at the mastoid processes.

Participants were exposed to i) a control condition (CTRL) with no stimulation, ii) a Direct Current stimulation (DC) at 2 mA used as a positive control, iii) Alternating Current stimulations (sinusoidal, peak ± 2 mA) given at 4 frequencies (20 Hz, 60 Hz, 120 Hz, and 160 Hz), and iv) alternating sinusoidal ELF-MF stimulations at the same frequencies.

As described by the following equation derived from Maxwell's third law:

$$\mathbf{E} = \frac{r}{2} \frac{dB}{dt} = \pi r f B$$

where E represents the induced E-Fields, r the radius of the Faraday's loop encompassing a homogeneous alternating MF of flux density B, and frequency f, the intensity of the stimulation is linearly proportional to the frequency of stimulation. To compare similar intensity AC stimulations to ELF-MF stimulations, we decreased the flux density proportionally to the stimulation frequency to keep a constant dB/dt level (chosen to be 12.3 T.s⁻¹) across frequencies. Table 4-1 summarizes the intensity levels reached at 3 cm from the casing of the coil where the vestibular system should be located (38).

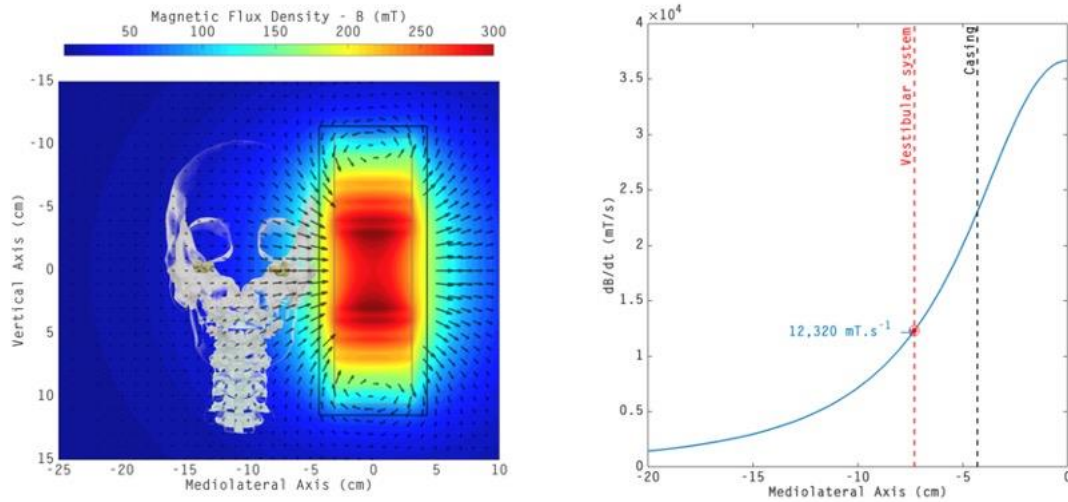


Figure 4-1 Magnetic flux density distribution around the exposure device for a 20Hz stimulation. On the left panel, the black lines show the outer boundaries casing, and the grey lines show the outer boundaries of the solenoid. The vestibular system (represented as the two yellow structures into the skull) lays approximately 3 cm from the casing of the coil. The right panel shows the dB/dt values along the Mediolateral axis at the level of the vestibular level. The dashed line represents the position of the coil casing (black) and the vestibular system (red) along the mediolateral axis.

For both ELF-MF and AC stimulations, we chose the frequencies following the subsequent rationale. As stated in the introduction, otoliths are best-tuned at 100 Hz, and responses progressively decline under and above this value (19–21). Therefore, we opted to investigate two frequencies above and two frequencies below 100 Hz. The main goal of this study is to study responses at 60 Hz (i.e. the powerline frequency in North America). Also, we chose 20 Hz since AC stimulations up to such frequency generate ocular torsions (39). Finally, we kept both 120 and 160 Hz since otolithic responses drop dramatically at 200 Hz (20).

Table 4-1 Alternating magnetic field intensity (in rms) expressed in mT and $T.s^{-1}$ at 3 cm from the casing of the coil for the four frequency conditions. We intentionally decreased the level of flux density to keep a stable dB/dt across frequency conditions.

	20 Hz	60 Hz	120 Hz	160 Hz
Intensity				
dB/dt ($\text{T}\cdot\text{s}^{-1}$)	12.3	12.3	12.3	12.3
Flux density B (mT)	98.0	32.8	16.4	12.3

4.2.3 Procedure

After giving written informed consent, we equipped the participants with the electric stimulation device. We saturated the circular 25 cm² Ag/AgCl electrodes (StarStim, Neuroelectronics, Spain) with 8 mL of saline solution to provide proper conduction between the electrodes and the skin. We then secured the electrodes using the StarStim exposure cap and tape. To ensure appropriate stimulations, we maintained electrodes' impedances strictly below 10 k Ω throughout the experiment following the manufacturer's recommendations. Before starting the testing, we exposed the participants to 5 seconds DC (2 mA) and AC (peak \pm 2 mA at 20 Hz) exposures while standing feet together, arms by their side, and eyes closed. This was done i) as familiarization samples and ii) to make sure that DC made participants sway towards the anodal side (for review (5)).

We asked the participants to sit on a sturdy stool during the time of the experiment. To avoid any environmental visual bias, we asked the participants to look through an open cone to a monitor displaying a dotted white line over a black background oriented towards the left with a random angle bounded between -25° and -20° . Participants' eyes were 43 cm away from the screen displaying a 15 cm long dotted line, representing a visual angle of 23° . We asked the participants to use the wheel of a mouse to control the angle of this white line and align it with what they perceived to be the gravitational vertical. We instructed the participants to press the left button of the mouse to validate the measurement and record the final angle of the line when they reached the final alignment. They performed two consecutive measurements during one 30-s stimulation and repeated each stimulation twice for a total of 20 stimulations. One-minute rest periods were given between trials to avoid participant fatigue and dissipate the stimulation effects in between blocks. A second investigator, blinded to the type of stimulation, was present at all times, to position the participants correctly at the beginning of each trial and to make sure they maintained the proper positioning throughout the trials. To conceal the noise generated by the coil, subjects wore earplugs throughout the experiment. We presented all conditions in a pseudo-

randomized order, where higher flux density conditions (i.e. four 20Hz) were distributed at an equal time interval from each other to allow the proper cooling time of the coil. We fully randomized all other stimulations.

4.2.4 Data collection and analysis

We collected the final angle of the line after adjustment (SVV), the initial angle of the line before the adjustment, and the adjustment time from the moment the line appeared on the screen to the button-click marking the final adjustment with a custom HTML/javascript program.

To account for the interindividual variability of SVV measurements and the known bias of the initial angle of presentation (40), we averaged the four measurements for each condition and subtracted the averaged SVV of each experimental condition from the CTRL averaged SVV. Thus, we obtained a difference to the CTRL value of the SVV angle that we will describe in the rest of this work as dSVVmean. We calculated the same difference for the standard deviations of the SVV over the four repetitions (dSVVstd). This dSVVstd represents how variable an adjustment was compared to the CTRL condition.

Finally, knowing that the initial angle was randomly chosen, to compare the adjustment time for every condition and every participant, we computed an adjustment velocity as the angular distance between the initial angle and the final angle over the adjustment time. This variable was also averaged and presented as a difference to CTRL and called dVel.

The data analysis was performed with python (v.3.7.6) and R (v.3.6.0). A level of significance of $\alpha = 0.05$ was adopted throughout data analysis. dSVV variables were computed by subtracting the averaged SVV from the CTRL averaged SVV. Therefore, the dSVV for CTRL is equal to zero (dSVV CTRL = CTRL minus CTRL). Since the theoretical true vertical would correspond to a normal Gaussian distribution centered on zero, we implemented this distribution to the TRUE vertical condition. As a consequence, the effect of DC stimulations can be tested as DC vs TRUE. A one-tailed one-sample t-test was conducted, with the expectation that dSVVmean for the DC condition to be below 0 (bias towards the anode expected).

We compared 2 stimulation types (AC and MF) and 4 stimulation frequencies (20 Hz, 60 Hz, 120 Hz, and 160 Hz) with 2-ways repeated measure ANOVAs on dSVVmean, dSVVstd, and dVel. We presented the generalized eta squared (η_G^2) as a measure of the effect size as it is recommended for repeated measures ANOVAs (41).

4.3 Results

The analysis of SVV angles shows that 3 participants demonstrated SVV angle $> 2.5^\circ$ in the CTRL conditions. Healthy participants are normally able to align the perceived vertical within ± 2 degrees of the true gravitational vertical [29]. Therefore, we decided to classify these 3 participants as outliers and to remove them from the statistical analysis

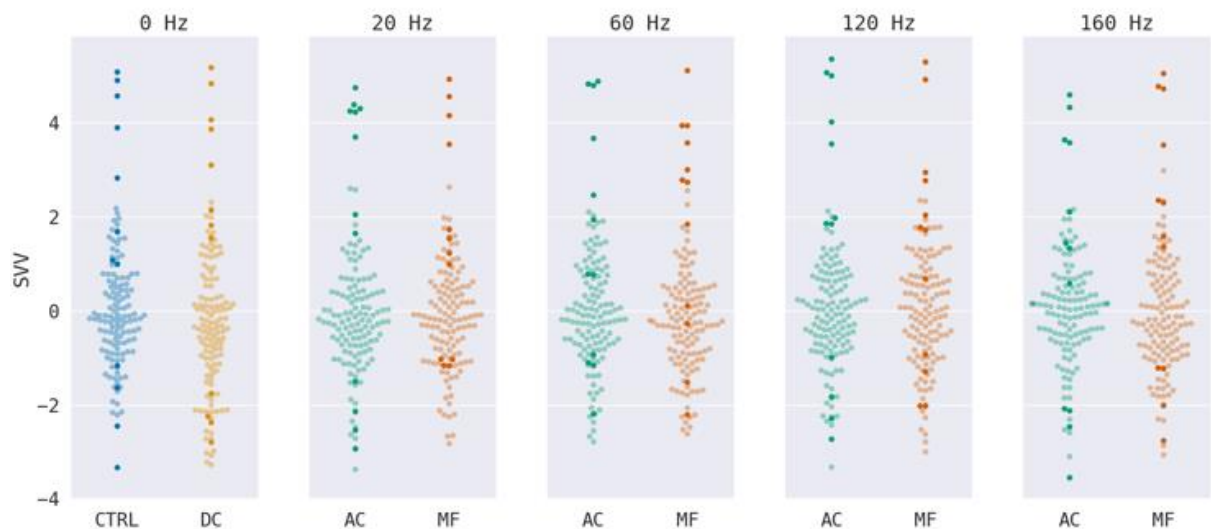


Figure 4-2 Swarm plot representation of SVV angle assessment for all participants overall experimental stimulations (CTRL: Control, DC: Direct Current, AC: Alternating Current, MF: Magnetic Field) by frequency conditions (from CTRL and DC on the left panel to 160 Hz for AC and MF on the right panel). The solid dots represent the data collected for the 3 participants exhibiting SVV angles $> 2.5^\circ$ in the CTRL condition. The shaded dots represent the measurements of SVV kept in the statistical analysis.

The results first consisted of comparing the effect of the DC stimulation on the perception of verticality. FIG. 4-2 shows the large variability among the participants in terms of SVV

angle perception. This variability is smaller when considering dSVV, which represents the difference in degrees between measurements in the CTRL condition and measurements in the experimental condition (i.e. DC, AC, or MF). By comparing these dSVV in the DC vs TRUE conditions, we are testing if the DC condition was significantly lower than a condition with no stimulation. As expected, [45,46], the t-test showed that dSVV for the DC condition was significantly lower than 0 ($t_{29} = -2.0104$, $p = 0.027$, $r^2 = 12\%$) which describes a misperception towards the anodal stimulation on the left side. The mean dSVV for DC was $-0.32^\circ \pm 0.8^\circ$.

FIG. 4-3 presents the $dSVV_{\text{mean}}$, $dSVV_{\text{std}}$, and $dVel$ results for both AC and MF stimulations. Two-way ANOVAs (2 stimulation modalities \times 4 frequencies) for repeated measures indicated no significant main effects of frequency conditions for $dSVV_{\text{mean}}$ ($F_{3,87} = 1.97$, $p = 0.12$), $dSVV_{\text{std}}$ ($F_{3,87} = 0.31$, $p = 0.82$), and $dVel$ ($F_{3,87} = 1.70$, $p = 0.18$).

Similarly, no significant stimulation main effect was found for $dSVV_{\text{mean}}$ ($F_{1,29} = 0.6$, $p = 0.45$). However, $dSVV_{\text{std}}$ ($F_{1,29} = 7.86$, $p = 0.009$, $\eta^2 = 2\%$) showed that while the variability of SVV is lower than CTRL for AC exposure, it is however greater than CTRL in the instance of MF stimulation (FIG. 4-3). Similarly, $dVel$ ($F_{1,29} = 9.04$, $p = 0.005$, $\eta^2 = 2\%$) showed that velocities to adjust the SVV measurement were greater in AC conditions than in the MF conditions. Finally, no interaction effects were found for $dSVV_{\text{mean}}$ ($F_{3,87} = 1.87$, $p = 0.14$), $dSVV_{\text{std}}$: ($F_{3,87} = 0.76$, $p = 0.52$) and for $dVel$: ($F_{3,87} = 0.27$, $p = 0.84$).

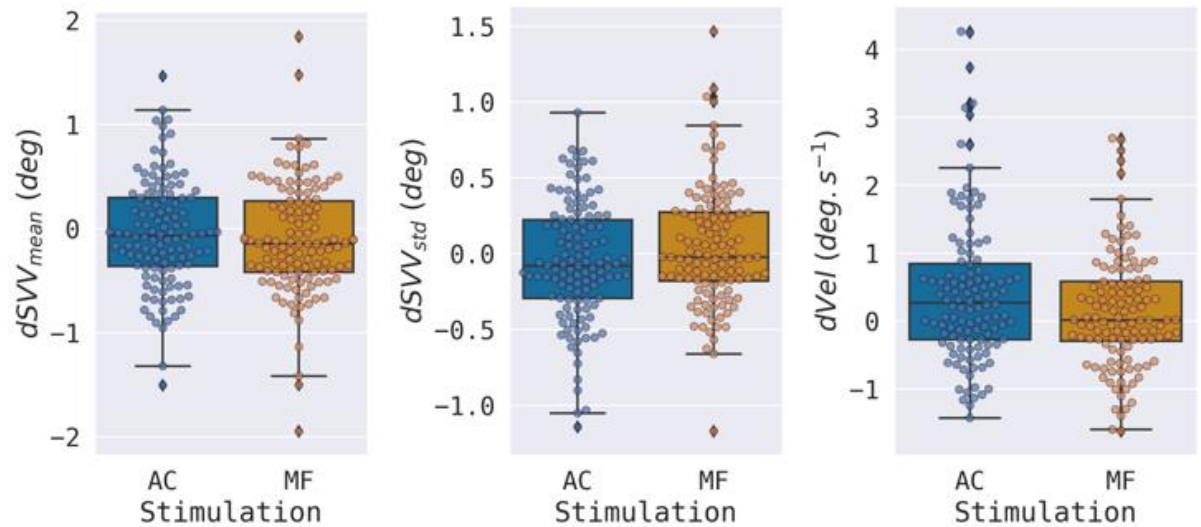


Figure 4-3 Boxplots representation of $dSVV_{mean}$, $dSVV_{std}$, and $dVel$ distributions comparing AC and MF stimulations. Individual measurements are presented as swarm plot over each boxplot. Only $dSVV_{std}$ and $dVel$ yielded significant differences between AC and MF.

4.4 Discussion

The current international standards and guidelines consider the impact of ELF-MF on neural networks through the paradigm of phosphene perception (42,43). The actual hypothesis regarding phosphenes is that they result from membrane potential modulations of graded potential retinal cells, impacting in cascade the continuous release of neurotransmitters through their ribbon synapses (12). Yet, the International Commission on Non-Ionizing Radiation Protection (ICNIRP) acknowledges uncertainties regarding how electrostimulation impacts human neurophysiology in the ELF-MF frequency range (44). In this perspective, this work was intended to shed light on some knowledge gap, by investigating other graded potential cells located in the vestibular system.

Considering previous work from our group (14,15), we argued that ELF-MF stimulations applied laterally would more specifically trigger the vestibular hair cells within the utricular subsystem. Hence, the first aim here was to study the potential acute effect of vestibular exposure to a power-frequency MF by investigating the SVV in which the utricle

plays a significant role (27). Furthermore, given potential differences between AC and MF, the second aim of this work was to compare the results from both stimulations.

We hypothesized more important modulations in SVV outcomes with MF than with AC given that i) the intensity related to AC is potentially dampened by the head's anatomical structures but not with MF and ii) the ELF-MF stimulations would more preferentially affect the utricular system than AC. Finally, given that the utricles are best-tuned at 100 Hz and eye muscle responses progressively decrease above and under such frequency (19–21), we also expected a frequency effect with our stimulations.

It is well known that DC impacts the SVV towards the anodal side of the stimulation (45,46). This was also the case in our study. Also, given that both the SVV dotted line appearance and the anodal side were oriented towards the left, DC shortened the time to set the SVV score.

Considering previously reported results, with the intensity used in this work, our DC result was likely due to ocular torsion (24,30,31,47–49). Thus, this validated DC as a positive control.

With AC, the current's polarity switches with frequency, and torsional eye movements should therefore be modulated accordingly. The same rationale applies to our ELF-MF stimulations given their sinusoidal nature. Therefore, we didn't expect a tonic response with a stable ocular torsion generating a constant SVV error towards the anodal side, but rather an increased variability in the SVV results.

Even though no effect was found on $dSVV_{\text{mean}}$, results show that ELF-MF performance was more variable compared to performance under AC, and it took more time for the participants to achieve verticality adjustments with the former than with the latter. This means that in order to get equivalent results, the adjustment performance was less optimal with ELF-MF than with AC. Therefore, we need to reflect on whether the E-Fields intensity was indeed higher in ELF-MF than with AC at the utricular level.

Depending on the frequency, the information coming from both vestibular subsystems does not seem to be equally integrated within the vestibular nuclei. Indeed, Carriot et al. (16)

showed that, as stimulation frequencies increases, more otolithic inputs than canalithic inputs are integrated. Given that our frequency range started at 20 Hz, which is considered as the upper physiological frequency limit for the vestibular system (50,51), the otolithic information was likely more integrated than the canalithic ones.

The electrical AC stimulations applied in this study used a classical binaural bipolar montage. Thomas et al. (52) showed that such a montage with a 1 mA stimulation intensity generates a maximum of 0.08 V/m at the vestibular system. However, such maximum E-Fields value is generated at the canalithic level whereas, due to the more resistive otolithic structures, less signal is spawned at the otolithic subsystem (52). Based on Thomas et al.'s results, our 2 mA AC stimulations would have produced a maximum of 0.04 V/m peak at the otoliths (52).

The ELF-MF stimulations used here were scaled to target a constant dB/dt value in the order of $12.3 \text{ T}\cdot\text{s}^{-1}_{\text{rms}}$. As in previous work from our group (14,15), the in-situ E-Fields at the vestibular level were estimated using the equation described in the methods. Considering a radius of 6 mm encompassing the entire vestibular system (53), the utricular E-Fields values can be estimated at 0.053 V/m peak (14).

Since E-Field values as low as 0.008 V/m are reported to be sufficient to start triggering ocular torsions (49), it confirms that both our AC and MF stimulations were sufficiently strong to trigger vestibular-related rotational eye responses.

Interestingly, the estimated E-Field level for ELF-MF was a little higher than the AC values at the utricle level (0.053 V/m peak vs 0.04 V/m peak) and could serve as a reason for the discrepancies found in our results.

However, only the E-Fields colinear to the neuronal cell body have a maximum neurophysiological impact (54). Therefore, depending on the orientation of the E-Fields relative to the hair cells, only a fraction of the absolute induced E-Fields values could have modulated them. Thus, the maximum peak values cannot by themselves explain our results and we need information relative to the E-Fields' orientation for both stimulation modalities.

Electric stimulation modalities are applied to the skin at the skull level (55). Given volume conduction as well as the anisotropic and non-homogeneous properties of the head's anatomical structures (56), the currents diffuse following the path of least resistance (35). Depending on how the local electric vector fields align with the utricular hair cells, the relevant E-Fields strength could have been much lower than the 0.04 V/m peak reported above. On the contrary, the ELF-MF goes through the anatomical structures without any hindrance, and the induced E-Fields are always orthogonal to the magnetic fields, constraining the currents in specific directions. In that regard, we have previously argued that lateral MF stimulations relative to the vestibular system induce E-Fields aligned with the utricular hair cells (14). Therefore, with MF, the utricle could have received all or close to 0.053 V/m peak E-Fields strength.

Furthermore, the vestibular montages used between the two stimulation modalities (AC and MF) differed and should also be considered. A binaural bipolar montage was used with AC. This implies that the vestibular systems on both sides of the head are modulated in antiphase, meaning that while one system is excited, the other is inhibited. This induces a greater firing rate difference between the two systems which the brain interprets as a greater acceleration of the head in one direction. On the contrary, a left monaural lateral stimulation was used with the ELF-MF stimulations. Therefore, in this case, the firing rate in the right ear remained constant throughout the trials. For a given stimulation intensity, the binaural montages usually induce larger vestibular outcomes. Hence, in order for the SVV results to be more variable with ELF-MF would mean that the monaural lateral MF stimulation, in this case, induced a greater difference between the two vestibular systems than the binaural bipolar montage used with AC. This could only be the case if the E-Fields strength at the utricular level was much higher with ELF-MF than with AC since higher stimulation intensity inflates vestibular outcome modulations (57).

In summary, stronger and more utricular-specific ELF-MF stimulations could explain the dSVVstd difference with the AC stimulation modalities

However, caution is still needed. Indeed, if ELF-MF more specifically targeted the utricles with higher E-Field levels, greater effect size would have been expected, which is only in the order of 2 % of the total variance here. Furthermore, since the utricular-specific Ovemps

responses are frequency-dependent (19–21), an effect resulting from a more important utricular modulation with ELF-MF should also lead to a frequency impact, which was not seen.

According to Dalmaijer et al. (24), with E-Fields levels tested in the current study, modulation of SVV perception should mostly result from eye torsion. However, torsional eye movement amplitudes decrease as stimulation frequencies increases (less than 0.2° at 20 Hz) (39). Therefore, a 20 Hz stimulation may result in too small ocular torsions to be able to modulate SVV. Moreover, it is also suggested that, with E-Fields, torsional eye movements are mostly related to canalithic activity (39,52,58), and that higher frequencies such as 20 Hz are known to promote otolithic instead of canalithic activation (16). All these aspects are justifying the possible contribution of an alternative explanation supporting our results.

The modulation of cortical regions activated by the ELF-MF signal cannot be excluded. Indeed, the position of the coil system is compatible with a potential direct effect on the temporoparietal cortices (FIG. 4-1 upper panel). According to the model (FIG. 4-1 lower panel), the dB/dt levels at these cortical regions are estimated at $20 \text{ T}\cdot\text{s}^{-1}_{\text{rms}}$ or higher.

Interestingly these cortical areas are implicated in spatial cognition, including the perception of spatial orientation (59). Otero-Millan et al. (60) found SVV perception alterations with transcranial magnetic stimulations, showing SVV bias shift uncorrelated with torsional eye movements. Moreover, patients with temporoparietal lesions also present SVV biases (61). Therefore, the ELF-MF stimulations could have impacted the higher levels of multisensory processing of vestibular, somatosensory, and visual information within those brain areas (50,62) leading to modulations of SVV outcomes.

Furthermore, temporoparietal brain areas are also involved in subjective mental time perception (63), especially during tasks implicating the vestibular system (64). This is consistent with the longer SVV adjustment time we found with MF than with AC. The fact that the MF-induced E-Fields were not aligned with the cortical neuronal structures limits the potential impact on the temporoparietal cortices, which may explain the small effect sizes accounting only for 2% of the total variance for both dSVVstd, and dVel.

In summary, SVV performance was less optimal with MF than with AC. This result could be due to a greater utricular activation with ELF-MF than with AC. However, given the lack of frequency effect expected for such stimulations, the position of our MF stimulation coil, and considering the dB/dt values generated at these sites, we cannot exclude temporoparietal cortices modulations with ELF-MF.

Further ELF-MF investigations should focus on vestibular biomarkers more specifically sensitive to E-Fields, like otolithic-specific assessments such as ocular (65–67) and cervical (68–70) vestibular evoked myogenic potentials. Lower stimulation frequencies should also be considered and the implementation of new eye-tracking techniques (39,71) could help confirm and better understand the possible eye impact reported here. Finally, targeting the temporoparietal cortices with ELF-MF stimulations would also help dissociate and disentangle the origins of the effects found herein.

4.5 Conclusion

Our results further shed light on the differential impacts between similar non-invasive AC and MF vestibular stimulations applied at the mastoid process. Variations in E-Fields orientation in space relative to neuronal anatomical structures modulate the E-Fields strength and thus the impact on such structures. These bricks of new knowledge are of paramount importance to expand the scientific bases at the foundation of international guidelines and standards, to broaden the protection of workers and the general public alike.

4.6 References

1. Zenner HP, Reuter G, Hong S, Zimmermann U, Gitter AH. Electrically evoked motile responses of mammalian type I vestibular hair cells. *J Vestib Res.* 1992;2(3):181–91.
2. Norris CH, Miller AJ, Perin P, Holt JC, Guth PS. Mechanisms and effects of transepithelial polarization in the isolated semicircular canal. *Hear Res.* 1998;123(1–2):31–40.
3. Gensberger KD, Kaufmann A-K, Dietrich H, Branoner F, Banchi R, Chagnaud BP, et al. Galvanic Vestibular Stimulation: Cellular Substrates and Response Patterns of

- Neurons in the Vestibulo-Ocular Network. *J Neurosci* [Internet]. 2016;36(35):9097–110.
4. Długaiczek J, Gensberger KD, Straka H. Galvanic vestibular stimulation: from basic concepts to clinical applications. *J Neurophysiol*. 2019;121(6):2237–55.
 5. Fitzpatrick RC, Day BL. Probing the human vestibular system with galvanic stimulation. *J Appl Physiol* [Internet]. 2004;96(6):2301–16.
 6. Van Nierop LE, Slottje P, Kingma H, Kromhout H. MRI-related static magnetic stray fields and postural body sway: A double-blind randomized crossover study. *Magn Reson Med*. 2013;70(1):232–40.
 7. Schaap K, Portengen L, Kromhout H. Exposure to MRI-related magnetic fields and vertigo in MRI workers. *Occup Environ Med*. 2015;161–6.
 8. Laakso I, Kännälä S, Jokela K. Computational dosimetry of induced electric fields during realistic movements in the vicinity of a 3 T MRI scanner. *Phys Med Biol* [Internet]. 2013;58(8):2625–40.
 9. IEEE. C95.6. IEEE standard for safety levels with respect to human exposure to electromagnetic fields, 0-3kHz. IEEE: New York. New York: The institute of Electrical and Electronics Engineers, Inc.; 2002.
 10. International Commission on Non-Ionizing Radiation Protection, ICNIRP, International Commission on Non-Ionizing Radiation Protection. Guidelines for limiting exposure to time-varying electric and magnetic fields (1 Hz to 100 kHz). *Health Phys*. 2010 Dec;99(6):818–36.
 11. Lövsund P, Öberg P, Nilsson SEG. Quantitative determination of thresholds of magnetophosphenes. *Radio Sci*. 1979;14(6 S):199–200.
 12. Attwell D. Interaction of low frequency electric fields with the nervous system: the retina as a model system. *Radiat Prot Dosimetry* [Internet]. 2003;106(4):341–8.
 13. Juusola M, French AS, Uusitalo RO, Weckström M. Information processing by

- graded-potential transmission through tonically active synapses. *Trends Neurosci.* 1996;19(7):292–7.
14. Bouisset N, Villard S, Legros A. Human Postural Responses to High Vestibular Specific Extremely Low-Frequency Magnetic Stimulations. *IEEE Access* [Internet]. 2020;8:165387–95.
 15. Bouisset N, Villard S, Legros A. Human Postural Control under High Levels of Extremely Low Frequency Magnetic Fields. *IEEE Access.* 2020;
 16. Carriot J, Jamali M, Brooks JX, Cullen KE. Integration of Canal and Otolith Inputs by Central Vestibular Neurons Is Subadditive for Both Active and Passive Self-Motion: Implication for Perception. *J Neurosci* [Internet]. 2015;35(8):3555–65.
 17. Curthoys IS, Grant JW, Burgess AM, Pastras CJ, Brown DJ, Manzari L. Otolithic receptor mechanisms for vestibular-evoked myogenic potentials: A review. *Front Neurol.* 2018;9(MAY):z.
 18. Curthoys IS. A critical review of the neurophysiological evidence underlying clinical vestibular testing using sound, vibration and galvanic stimuli. *Clin Neurophysiol* [Internet]. 2010;121(2):132–44.
 19. Todd NPM, Rosengren SM, Colebatch JG. A utricular origin of frequency tuning to low-frequency vibration in the human vestibular system? *Neurosci Lett.* 2009;451(3):175–80.
 20. Todd NPM, Rosengren SM, Colebatch JG. Tuning and sensitivity of the human vestibular system to low-frequency vibration. *Neurosci Lett.* 2008;444(1):36–41.
 21. Zhang AS, Govender S, Colebatch JG. Tuning of the ocular vestibular evoked myogenic potential to bone-conducted sound stimulation. *J Appl Physiol* [Internet]. 2012;112(8):1279–90.
 22. Oman C. Spatial orientation and navigation in microgravity. *Spat Process Navig Imag Percept.* 2007;209–47.

23. Akin FW, Murnane O. Subjective Visual Vertical Test. *Semin Hear.* 2009 Nov;30(04):281–6.
24. Dalmaijer E. Beyond the Vestibulo-Ocular Reflex: Vestibular Input is Processed Centrally to Achieve Visual Stability. *Vision.* 2018;2(2):16.
25. Friedmann G. The judgement of the visual vertical and horizontal with peripheral and central vestibular lesions. *Brain.* 1970;93(2):313–28.
26. Kumagami H, Sainoo Y, Fujiyama D, Baba A, Oku R, Takasaki K, et al. Subjective Visual Vertical in Acute Attacks of Ménière’s Disease. *Otol Neurotol.* 2009 Feb;30(2):206–9.
27. Jaeger R, Kondrachuk A V., Haslwanter T. The distribution of otolith polarization vectors in mammals: Comparison between model predictions and single cell recordings. *Hear Res.* 2008;239(1–2):12–9.
28. Mars F, Popov K, Vercher JL. Supramodal effects of galvanic vestibular stimulation on the subjective vertical. *Neuroreport.* 2001;12(13):2991–4.
29. Volkening K, Bergmann J, Keller I, Wuehr M, Müller F, Jahn K. Verticality perception during and after galvanic vestibular stimulation. *Neurosci Lett [Internet].* 2014;581:75–9.
30. Zink R, Steddin S, Weiss A, Brandt T, Dieterich M. Galvanic vestibular stimulation in humans : effects on otolith function in roll. *Neurosci Lett.* 1997;232(1):171–4.
31. Zink R, Bucher SF, Weiss A, Brandt T, Dieterich M. Effects of galvanic vestibular stimulation on otolithic and semicircular canal eye movements and perceived vertical. *Electroencephalogr Clin Neurophysiol.* 1998;107(3):200–5.
32. Zink R, Bucher SF, Weiss A, Brandt T, Dieterich M. Effects of galvanic vestibular stimulation on otolithic and semicircular canal eye movements and perceived vertical. *Electroencephalogr Clin Neurophysiol.* 1998;107(3):200–5.
33. Lövsund P, Oberg PA, Nilsson SEG. Magneto- and electrophosphenes : a

- comparative study. *Med Biol Eng Comput.* 1980;758–64.
34. Srinivasan R, Tucker DM, Murias M. Estimating the spatial Nyquist of the human EEG. *Behav Res Methods, Instruments, Comput.* 1998;30(1):8–19.
 35. Laakso I, Hirata A. Computational analysis shows why transcranial alternating current stimulation induces retinal phosphenes. *J Neural Eng.* 2013;10(2008):046009.
 36. Day BL, Ramsay E, Welgampola MS, Fitzpatrick RC. The human semicircular canal model of galvanic vestibular stimulation. *Exp Brain Res.* 2011;210(3–4):561–8.
 37. Kwan A, Forbes PA, Mitchell DE, Blouin J-S, Cullen KE. Neural substrates, dynamics and thresholds of galvanic vestibular stimulation in the behaving primate. *Nat Commun [Internet].* 2019;10(1):1904.
 38. Yu JF, Lee KC, Wang RH, Chen YS, Fan CC, Peng YC, et al. Anthropometry of external auditory canal by non-contactable measurement. *Appl Ergon [Internet].* 2015;50:50–5.
 39. Mackenzie SW, Reynolds RF. Ocular torsion responses to sinusoidal electrical vestibular stimulation. *J Neurosci Methods.* 2018;294:116–21.
 40. Pagarkar W, Bamiou D-E, Ridout D, Luxon LM. Subjective Visual Vertical and Horizontal. *Arch Otolaryngol Neck Surg.* 2013;134(4):394–401.
 41. Bakeman R. Recommended effect size statistics for repeated measures designs. *Behav Res Methods.* 2005 Aug;37(3):379–84.
 42. IEEE. IEEE Standard for Safety Levels With Respect to Human Exposure to Electric, Magnetic, and Electromagnetic Fields, 0 Hz to 300 GHz. Vol. 2005, IEEE Std C95.1-2005 (Revision of IEEE Std C95.1-1991). 2019. 0_1-238.
 43. ICNIRP. Guidelines for limiting exposure to time-varying electric and magnetic fields (1 Hz to 100 kHz). *Health Phys [Internet].* 2010;99(6):818–36.

44. ICNIRP. Gaps in Knowledge Relevant to the “Guidelines for Limiting Exposure to Time-Varying Electric and Magnetic Fields (1 Hz-100 kHz).” *Health Phys.* 2020;118(5):533–42.
45. Mars F, Popov K, Vercher JL. Supramodal effects of galvanic vestibular stimulation on the subjective vertical. *Neuroreport.* 2001;12(13):2991–4.
46. Volkening K, Bergmann J, Keller I, Wuehr M, Müller F, Jahn K. Verticality perception during and after galvanic vestibular stimulation. *Neurosci Lett.* 2014 Oct;581:75–9.
47. Watson SRD, Brizuela AE, Curthoys IS, Colebatch JG, MacDougall HG, Halmagyi GM. Maintained ocular torsion produced by bilateral and unilateral galvanic (DC) vestibular stimulation in humans. *Exp Brain Res.* 1998;122(4):453–8.
48. Schneider E, Glasauer CAS, Dieterich M. Central processing of human ocular torsion analyzed by galvanic vestibular stimulation. *Neuroreport.* 2000;11(7):1559–63.
49. Severac Cauquil A, Faldon M, Popov K, Day BL, Bronstein AM. Short-latency eye movements evoked by near-threshold galvanic vestibular stimulation. *Exp Brain Res.* 2003;148:414–8.
50. Cullen KE. Vestibular processing during natural self-motion: implications for perception and action. *Nat Rev Neurosci* [Internet]. 2019.
51. Goldberg JM, Wilson VJ, Cullen KE, Angelaki DE, Broussard DM, Buttner-Ennever J, et al. *The Vestibular System: A Sixth Sense.* The Vestibular System: A Sixth Sense. Oxford University Press; 2012. 1–560 p.
52. Thomas C, Truong D, Clark TK, Datta A. Understanding current flow in Galvanic Vestibular Stimulation: A Computational Study*. In: 2020 42nd Annual International Conference of the IEEE Engineering in Medicine & Biology Society (EMBC) [Internet]. Montreal, QC, Canada,: IEEE; 2020. p. 2442–6.
53. Baloh RW, Honrubia V, Kerber A. Clinical neurophysiology of the vestibular

system. 4th Edition. Contemporary neurology series. New York: Oxford University Press, Inc; 2011. 1–455 p.

54. Radman T, Ramos RL, Brumberg JC, Bikson M. Role of cortical cell type and morphology in subthreshold and suprathreshold uniform electric field stimulation in vitro. *Brain Stimul* [Internet]. 2009;2(4):215-228.e3.
55. Utz KS, Dimova V, Oppenländer K, Kerkhoff G. Electrified minds: Transcranial direct current stimulation (tDCS) and Galvanic Vestibular Stimulation (GVS) as methods of non-invasive brain stimulation in neuropsychology-A review of current data and future implications. *Neuropsychologia*. 2010;48(10):2789–810.
56. Nunez PL, Srinivasan R. *Electric Fields of the Brain: The neurophysics of EEG*. 2006.
57. Aw ST, Todd MJ, Halmagyi GM. Latency and initiation of the human vestibuloocular reflex to pulsed galvanic stimulation. *J Neurophysiol* [Internet]. 2006;96(2):925–30.
58. Reynolds RF, Osler CJ. Galvanic vestibular stimulation produces sensations of rotation consistent with activation of semicircular canal afferents. *Front Neurol*. 2012;JUN(June):1–2.
59. Hitier M, Besnard S, Smith PF. Vestibular pathways involved in cognition. *Front Integr Neurosci* [Internet]. 2014;8(July):59.
60. Otero-Millan J, Winnick A, Kheradmand A. Exploring the role of temporoparietal cortex in upright perception and the link with torsional eye position. *Front Neurol*. 2018;9(APR).
61. Brandt T, Dieterich M, Danek A. Vestibular cortex lesions affect the perception of verticality. *Ann Neurol*. 1994;35(4):403–12.
62. Angelaki DE, Cullen KE. Vestibular System: The Many Facets of a Multimodal Sense. *Annu Rev Neurosci* [Internet]. 2008;31(1):125–50.

63. Arzy S, Collette S, Ionta S, Fornari E, Blanke O. Subjective mental time: The functional architecture of projecting the self to past and future. *Eur J Neurosci*. 2009;30(10):2009–17.
64. Kaski D, Quadir S, Nigmatullina Y, Malhotra PA, Bronstein AM, Seemungal BM. Temporoparietal encoding of space and time during vestibular-guided orientation. *Brain*. 2016;139(2):392–403.
65. Rosengren SM, Jombik P, Halmagyi GM, Colebatch JG. Galvanic ocular vestibular evoked myogenic potentials provide new insight into vestibulo-ocular reflexes and unilateral vestibular loss. *Clin Neurophysiol*. 2009;120(3):569–80.
66. Rosengren SM, Welgampola MS, Colebatch JG. Vestibular evoked myogenic potentials: Past, present and future. *Clin Neurophysiol [Internet]*. 2010;121(5):636–51.
67. Cheng PW, Chen CC, Wang SJ, Young YH. Acoustic, mechanical and galvanic stimulation modes elicit ocular vestibular-evoked myogenic potentials. *Clin Neurophysiol [Internet]*. 2009;120(10):1841–4.
68. Watson SRD, Fagan P, Colebatch JG. Galvanic stimulation evokes short-latency EMG responses in sternocleidomastoid which are abolished by selective vestibular nerve section. *Electroencephalogr Clin Neurophysiol - Electromyogr Mot Control*. 1998;109(6):471–4.
69. Watson S, Colebatch J. Vestibulocollic reflexes evoked by short-duration galvanic stimulation in man. *J Physiol*. 1998;513 (Pt 2(1998):587–97.
70. Murofushi T, Monobe H, Ochiai A, Ozeki H, T. M, H. M, et al. The site of lesion in “vestibular neuritis”: study by galvanic VEMP. *Neurology [Internet]*. 2003;61(3):417–8.
71. Otero-Millan J, Roberts DC, Lasker A, Zee DS, Kheradmand A. Knowing what the brain is seeing in three dimensions: A novel, noninvasive, sensitive, accurate, and low-noise technique for measuring ocular torsion. *J Vis [Internet]*. 2015;15(14):1–

15.

5 General discussion and conclusion

5.1 General discussion

Extremely Low-Frequency Magnetic Fields (ELF-MF) are ubiquitous in modern societies and raise health and safety concerns for both workers and the general public (1–5). More than four decades of research have amassed a large body of evidence on the impact of ELF-MF on retinal photoreceptors. This research has identified that the well-known phenomenon of magnetophosphenes is thought to result from modulation of the rods' membrane potential (6). Being the most sensitive response to ELF-MF, magnetophosphenes form the basis for the 0.075 V/m peak synaptic threshold (4). This threshold is generalized for the entire ELF frequency range to all of the neurological structures within the central nervous system. Yet, such threshold relies upon a subjective report of a visual perception and accordingly is limited. Guidelines would gain in precision from setting their threshold on more objective measures of ELF-MF's impact on human neurophysiology. However, such objective outcomes are yet to be defined and proven.

The fact that the retinal photoreceptors are graded potential cells is hypothesized as the mechanism for producing phosphenes (6). Interestingly, the vestibular hair cells are also graded potential cells (7,8) and are sensitive to E-Fields (9–11). In addition, when triggered, the vestibular system provides precise motor outputs that can be easily recorded and observed (12,13). Thus, the vestibular system could potentially be an alternative model for setting safe thresholds. This thesis was, therefore, an attempt to investigate whether the vestibular system was indeed a good candidate for such an alternative model.

International guidelines and standards base their ELF-MF threshold on the most sensitive responses to such fields, which currently are phosphenes (1–5). This enables them to set the lowest possible threshold (0.075 V/m peak) to keep both the workers and the public safe from potential adverse effects (1–5). The first step was therefore to figure whether a lower threshold than the currently established synaptic threshold (1–4) could be found with the vestibular system.

In Chapter 1, I attempted to estimate the lowest E-Field threshold triggering a vestibular modulation. Given that we looked at postural control in our two first studies (Chapter 2 and 3), I needed to find a theoretical postural threshold first. This estimation was mainly based on two published papers. In 2015, Yang et al (14), provided evidence showing that only 0.32 mA at the mastoid processes starts producing vestibulospinal outcomes. Additionally, Huang et al.(15) showed that 1 mA at the skull could generate 0.2 V/m at both the cortex level and deeper structures within the brain. Given the information provided in Huang et al.(15), this was thought to be generalizable to the entire brain and, therefore, to the vestibular system as well. Given the linear relationship between the intensity of the current in mA and the induced E-Fields, I estimated a 0.06 V/m vestibulospinal threshold. Interestingly this threshold is already lower than the 0.075 V/m peak synaptic phosphene perception threshold (4). However, the results from Huang et al.(15), may not be directly relevant to the vestibular system. According to the first dosimetry vestibular specific estimation (16), 1 mA at the mastoid processes could, in fact, generate 0.08 V/m at the vestibular system level. Furthermore, given that Severac-Cauquil et al. (13) showed that 0.1 mA applied at the mastoid process triggered vestibulo-ocular outcomes, a more sensitive and precise vestibulomotor threshold could potentially be found as low as 0.008 V/m. Of course, further dosimetry studies will need to be conducted to confirm whether this is actually the case. Nonetheless, the E-Fields sensitivity of the vestibular system was indeed worth studying within the context of the guidelines since, theoretically, vestibular outcomes could be triggered at lower E-Fields levels than the actual phosphene threshold.

However, altogether, the results presented in this thesis provide converging evidence that the vestibular outcomes cannot dethrone the phosphenes so easily. Although, as estimated in Chapter 1, the hair cells could trigger vestibular responses with E-Fields levels under the threshold found within the guidelines (1–5), the translation from a hair cell's potential membrane modulation to an overt measurable vestibular outcome is not straight forward.

For instance, in the context of our behavioural postural control studies (Chapters 2 and 3) no modulations were observed. Yet, in both cases the highest *in-situ* E-Fields at the vestibular system was found at 0.432 V/m in Chapter 3 and at 1 V/m in Chapter 2. Although, being respectively more than fivefold (Chapter 3) and tenfold (Chapters 2) above the guideline's

0.075 V/m peak synaptic threshold (1–5), no objectively measured outcomes were observed in both postural control experiments. On the other hand, we detected a small effect on the perception of verticality with *in-situ* E-Fields estimated at 0.053 V/m peak at the vestibular system (Chapter 4), approximately 30% below the guidelines' 0.075 V/m peak synaptic threshold. This could advocate in favor of SVV as an alternative approach to phosphenes. However, phosphenes are quite a consistent response to ELF-MF stimulations and given the very small effect size found in our last study (Chapter 4), caution is therefore needed before switching from phosphenes to vestibular responses to substantiate guidelines.

Nonetheless, our results question the main basis on which the guidelines are actually set. Indeed, for the full ELF-MF frequency range, the guidelines and standard threshold are set and expressed in terms of a single *in-situ* E-Field strength at the synaptic level (2,4). Yet, we have demonstrated, with a very sensitive sensory system, having close neurophysiological properties to both the retina and the brain (6,17), that stimuli above the guideline threshold could lead to no observable sensorimotor response (Chapters 2 and 3).

Secondly, orientation of the fields is not considered at the guidelines and recommendations level and should be taken into account in the future. We have argued that depending on top-down or mediolateral orientation of the fields, the hair cells within the vestibular system could be either impacted (Chapters 3) or not (Chapters 2), potentially being observed with the right orientation depending on the type of outcomes analyzed (Chapter 4 vs Chapter 2). Thus, as shown for the retina (18) and other brain neural structures (19,20), ELF-MF field orientation is of paramount importance. Nonetheless, with the same mediolateral field orientation, SVV effects could also be observed with 0.053 V/m (Chapter 4), whereas postural modulations were not with 0.423 V/m (Chapter 3). Therefore, it appears that the E-Field values must be considered together with the orientation (Chapter 4).

Frequency specificity is also overlooked in the guidelines. Although the guidelines acknowledge that the threshold could be frequency dependent, they mainly consider a single *in-situ* E-Field value of 0.075 V/m peak for the entire ELF frequency range (1,4). Yet, as shown by Carriot et al (21), for the vestibular system, the integration of the afferents' inputs vary depending on the stimulation frequency. Indeed, as stimulation frequency increases, the weight of otolithic information being integrated is more important

while the opposite occurs with the canalithic inputs (21). Frequency specificity is also important at the retinal photoreceptors level, as phosphenes threshold responses also rely on different frequency levels (22–25). Furthermore, frequency dependency varies between tasks. Studies have shown evidence that in a postural control context, frequencies could be low-pass filtered (26–29) resulting in an absence of outcome modulation, while the hair cells themselves could be efficiently triggered at the same or higher frequencies (9,30). This was further demonstrated in this thesis, as for the same frequency range, small effects were observed with SVV (Chapter 4) but not with the postural tasks (Chapters 2 and 3). Therefore, a single threshold for the entire ELF frequency range applied indiscriminately to all neural structures does not seem appropriate for guidelines trying to protect the workers and the public alike.

5.2 General limitations

The first limitation was the use of high stimulation frequencies throughout this thesis. Physiologically, it has been hypothesized that for the biomechanical system to work efficiently, only frequencies required to control task-specific muscle physiology are used (27). Evidence suggests that depending on the task and the needs, high frequency currents could be low-pass filtered at several stages (26). First neurologically when being integrated and transferred through different vestibulospinal pathways (31), then at the muscle level (26,27,29), and then finally be further biomechanically low-pass filtered by the inertia of the body (32). Indeed, non-invasive electric vestibular stimulation up to 300 Hz trigger myogenic responses in the neck (31), whereas leg muscles only respond below 20 Hz (33), while 95% of the spectral power of COP time-series is located below 5 Hz (34,35). Therefore, in both of the postural studies (Chapter 2 and 3), but more so in Chapter 3 where it was hypothesized that an impact could have been generated at the utricle level, these low-pass filtering effects could have further dampened the small net acceleration signal from the utricle. Altogether, our stimulations could have produced responses that were too small to observe through postural sway analysis. In our third study (Chapter 4), given that SVV is hypothesized as a torsional eye movement due to the E-Fields, the filtering mechanisms were less likely to impact the outcome (26). Nonetheless, the high frequencies could have also limited the effect obtained and yielded variable results. Indeed, as

frequencies of the stimulations increase, the amplitude of the torsional eye response decreases accordingly, and at 20 Hz, eye torsion is already smaller than 0.2° (36). Therefore, considering lower frequencies could have provided a greater impact and such frequency reduction will need to be considered in future studies.

A second limitation for the first two studies (Chapters 2 and 3) was the choice of postural sway as the sole outcome measure and different parameters could have sensitized the analysis. Modulating head orientations could have been an interesting parameter to change during our postural control experiments. Because the vestibular system is fixed to the head, the information it provides to the CNS lies within a craniocentric reference frame (37). However, for the brain to compute accurate motor control and balance, the information provided by the vestibular system must be translated into a body reference frame (37). For the brain to make this reference frame transformation accurately, it needs to rely on other sensory inputs as well as motor-related information (37,38). Neck proprioception seems to play a crucial role in the transformation process. In 1983, Lund & Broberg (39) showed that by modulating head orientation in space relative to the feet, the electric vestibular stimulation outcome was expressed in a different plane. As the head faced forward, even if the trunk is rotated, the outcome will be expressed in the frontal plane. However, if the participants had their heads tilted toward one side, about the yaw axis, the outcome was expressed in the sagittal plane (39). By giving information concerning where the head lies in reference to the body, proprioception, therefore, helps the brain coordinate vestibulospinal reflexes accordingly to stabilize our body in space if needed. Therefore, head orientation modifications around the yaw axis, directly impact the orientation of postural outcome and therefore axial muscle activity. Tilting the head could have sensitized information concerning the directions of sway analyzed in both postural studies (Chapters 2 and 3). Also, by emphasizing axial muscle activity, turning the head along the yaw axis, could have been evaluated through the use of electromyographic (EMG) analysis which is a more sensitive outcome measure than postural sway during a balance task (26–29,31,40–42).

Another limitation in this thesis was the population investigated. Most of our participants were active university students in their early twenties. The fact that regular sports practice can reduce the effects of E-Fields on postural control (43) might have been an issue in the

two first postural studies of this thesis (Chapters 2 and 3). Also, given that our population samples consisted mostly of young adults, the results reported in this thesis cannot be generalized to other age groups, since age-related changes have been observed when E-Fields specifically impact the vestibular system (44–46).

Finally, both postural control (Chapters 2 and 3) and SVV (Chapter 4) are highly integrated outcomes. In that regard, vestibular perception, for instance, could have also been a limitation of this work. Although the vestibular system is very quick to stabilize the eye in the orbit (7 ms for the vestibulo-ocular pathways) and the head on the torso (~8–10 ms for the vestibulo-collic pathways) (26), for multisensory integration purposes (47), it seems to be slow when it comes to perception (48). Even though the natural frequency bandwidth of the vestibular system ranges up to 30 Hz (49), no human vestibular perception is recorded above 5 Hz (38). On average vestibular perception starts 438 ms after GVS onset (47). The greatest vestibular perceptions are felt under 2 Hz (50) corresponding to a 500 ms period. Moreover, as the frequency of stimulation increases the percentage of participants perceiving a sensation of self-motion decreases (50). Therefore, with the direct current stimulations, the time delays needed for perceived head movement could have been enough to induce both the postural (Chapters 2 and 3) as well as the SVV (Chapter 4) changes seen with our positive control results. Yet, with a sinusoidal stimulation at 20 Hz, the current period is 50 ms while at 160 Hz it drops to 6 ms. While this is enough to induce reflexive myogenic responses (31), it may not be enough to be perceived. This may explain why no specific vestibular perceptions were observed in all of the studies included in this thesis (Chapters 2, 3, and 4). Given the high cognitive processes occurring in all of the tasks used in this thesis, this might explain why our stimulations between 20 Hz and 160 Hz, appeared ineffective in strongly modulating vestibular outputs.

The vestibular perception argument could indeed be paramount and have safety consequences. Indeed, both workers and the public can be exposed to ELF-MF levels exceeding the guidelines' synaptic threshold. Vestibular perception is, therefore, an important point to consider in the health and safety contexts. Using a synaptosome model, Masoudian et al., (51) found that considering the time of exposure, the strength of the flux density, and the exposition frequency, ELF-MF stimulations could modulate glutamate

concentrations within the synaptic cleft. Depending on how these three parameters are combined, an increase in glutamate concentration occurs (51). These results are important given that glutamate is the main neurotransmitter of the vestibular system. Furthermore, when in excess in the synaptic cleft, glutamate leads to neuronal death through the excitotoxicity phenomenon (52,53). This is extremely important since power lines ELF-MFs oscillating at 50 Hz or at 60 Hz worldwide are ubiquitous in our daily lives, but no vestibular perception is felt; accordingly people could be unaware of potential adverse effects. Considering the important issue of protection of the public and workers in ELF-MF environments, this knowledge gap needs to be addressed in future studies, to contribute to the literature supporting MF safety exposure guidelines for workers and the public.

5.3 Future studies

The current thesis was the first steppingstone in investigating specific ELF-MF interactions on the vestibular system and provides the foundation for many important directions for future research. Future studies on powerline frequency vestibular specific ELF-MF stimulations should first avoid any perception vestibular tasks as in our thesis and fully concentrate on less integrated outcome measures. Vestibular reflexes should, therefore, be a priority.

5.3.1 Eye movement analysis

Electrical vestibular stimulations modulate eye movement (13,54–59). With such stimulations, small amplitude ocular torsions could be recorded with E-Fields potentially as low as 0.008 V/m (see above). The vestibulo-ocular reflex could respond to frequencies up to 70 Hz and probably higher (26) and could therefore be impacted by ELF-MF power line stimulations. Nystagmus amplitudes are proportional to current intensity (60) meaning that outcomes should increase with E-Field strength. However, they decrease with increasing frequencies (36). Therefore, the angular resolution of the analysis will need to be taken into consideration in a future study. Otero-Millan et al. (61) have described a new 3D eye-tracking analysis technique which they claim to be better than the scleral search

coil, considered as the actual gold standard. Therefore, this technique could be implemented in future protocols investigating ELF-MF VOR responses.

5.3.2 Myogenic responses

Vestibular-evoked myogenic potentials (VEMPs) seem also to be an interesting investigation choice. First, VEMPs are recognized as specific otolithic tests (62) and have been researched thoroughly both on healthy participants (63) and patients (64–68). They can be used to investigate both vestibulospinal (cVEMPs) (27,41,69–71) and vestibulo-ocular (oVEMPs) (72–75) pathways. CVEMPs mostly rely on ipsilateral saccular irregular afferents while oVEMPs test the utricular macula of the contralateral ear (76,77).

Second, otoliths can phase-lock with high-frequency stimuli up to 2000 Hz (30) and important VEMPS responses can be recorded at power line frequencies (78–80). VEMPS can be obtained using electric vestibular stimulations (62,69,70,73,81). Furthermore, these galvanic induced VEMPs are as reliable as the more classical ones evoked by sounds or vibrations (69,70,72,73). Our SVV results suggest that monaural lateral ELF-MF stimulations could be utricular specific when the head is upright. Therefore, with the head upright, powerline frequency ELF-MF could induce oVemp responses. Furthermore, with the neck completely flexed, the ELF-MF stimulations could become more saccular specific and induce cVEMP responses. Thus, depending on field orientations and head position, the specificity of those tests could help better understand whether ELF MF stimulations precisely trigger a specific vestibular region.

5.3.3 Cortical activity

Brain imaging studies show activation and deactivation of specific cortical areas when the vestibular system is stimulated (50,82–84). Most of the studies related to that subject reveal vestibular responses in the insular, temporoparietal, somatosensory, cingulate, and frontal cortices as well as in the cerebellum and the hippocampus (50,85–88).

In that context, EEG seems an interesting technique to consider. EEG recordings have been obtained with different types of vestibular stimulations such as natural types of movements (89–92), caloric stimulation (93), auditory stimuli made by clicks and short-tone bursts

(94) and electric vestibular stimulations (95–97). Comparisons and matching activations at cortical level with vestibular specific ELF-MF stimulations would therefore be informative. Indeed, if the induced currents activate the vestibular system in a similar way, the same type of activation should be recorded. Functional Near-Infrared Spectroscopy (fNIRS) could also be an alternative as specific vestibulo cortical recordings have also been done with this technique (98–101). Yet, fNIRS as a lower temporal resolution and EEG could therefore be favored for power line frequency stimulations.

5.3.4 Autonomous responses

The vestibular system is systematically triggered when one is in movement or must regulate his posture. Research findings have shown a link between the vestibular system and the autonomous system. While adjusting posture or when moving through space, the vestibular system regulates both respiratory and cardiovascular systems accordingly (102). The superior canal via a neurological connection with the abdominal muscles could play a major role in the breathing processes (103). The vestibular system is equally engaged in adjusting cardiovascular responses (104). The vestibular system senses both the linear and the angular accelerations of the head through the otolithic and canalithic system respectfully. Participants subjected to head accelerations see an increase in their blood pressure as well as a modulation of their electrocardiogram output (105). Heart rate variability can also be modulated by vestibular electrical stimulations (106). Acute vestibular symptoms include nausea, tachycardia, sweatiness, palpitations, and vomiting which can be also induced when stimulated by specific electrical currents applied to the vestibular system (102).

Pupillometry could also be of interest. Asymmetry in pupil size known as anisocoria occurs in vestibular pathologies (107). In the introduction of their paper, Chin Tang and Gernandt (108) acknowledge pupil reactions to vestibular stimulations. Indeed pupillary reactions to vestibular stimulations have been recorded using different types of vestibular stimulation such as rotational or caloric stimulations (109). Also, specific utricular stimulations can trigger rhythmic dilatations and constrictions of the pupils (110).

5.3.5 Animal models and C-Fos

C-Fos is a good neuroanatomical biomarker indicating increased activity within the investigated area and is commonly used to provide evidence of vestibular end-organs stimulation (111–113). Interestingly, both ELF-MF (114) and sinusoidal vestibular stimulations (115) produce the same C-Fos-labeled neurons in the vestibular nuclei, indicating that both stimulations activate the vestibular end-organs. Although these results relate to animal models with very different vestibular sensitivity than in humans, these results are nonetheless promising in providing evidence of exclusive ELF-MF stimulations modulating the vestibular end-organs and could be considered in future studies.

5.4 General conclusion

Altogether this thesis underlines that generalizing the retinal outcomes to the entire SNC is inappropriate. Indeed, other sensory systems and the brain neurological structures may ultimately not behave similarly as the photoreceptors. Sensory and structural specificities as well as how the afferences are integrated should also be considered.

As far as powerline frequencies are concerned, vestibulomotor outcomes could start being triggered at 0.008 V/m peak and may not be consciously perceived. Therefore, the notion of 0.075 V/m peak as a one size fits all synaptic threshold for the entire ELF range is likely not appropriate. Paramount parameters such as frequency specificities and E-Fields orientation will need to be more emphasized in future guidelines and standards.

5.5 References

1. ICNIRP. Guidelines for limiting exposure to time-varying electric and magnetic fields (1 Hz to 100 kHz). *Health Phys* [Internet]. 2010;99(6):818–36.
2. ICNIRP. Gaps in Knowledge Relevant to the “Guidelines for Limiting Exposure to Time-Varying Electric and Magnetic Fields (1 Hz-100 kHz).” *Health Phys*. 2020;118(5):533–42.
3. IEEE. IEEE Standard for Safety Levels with Respect to Human Exposure to

Electromagnetic Fields, 0–3 kHz. Technology. 2002.

4. IEEE. IEEE Standard for Safety Levels With Respect to Human Exposure to Electric, Magnetic, and Electromagnetic Fields, 0 Hz to 300 GHz. Vol. 2005, IEEE Std C95.1-2005 (Revision of IEEE Std C95.1-1991). 2019. 0_1-238.
5. WHO. Extremely Low Frequency Fields Environmental Health Criteria Monograph No.238. [Internet]. WHO,. Geneva; 2007.
6. Attwell D. Interaction of low frequency electric fields with the nervous system: the retina as a model system. *Radiat Prot Dosimetry* [Internet]. 2003;106(4):341–8.
7. Eatock RA, Songer JE. Vestibular Hair Cells and Afferents: Two Channels for Head Motion Signals [Internet]. Vol. 34, *Annual Review of Neuroscience*. 2011. 501–534 p.
8. Sadeghi SG, Pyott SJ, Yu Z, Glowatzki E. Glutamatergic Signaling at the Vestibular Hair Cell Calyx Synapse. 2014;34(44):14536–50.
9. Zenner HP, Reuter G, Hong S, Zimmermann U, Gitter AH. Electrically evoked motile responses of mammalian type I vestibular hair cells. *J Vestib Res*. 1992;2(3):181–91.
10. Norris CH, Miller AJ, Perin P, Holt JC, Guth PS. Mechanisms and effects of transepithelial polarization in the isolated semicircular canal. *Hear Res*. 1998;123(1–2):31–40.
11. Gensberger KD, Kaufmann A-K, Dietrich H, Branoner F, Banchi R, Chagnaud BP, et al. Galvanic Vestibular Stimulation: Cellular Substrates and Response Patterns of Neurons in the Vestibulo-Ocular Network. *J Neurosci* [Internet]. 2016;36(35):9097–110.
12. Fitzpatrick RC, Day BL. Probing the human vestibular system with galvanic stimulation. *J Appl Physiol* [Internet]. 2004;96(6):2301–16.

13. Severac Cauquil A, Faldon M, Popov K, Day BL, Bronstein AM. Short-latency eye movements evoked by near-threshold galvanic vestibular stimulation. *Exp Brain Res*. 2003;148:414–8.
14. Yang Y, Pu F, Lv X, Li S, Li J, Li D, et al. Comparison of postural responses to galvanic vestibular stimulation between pilots and the general populace. *Biomed Res Int*. 2015;2015.
15. Huang Y, Liu AA, Lafon B, Friedman D, Dayan M, Wang X, et al. Measurements and models of electric fields in the in vivo human brain during transcranial electric stimulation. *Elife*. 2017;6:1–27.
16. Thomas C, Truong D, Clark TK, Datta A. Understanding current flow in Galvanic Vestibular Stimulation: A Computational Study*. In: 2020 42nd Annual International Conference of the IEEE Engineering in Medicine & Biology Society (EMBC) [Internet]. Montreal, QC, Canada,: IEEE; 2020. p. 2442–6.
17. Juusola M, French AS, Uusitalo RO, Weckström and M. Information processing by graded-potential transmission through tonically active synapses. *Trends Neurosci*. 1996;(19.):292–297.
18. Hirata A, Takano Y, Fujiwara O, Dovan T, Kavet R. An electric field induced in the retina and brain at threshold magnetic flux density causing magnetophosphenes. *Phys Med Biol*. 2011;
19. Liu A, Vöröslakos M, Kronberg G, Henin S, Krause MR, Huang Y, et al. Immediate neurophysiological effects of transcranial electrical stimulation. *Nat Commun* [Internet]. 2018;9(1).
20. Radman T, Ramos RL, Brumberg JC, Bikson M. Role of cortical cell type and morphology in subthreshold and suprathreshold uniform electric field stimulation in vitro. *Brain Stimul* [Internet]. 2009;2(4):215-228.e3.
21. Carriot J, Jamali M, Brooks JX, Cullen KE. Integration of Canal and Otolith Inputs by Central Vestibular Neurons Is Subadditive for Both Active and Passive Self-

- Motion: Implication for Perception. *J Neurosci* [Internet]. 2015;35(8):3555–65.
22. Evans ID, Palmisano S, Loughran SP, Legros A, Croft RJ. Frequency-dependent and montage-based differences in phosphene perception thresholds via transcranial alternating current stimulation. *Bioelectromagnetics*. 2019;40(6):365–74.
 23. Lövsund P, Öberg PÅ, Nilsson SEG, Reuter T. Magnetophosphenes: a quantitative analysis of thresholds. *Med Biol Eng Comput*. 1980;18(3):326–34.
 24. Lövsund P, Oberg PA, Nilsson SEG. Magneto- and electrophosphenes : a comparative study. *Med Biol Eng Comput*. 1980;758–64.
 25. Lövsund P, Öberg P, Nilsson SEG. Quantitative determination of thresholds of magnetophosphenes. *Radio Sci*. 1979;14(6 S):199–200.
 26. Forbes PA, Siegmund GP, Schouten AC, Blouin J-S. Task, muscle and frequency dependent vestibular control of posture. *Front Integr Neurosci* [Internet]. 2014;8(January):94.
 27. Forbes P a, Dakin CJ, Vardy AN, Happee R, Siegmund GP, Schouten AC, et al. Frequency response of vestibular reflexes in neck, back, and lower limb muscles. *J Neurophysiol* [Internet]. 2013;110(July 2013):1869–81.
 28. Dakin CJ, Son GML, Inglis JT, Blouin J-S. Frequency response of human vestibular reflexes characterized by stochastic stimuli. *J Physiol* [Internet]. 2007;583(Pt 3):1117–27.
 29. Dakin CJ, Luu BL, van den Doel K, Inglis JT, Blouin J-S. Frequency-specific modulation of vestibular-evoked sway responses in humans. *J Neurophysiol* [Internet]. 2010;103(2):1048–56.
 30. Curthoys IS. The new vestibular stimuli: sound and vibration—anatomical, physiological and clinical evidence. *Exp Brain Res* [Internet]. 2017;235(4):957–972.

31. Forbes PA, Kwan A, Rasman XBG, Mitchell DE, Cullen XKE, Blouin JS. Neural mechanisms underlying high-frequency vestibulocollic reflexes in humans and monkeys. *J Neurosci*. 2020;40(9):1874–87.
32. Fitzpatrick R, Burke D, Gandevia SC. Loop gain of reflexes controlling human standing measured with the use of postural and vestibular disturbances. *J Neurophysiol* [Internet]. 1996;76(6):3994–4008.
33. Dakin CJ, Son GML, Inglis JT, Blouin J-S. Frequency response of human vestibular reflexes characterized by stochastic stimuli. *J Physiol* [Internet]. 2007;583(Pt 3):1117–27.
34. Dozza M, Chiari L, Horak FB. Audio-biofeedback improves balance in patients with bilateral vestibular loss. *Arch Phys Med Rehabil*. 2005;86(7):1401–3.
35. Chiari L, Rocchi L, Cappello A. Stabilometric parameters are affected by anthropometry and foot placement. *Clin Biomech*. 2002;17(9–10):666–77.
36. Mackenzie SW, Reynolds RF. Ocular torsion responses to sinusoidal electrical vestibular stimulation. *J Neurosci Methods*. 2018;294:116–21.
37. Angelaki DE, Cullen KE. Vestibular System: The Many Facets of a Multimodal Sense. *Annu Rev Neurosci* [Internet]. 2008;31(1):125–50.
38. Cullen KE. Vestibular processing during natural self-motion: implications for perception and action. *Nat Rev Neurosci* [Internet]. 2019;
39. Lund S, Broberg C. Effects of different head positions on postural sway in man induced by a reproducible vestibular error signal. *Acta Physiol Scand*. 1983;117(2):307–9.
40. Kwan A, Forbes PA, Mitchell DE, Blouin J-S, Cullen KE. Neural substrates, dynamics and thresholds of galvanic vestibular stimulation in the behaving primate. *Nat Commun* [Internet]. 2019;10(1):1904.

41. Forbes PA, Luu BL, Van der Loos HFM, Croft EA, Inglis JT, Blouin J-S. Transformation of vestibular signals for the control of standing in humans. *J Neurosci*. 2016;36(45):11510–20.
42. Forbes PA, Fice JB, Siegmund GP, Blouin J-S. Electrical Vestibular Stimuli Evoke Robust Muscle Activity in Deep and Superficial Neck Muscles in Humans. *Front Neurol* [Internet]. 2018;9(July):1–8.
43. Maitre J, Paillard T. Postural effects of vestibular manipulation depend on the physical activity status. *PLoS One* [Internet]. 2016;11(9):1–13.
44. Chang CM, Cheng PW, Young YH. Aging effect on galvanic vestibular-evoked myogenic potentials. *Otolaryngol - Head Neck Surg* [Internet]. 2010;143(3):418–21.
45. Chang C-M, Young Y-H, Cheng P-W. Age-related changes in ocular vestibular-evoked myogenic potentials via galvanic vestibular stimulation and bone-conducted vibration modes. *Acta Otolaryngol* [Internet]. 2012;132(12):1295–300.
46. Jahn K, Naessl A, Schneider E, Strupp M, Brandt T, Dieterich M. Inverse U-shaped curve for age dependency of torsional eye movement responses to galvanic vestibular stimulation. *Brain* [Internet]. 2003;126(Pt 7):1579–89.
47. Barnett-cowan M, Harris LR. Perceived timing of vestibular stimulation relative to touch , light and sound. *Exp Brain Res*. 2009;198:221–31.
48. Barnett-cowan M. Vestibular Perception is Slow : A Review. *Multisens Res*. 2013;26:387–403.
49. Carriot J, Jamali M, Chacron MJ, Cullen KE. Statistics of the Vestibular Input Experienced during Natural Self-Motion : Implications for Neural Processing. *J Neurosci*. 2014;34(24):8347–57.
50. Stephan T, Deutschländer A, Nolte A, Schneider E, Wiesmann M, Brandt T, et al. Functional MRI of galvanic vestibular stimulation with alternating currents at

- different frequencies. *Neuroimage*. 2005;26(3):721–32.
51. Masoudian N, Riazi GH, Afrasiabi A, Modaresi SMS, Dadras A, Rafiei S, et al. Variations of Glutamate Concentration Within Synaptic Cleft in the Presence of Electromagnetic Fields: An Artificial Neural Networks Study. *Neurochem Res*. 2015;40(4):629–42.
 52. Smith PF. Are vestibular hair cells excited to death by aminoglycoside antibiotics? *J Vestib Res*. 2000;10:1–5.
 53. Sedó-Cabezón L, Boadas-Vaello P, Soler-Martín C, Llorens J. Vestibular damage in chronic ototoxicity: A mini-review. *Neurotoxicology*. 2014;43:21–7.
 54. Schneider E, Glasauer S, Dieterich M. Central processing of human ocular torsion analyzed by galvanic vestibular stimulation. *Neuroreport* [Internet]. 2000;11(7):1559–63.
 55. Schlosser HG, Unterberg A, Clarke A. Using video-oculography for galvanic evoked vestibulo-ocular monitoring in comatose patients. *J Neurosci Methods*. 2005;145(1–2):127–31.
 56. Schneider E, Glasauer S, Dieterich M. Comparison of Human Ocular Torsion Patterns During Natural and Galvanic Vestibular Stimulation. *J Neurophysiol*. 2002;87:2064–73.
 57. Kleine JF, Guldin WO, Clarke AH. Variable otolith contribution to the galvanically induced vestibulo-ocular reflex. *Neuroreport*. 1999;10(5):1143–8.
 58. MacDougall HG, Brizuela AE, Burgess AM, Curthoys IS. Between-subject variability and within-subject reliability of the human eye-movement response to bilateral galvanic (DC) vestibular stimulation. *Exp Brain Res*. 2002;144(1):69–78.
 59. Mackenzie SW, Irving R, Monksfield P, Kumar R, Dezso A, Reynolds RF. Ocular torsion responses to electrical vestibular stimulation in vestibular schwannoma. *J Neurosci Methods* [Internet]. 2018;129:2350–60.

60. Aw ST, Todd MJ, Halmagyi GM. Latency and initiation of the human vestibuloocular reflex to pulsed galvanic stimulation. *J Neurophysiol* [Internet]. 2006;96(2):925–30.
61. Otero-Millan J, Roberts DC, Lasker A, Zee DS, Kheradmand A. Knowing what the brain is seeing in three dimensions: A novel, noninvasive, sensitive, accurate, and low-noise technique for measuring ocular torsion. *J Vis* [Internet]. 2015;15(14):1–15.
62. Curthoys IS. A critical review of the neurophysiological evidence underlying clinical vestibular testing using sound, vibration and galvanic stimuli. *Clin Neurophysiol* [Internet]. 2010;121(2):132–44.
63. Cunha LCM, Labanca L, Tavares MC, Gonçalves DU. Vestibular evoked myogenic potential (VEMP) with galvanic stimulation in normal subjects. *Braz J Otorhinolaryngol* [Internet]. 2014;80(1):48–53.
64. Caporali JF de M, Utsch Gonçalves D, Labanca L, Dornas de Oliveira L, Vaz de Melo Trindade G, de Almeida Pereira T, et al. Vestibular Evoked Myogenic Potential (VEMP) Triggered by Galvanic Vestibular Stimulation (GVS): A Promising Tool to Assess Spinal Cord Function in Schistosomal Myeloradiculopathy. *PLoS Negl Trop Dis*. 2016;10(4):1–11.
65. Fujimoto C, Iwasaki S, Matsuzaki M, Murofushi T. Lesion site in idiopathic bilateral vestibulopathy: a galvanic vestibular-evoked myogenic potential study. *Acta Otolaryngol* [Internet]. 2005;125(4):430–2.
66. Iwasaki S, Takai Y, Ozeki H, Ito K, Karino S, Murofushi T. Extent of Lesions in Idiopathic Sudden Hearing Loss With Vertigo. *Acta Otolaryngol Head Neck Surg*. 2005;131:857–62.
67. Monobe H, Murofushi T. Vestibular testing by electrical stimulation in patients with unilateral vestibular deafferentation: Galvanic evoked myogenic responses testing versus galvanic body sway testing. *Clin Neurophysiol*. 2004;115(4):807–

- 11.
68. Ozeki H, Iwasaki S, Ushio M, Takeuchi N, Murofushi T. The lesion site of vestibular dysfunction in Ramsay Hunt syndrome: a study by click and galvanic VEMP. *J Vestib Res.* 2006;16(4–5):217–22.
69. Watson SRD, Fagan P, Colebatch JG. Galvanic stimulation evokes short-latency EMG responses in sternocleidomastoid which are abolished by selective vestibular nerve section. *Electroencephalogr Clin Neurophysiol - Electromyogr Mot Control.* 1998;109(6):471–4.
70. Watson S, Colebatch J. Vestibulocollic reflexes evoked by short-duration galvanic stimulation in man. *J Physiol.* 1998;513 (Pt 2(1998):587–97.
71. Murofushi T, Monobe H, Ochiai A, Ozeki H, T. M, H. M, et al. The site of lesion in “vestibular neuritis”: study by galvanic VEMP. *Neurology [Internet].* 2003;61(3):417–8.
72. Rosengren SM, Jombik P, Halmagyi GM, Colebatch JG. Galvanic ocular vestibular evoked myogenic potentials provide new insight into vestibulo-ocular reflexes and unilateral vestibular loss. *Clin Neurophysiol [Internet].* 2009;120(3):569–80.
73. Rosengren SM, Welgampola MS, Colebatch JG. Vestibular evoked myogenic potentials: Past, present and future. *Clin Neurophysiol [Internet].* 2010;121(5):636–51.
74. Todd NPM, Rosengren SM, Aw ST, Colebatch JG. Ocular vestibular evoked myogenic potentials (OVEMPs) produced by air- and bone-conducted sound. *Clin Neurophysiol.* 2007;118(2):381–90.
75. Cheng PW, Chen CC, Wang SJ, Young YH. Acoustic, mechanical and galvanic stimulation modes elicit ocular vestibular-evoked myogenic potentials. *Clin Neurophysiol [Internet].* 2009;120(10):1841–4.

76. Rosengren SM, Colebatch JG, Borire A, Straumann D, Weber KP. cVEMP morphology changes with recording electrode position, but single motor unit activity remains constant. *J Appl Physiol*. 2016;120(8):833–42.
77. Curthoys IS. The interpretation of clinical tests of peripheral vestibular function. *Laryngoscope*. 2012;122(6):1342–52.
78. Todd NPM, Rosengren SM, Colebatch JG. A utricular origin of frequency tuning to low-frequency vibration in the human vestibular system? *Neurosci Lett*. 2009;451(3):175–80.
79. Todd NPM, Rosengren SM, Colebatch JG. Tuning and sensitivity of the human vestibular system to low-frequency vibration. *Neurosci Lett*. 2008;444(1):36–41.
80. Zhang AS, Govender S, Colebatch JG. Tuning of the ocular vestibular evoked myogenic potential to bone-conducted sound stimulation. *J Appl Physiol* [Internet]. 2012;112(8):1279–90.
81. Lue JH, Day AS, Cheng PW, Young YH. Vestibular evoked myogenic potentials are heavily dependent on type I hair cell activity of the saccular macula in guinea pigs. *Audiol Neurotol*. 2008;14(1):59–66.
82. Lopez C, Blanke O, Mast FW. The human vestibular cortex revealed by coordinate-based activation likelihood estimation meta-analysis. *Neuroscience* [Internet]. 2012;212:159–79.
83. Bense S, Stephan T, Yousry TA, Brandt T, Dieterich M. Multisensory cortical signal increases and decreases during vestibular galvanic stimulation (fMRI). *J Neurophysiol* [Internet]. 2001;85(2):886–99.
84. Bucher SF, Dieterich M, Wiesmann M, Weiss A, Zink R, Yousry TA, et al. Cerebral functional magnetic resonance imaging of vestibular, auditory, and nociceptive areas during galvanic stimulation. *Ann Neurol*. 1998;44(1):120–5.
85. Bottini G, Sterzi R, Paulesu E, Vallar G, Cappa SF, Erminio F, et al. Identification

- of the central vestibular projections in man: a positron emission tomography activation study. *Exp Brain Res*. 1994;99(1):164–9.
86. Lobel E, Kleine JF, Bihan DL, Leroy-Willig a, Berthoz a. Functional MRI of galvanic vestibular stimulation. *J Neurophysiol*. 1998;80(5):2699–709.
 87. Vitte E, Derosier C, Caritu Y, Berthoz A, Hasboun D, Soulié D. Activation of the hippocampal formation by vestibular stimulation: a functional magnetic resonance imaging study. *Exp Brain Res [Internet]*. 1996;112(3):523–6.
 88. Lopez C, Blanke O. The thalamocortical vestibular system in animals and humans. *Brain Res Rev [Internet]*. 2011;67(1–2):119–46.
 89. Ehinger B V, Fischer P, Gert AL, Kaufhold L, Weber F, Pipa G, et al. Kinesthetic and vestibular information modulate alpha activity during spatial navigation: a mobile EEG study. *Front Hum Neurosci [Internet]*. 2014;8(February):71.
 90. Hood J., Kayan A. OBSERVATIONS UPON THE EVOKED RESPONSES TO NATURAL VESTIBULAR STIMULATION. *Electroencephalogr Clin Neurophysiol*. 1985;62:266–76.
 91. Nolan H, Whelan R, Reilly RB, Bühlhoff HH, Butler JS. Acquisition of human EEG data during linear self-motion on a Stewart platform. 2009 4th Int IEEE/EMBS Conf Neural Eng NER '09. 2009;585–8.
 92. Gale S, Prsa M, Schurger A, Gay A, Paillard A, Herbelin B, et al. Oscillatory neural responses evoked by natural vestibular stimuli in humans. *J Neurophysiol [Internet]*. 2016;115(3):1228–42.
 93. Brkic F, Gortan D, Kapidzic A, Sinanovic O, Brkic S. The effects of caloric vestibular stimulation on EEGs in patients with central vertigo. *Eur Arch Otorhinolaryngol [Internet]*. 2002;259(6):334–8.
 94. McNerney KM, Lockwood AH, Coad M Lou, Wack DS, Burkard RF. Use of 64-channel electroencephalography to study neural otolith-evoked responses. *J Am*

- Acad Audiol [Internet]. 2011;22(3):143–55.
95. Kim DJ, Yogendrakumar V, Chiang J, Ty E, Wang ZJ, McKeown MJ. Noisy Galvanic Vestibular Stimulation Modulates the Amplitude of EEG Synchrony Patterns. *PLoS One*. 2013;8(7).
 96. Wilkinson D, Ferguson HJ, Worley A. Galvanic vestibular stimulation modulates the electrophysiological response during face processing. *Vis Neurosci* [Internet]. 2012;29(4–5):255–62.
 97. Lee J-W, Lee G-E, An J-H, Yoon S-W, Heo M, Kim H-Y. Effects of galvanic vestibular stimulation on visual memory recall and EEG. *J Phys Ther Sci* [Internet]. 2014;26(9):1333–6.
 98. Karim H, Fuhrman SI, Sparto P, Furman J, Huppert T. Functional Brain Imaging of Multi-sensory Vestibular Processing during Computerized Dynamic Posturography using NearInfrared Spectroscopy. *Neuroimage*. 2013;74(1):318–25.
 99. Karim HT, Fuhrman SI, Furman JM, Huppert TJ. Neuroimaging to detect cortical projection of vestibular response to caloric stimulation in young and older adults using functional near-infrared spectroscopy (fNIRS). *Neuroimage* [Internet]. 2013;76(July 2014):1–10.
 100. Kobayashi A, Cheung B. Detection of cerebral oxyhaemoglobin changes during vestibular Coriolis cross-coupling stimulation using near infrared spectroscopy. *Neurosci Lett*. 2006;394(2):83–7.
 101. Iida M, Haida M, Igarashi M. Vertigo and cerebral hemoglobin changes during unilateral caloric stimulation: A near-infrared spectroscopy study. *Ann N Y Acad Sci*. 2009;1164:386–9.
 102. Yates BJ, Bolton PS, Macefield VG. Vestibulo-Sympathetic Responses. *Compr Physiol*. 2015;4(2):851–87.
 103. Jauregui-Renaud K, Gresty MA, Reynolds R, Bronstein AM. Respiratory

responses of normal and vestibular defective human subjects to rotation in the yaw and pitch planes. *Neurosci Lett*. 2001;298:17–20.

104. Watenpaugh DE, Cothron A V, L WS, Wasmund WL, Carter R, Muentner N, et al. Do vestibular otolith organs participate in human orthostatic blood pressure control ? *Auton Neurosci*. 2002;100:77–83.
105. Yates BJ, Bronstein AM. The effects of vestibular system lesions on autonomic regulation: Observations, mechanisms, and clinical implications. *J Vestib Res*. 2005;15:119–29.
106. Yamamoto Y, Struzik ZR, Soma R, Ohashi K, Kwak S. Noisy vestibular stimulation improves autonomic and motor responsiveness in central neurodegenerative disorders. *Ann Neurol*. 2005;58(2):175–81.
107. Wanabe I, Nishida H. Anisocoria in Meniere’s Disease. *Equilibrium*. 1971;(2):71–8.
108. Chin Tang P, Gernandt BE. Autonomic Responses to Vestibular Stimulation. *Exp Neurol*. 1969;24:558–78.
109. Spiegel EA. EFFECT OF LABYRINTHINE REFLEXES ON THE VEGETATIVE NERVOUS SYSTEM : A Review. *Arch Otolaryngol Head Neck Surg*. 1939;12:61–72.
110. De Santis M, Gernandt BE. Effect of on Vestibular Stimulation on Pupillary Size. *Exp Neurol*. 1971;30:66–77.
111. Cason AM, Kwon B, Smith JC, Houpt TA. Labyrinthectomy abolishes the behavioral and neural response of rats to a high-strength static magnetic field. *Physiol Behav [Internet]*. 2009;97(1):36–43.
112. Houpt TA, Kwon B, Houpt CE, Neth B, Smith JC. Orientation within a high magnetic field determines swimming direction and laterality of c-Fos induction in mice. *Am J Physiol Regul Integr Comp Physiol [Internet]*. 2013;305(7):R793-803.

113. Keary N, Bischof HJ. Activation changes in zebra finch (*Taeniopygia guttata*) brain areas evoked by alterations of the earth magnetic field. *PLoS One*. 2012;7(6).
114. Nimpf S, Nordmann GC, Kagerbauer D, Colombini M, Mason MJ, Nimpf S, et al. Report A Putative Mechanism for Magnetoreception by Electromagnetic Induction in the Pigeon Inner Ear. *Curr Biol [Internet]*. 2019;1–8.
115. Holstein GR, Friedrich VL, Martinelli GP, Ogorodnikov D, Yakushin SB, Cohen B. Fos expression in neurons of the rat vestibulo-autonomic pathway activated by sinusoidal galvanic vestibular stimulation. *Front Neurol*. 2012;FEB(February):1–15.

Appendices



**Western
Research**

Research Ethics

**Western University Health Science Research Ethics Board
HSREB Full Board Initial Approval Notice**

Principal Investigator: Dr. Alexandre Legros
Department & Institution: Schulich School of Medicine and Dentistry/Medical Biophysics, Lawson Health Research Institute

HSREB File Number: 106122
Study Title: Impact of extremely low-frequency (<300Hz) magnetic fields (up to 100 mT) on postural control in humans
Sponsor:

HSREB Initial Approval Date: March 02, 2015
HSREB Expiry Date: March 02, 2016

Documents Approved and/or Received for Information:

Document Name	Comments	Version Date
Other	Appendix 1 Phone Questionnaire	2014/12/02
Western University Protocol		2015/01/01
Advertisement	Appendix 2 - Advertisement	2015/01/01
Letter of Information & Consent	Appendix 3 - Letter of Information and Consent Form	2015/01/01
Instruments	Appendix 4 - Field Status Questionnaire	2015/01/01

The Western University Health Science Research Ethics Board (HSREB) has reviewed and approved the above named study, as of the HSREB Initial Approval Date noted above.

HSREB approval for this study remains valid until the HSREB Expiry Date noted above, conditional to timely submission and acceptance of HSREB Continuing Ethics Review. If an Updated Approval Notice is required prior to the HSREB Expiry Date, the Principal Investigator is responsible for completing and submitting an HSREB Updated Approval Form in a timely fashion.

The Western University HSREB operates in compliance with the Tri-Council Policy Statement Ethical Conduct for Research Involving Humans (TCPS2), the International Conference on Harmonization of Technical Requirements for Registration of Pharmaceuticals for Human Use Guideline for Good Clinical Practice (ICH E6 R1), the Ontario Personal Health Information Protection Act (PHIPA, 2004), Part 4 of the Natural Health Product Regulations, Health Canada Medical Device Regulations and Part C, Division 5, of the Food and Drug Regulations of Health Canada.

Members of the HSREB who are named as Investigators in research studies do not participate in discussions related to, nor vote on such studies when they are presented to the REB.

The HSREB is registered with the U.S. Department of Health & Human Services under the IRB registration number IRB 00000940.



Ethics Officer to Contact for Further Information



This is an official document. Please retain the original in your files.

Western University, Research, Support Services Bldg., Rm. 5150
London, ON, Canada N6A 3K7 T. 519.661.3036 F. 519.850.2466 www.uwo.ca/research/services/ethics

Appendices 1. Ethics Approval # 106122 for postural studies (Chapters 2 & 3)



Date: 24 April 2018

To: Dr. Alexandre Legros

Project ID: 109161

Study Title: Acute effect of extremely low frequency magnetic fields on the vestibular system: perception of verticality

Application Type: HSREB Amendment Form

Review Type: Delegated

Meeting Date / Full Board Reporting Date: 01/May/2018

Date Approval Issued: 24/Apr/2018

REB Approval Expiry Date: 09/May/2019

Dear Dr. Alexandre Legros ,

The Western University Health Sciences Research Ethics Board (HSREB) has reviewed and approved the WREM application form for the amendment, as of the date noted above.

Documents Approved:

Document Name	Document Type	Document Date	Document Version
109161.v0418_Resp	Protocol	17/Apr/2018	v0418_Resp
109161LOICS.v0418	Consent Form	16/Apr/2018	v0418

REB members involved in the research project do not participate in the review, discussion or decision.

The Western University HSREB operates in compliance with, and is constituted in accordance with, the requirements of the TriCouncil Policy Statement: Ethical Conduct for Research Involving Humans (TCPS 2); the International Conference on Harmonisation Good Clinical Practice Consolidated Guideline (ICH GCP); Part C, Division 5 of the Food and Drug Regulations; Part 4 of the Natural Health Products Regulations; Part 3 of the Medical Devices Regulations and the provisions of the Ontario Personal Health Information Protection Act (PHIPA 2004) and its applicable regulations. The HSREB is registered with the U.S. Department of Health & Human Services under the IRB registration number IRB 00000940.

Please do not hesitate to contact us if you have any questions.

Sincerely,

Note: This correspondence includes an electronic signature (validation and approval via an online system that is compliant with all regulations).

Creative Commons Attribution License (CCBY)

Human Postural Control Under High Levels of Extremely Low Frequency Magnetic Fields

Boulsset, Nicolas; Villard, Sebastien; Legros, Alexandre

IEEE Access

By clicking the checkbox at the bottom of this page you, as the author or representative of the author, confirm that your work is licensed to IEEE under the Creative Commons Attribution 4.0(CC BY 4.0). As explained by the Creative Commons web site, this license states that IEEE is free to share, copy, distribute and transmit your work under the following conditions:

- Attribution - Users must attribute the work in the manner specified by the author or licensor (but not in any way that suggests that they endorse the users or their use of the work).
- Noncommercial - Users may not use this work for commercial purposes.
- No Derivative Works - Users may not alter, transform, or build upon this work.

With the understanding that:

- **Waiver** - Any of the above conditions can be waived if users get permission from the copyright holder.
- **Public Domain** - Where the work or any of its elements is in the public domain under applicable law, that status is in no way affected by the license.
- **Other Rights** - In no way are any of the following rights affected by the license:
 - A user's fair dealing or fair use rights, or other applicable copyright exceptions and limitations;
 - The author's moral rights;
 - Rights other persons may have either in the work itself or in how the work is used, such as publicity or privacy rights.

For any reuse or distribution, users must make clear to others the license terms of this work.

Upon clicking on the checkbox below, you will not only confirm that your submission is under the CCBY license but you will also be taken to IEEE's Terms of Use, which will require your signature.

I confirm the submitted work is licensed to IEEE under the Creative Commons Attribution 4.0 United States (CC BY 4.0)

TERMS AND CONDITIONS OF AN AUTHOR'S USE OF THE CREATIVE COMMONS ATTRIBUTION LICENSE (CCBY)

1. Creative Commons Licensing

To grow the commons of free knowledge and free culture, all users are required to grant broad permissions to the general public to re-distribute and re-use their contributions freely. Therefore, for any text, figures, or other work in any medium you hold the copyright to, by submitting it, you agree to license it under the Creative Commons Attribution 4.0 Unported License.

2. Attribution

As an author, you agree to be attributed in any of the following fashions: a) through a hyperlink (where possible) or URL to the article or articles you contributed to, b) through a hyperlink (where possible) or URL to an alternative, stable online copy which is freely accessible, which conforms with the license, and which provides credit to the authors in a manner equivalent to the credit given on this website, or c) through a list of all authors.

3. Terms of Publication

- A. By submitting your work to IEEE, you agree to comply with the IEEE Publication Services and Products Board Operations Manual (the "Operations Manual"), including, but not limited to, the specific provisions referenced herein (except to the extent any provision of the Operations Manual requires assignment of copyright in your work to IEEE).
- B. Submission to this IEEE journal does not guarantee publication. By submitting your work to this journal you, as author, recognize that your work may be rejected for any reason. All submissions shall be reviewed by the Editor in accordance with section 8.2.2 of the Operations Manual.
- C. Should your paper be rejected IEEE will not exercise any of the rights granted to it under the [Creative Commons Attribution 4.0 Unported License](#).
- D. IEEE takes intellectual property protection seriously and is opposed to plagiarism in any fashion. Accordingly, you consent to having your work submitted to a plagiarism detection tool and to be bound by IEEE policies concerning plagiarism and author misconduct.
- E. IEEE distributes its technical publications throughout the world and wants to ensure that the material submitted to its publications is properly available to the readership of those publications. You must ensure that your work meets the requirements as stated in section 8.2.1 of the Operations Manual, including provisions covering originality, authorship, author responsibilities and author misconduct. More information on IEEE's publishing policies may be found at <https://www.ieee.org/publications/rights/author-rights-responsibilities.html>.
- F. You warrant that your work, including and any accompanying materials, is original and that you are the author of the work. To the extent your work incorporates text passages, figures, data or other material from the works of others, you represent and warrant that you have obtained all third party permissions and consents to grant the rights herein and have provided copies of such permissions and consents to IEEE. As stated in section 8.2.1B12 of the Operations Manual: "It is the responsibility of the authors, not the IEEE, to determine whether disclosure of their material requires the prior consent of other parties and, if so, to obtain it."
- G. You are advised of Operations Manual section 8.1.1B: "Statements and opinions given in work published by the IEEE are the expression of the authors."
- H. You agree that publication of a notice of violation as a corrective action for a confirmed case of plagiarism, as described in Section 8.2.4 of the IEEE PSPB Publications Operations Manual, does not violate any of your moral rights.
- I. You agree to indemnify and hold IEEE and its parents, subsidiaries, affiliates, officers, employees, agents, partners and licensors harmless from any claim or demand, including reasonable attorneys' fees, due to or arising out of: (1) content you submit, post, transmit or otherwise make available through IEEE's publishing program; (2) your use of this IEEE journal; (3) your violation of these Terms of Use; or (4) your violation of any rights of another party.

BY TYPING IN YOUR FULL NAME BELOW AND CLICKING THE SUBMIT BUTTON, YOU CERTIFY THAT SUCH ACTION CONSTITUTES YOUR ELECTRONIC SIGNATURE TO THIS FORM IN ACCORDANCE WITH UNITED STATES LAW, WHICH AUTHORIZES ELECTRONIC SIGNATURE BY AUTHENTICATED REQUEST FROM A USER OVER THE INTERNET AS A VALID SUBSTITUTE FOR A WRITTEN SIGNATURE.

Signature

22-05-2020

Date

**Questions about the submission of the form or manuscript must be sent to the publication's editor. Please direct all questions about IEEE copyright policy to:
IEEE Intellectual Property Rights Office, copyrights@ieee.org, +1-732-562-3966**

Appendices 3. Copyright release from IEEE-Access (Chapter 2)

Creative Commons Attribution License (CCBY)

Human Postural Responses to High Vestibular Specific Extremely Low-Frequency Magnetic Stimulations

Boulsset, Nicolas; Villard, Sebastien; Legros, Alexandre

IEEE Access

By clicking the checkbox at the bottom of this page you, as the author or representative of the author, confirm that your work is licensed to IEEE under the Creative Commons Attribution 4.0(CCBY 4.0). As explained by the Creative Commons web site, this license states that IEEE is free to share, copy, distribute and transmit your work under the following conditions:

- Attribution - Users must attribute the work in the manner specified by the author or licensor (but not in any way that suggests that they endorse the users or their use of the work).
- Noncommercial - Users may not use this work for commercial purposes.
- No Derivative Works - Users may not alter, transform, or build upon this work.

With the understanding that:

- **Waiver** - Any of the above conditions can be waived if users get permission from the copyright holder.
- **Public Domain** - Where the work or any of its elements is in the public domain under applicable law, that status is in no way affected by the license.
- **Other Rights** - In no way are any of the following rights affected by the license:
 - A user's fair dealing or fair use rights, or other applicable copyright exceptions and limitations;
 - The author's moral rights;
 - Rights other persons may have either in the work itself or in how the work is used, such as publicity or privacy rights.

For any reuse or distribution, users must make clear to others the license terms of this work.

Upon clicking on the checkbox below, you will not only confirm that your submission is under the CCBY license but you will also be taken to IEEE's Terms of Use, which will require your signature.

I confirm the submitted work is licensed to IEEE under the Creative Commons Attribution 4.0 United States (CCBY 4.0)

TERMS AND CONDITIONS OF AN AUTHOR'S USE OF THE CREATIVE COMMONS ATTRIBUTION LICENSE (CCBY)

1. Creative Commons Licensing

To grow the commons of free knowledge and free culture, all users are required to grant broad permissions to the general public to re-distribute and re-use their contributions freely. Therefore, for any text, figures, or other work in any medium you hold the copyright to, by submitting it, you agree to license it under the Creative Commons Attribution 4.0 Unported License.

2. Attribution

As an author, you agree to be attributed in any of the following fashions: a) through a hyperlink (where possible) or URL to the article or articles you contributed to, b) through a hyperlink (where possible) or URL to an alternative, stable online copy which is freely accessible, which conforms with the license, and which provides credit to the authors in a manner equivalent to the credit given on this website, or c) through a list of all authors.

3. Terms of Publication

- A. By submitting your work to IEEE, you agree to comply with the IEEE Publication Services and Products Board Operations Manual (the "Operations Manual"), including, but not limited to, the specific provisions referenced herein(except to the extent any provision of the Operations Manual requires assignment of copyright in your work to IEEE).
- B. Submission to this IEEE journal does not guarantee publication. By submitting your work to this journal you, as author, recognize that your work may be rejected for any reason. All submissions shall be reviewed by the Editor in accordance with section 8.2.2 of the Operations Manual.
- C. Should your paper be rejected IEEE will not exercise any of the rights granted to it under the [Creative Commons Attribution 4.0 Unported License](#).
- D. IEEE takes intellectual property protection seriously and is opposed to plagiarism in any fashion. Accordingly, you consent to having your work submitted to a plagiarism detection tool and to be bound by IEEE policies concerning plagiarism and author misconduct.
- E. IEEE distributes its technical publications throughout the world and wants to ensure that the material submitted to its publications is properly available to the readership of those publications. You must ensure that your work meets the requirements as stated in section 8.2.1 of the Operations Manual, including provisions covering originality, authorship, author responsibilities and author misconduct. More information on IEEE's publishing policies may be found at <https://www.ieee.org/publications/rights/author-rights-responsibilities.html>.
- F. You warrant that your work, including and any accompanying materials, is original and that you are the author of the work. To the extent your work incorporates text passages, figures, data or other material from the works of others, you represent and warrant that you have obtained all third party permissions and consents to grant the rights herein and have provided copies of such permissions and consents to IEEE. As stated in section 8.2.1B12 of the Operations Manual: "It is the responsibility of the authors, not the IEEE, to determine whether disclosure of their material requires the prior consent of other parties and, if so, to obtain it."
- G. You are advised of Operations Manual section 8.1.1B: "Statements and opinions given in work published by the IEEE are the expression of the authors."
- H. You agree that publication of a notice of violation as a corrective action for a confirmed case of plagiarism, as described in Section 8.2.4 of the IEEE PSPB Publications Operations Manual, does not violate any of your moral rights.
- I. You agree to indemnify and hold IEEE and its parents, subsidiaries, affiliates, officers, employees, agents, partners and licensors harmless from any claim or demand, including reasonable attorneys' fees, due to or arising out of: (1) content you submit, post, transmit or otherwise make available through IEEE's publishing program; (2) your use of this IEEE journal; (3) your violation of these Terms of Use; or (4) your violation of any rights of another party.

BY TYPING IN YOUR FULL NAME BELOW AND CLICKING THE SUBMIT BUTTON, YOU CERTIFY THAT SUCH ACTION CONSTITUTES YOUR ELECTRONIC SIGNATURE TO THIS FORM IN ACCORDANCE WITH UNITED STATES LAW, WHICH AUTHORIZES ELECTRONIC SIGNATURE BY AUTHENTICATED REQUEST FROM A USER OVER THE INTERNET AS A VALID SUBSTITUTE FOR A WRITTEN SIGNATURE.

Signature

04-09-2020
Date

Questions about the submission of the form or manuscript must be sent to the publication's editor. Please direct all questions about IEEE copyright policy to:

IEEE Intellectual Property Rights Office, copyrights@ieee.org, +1-732-562-3966

Appendices 4. Copyright releases from IEEE-Access (Chapter 3)

Curriculum Vitae

BOUISSET Nicolas

Born March 24th, 1976 in Montpellier (FRANCE)

ORCID [0000-0001-9068-8643](https://orcid.org/0000-0001-9068-8643)

Web of Science ResearcherID [AAJ-9520-2020](https://orcid.org/AAJ-9520-2020)

Professional Experience

2016-2020:

- PhD student under Dr Villard's supervision (Western University, London, Ontario Canada)

2011 – now:

- Consultant and translator for KPTEN (physiotherapy seminars company)

2003 – 2016:

- Physiotherapist in Private practice

21/06/2007 – 27/06/2007:

- Physiotherapist for the Crédit Agricole professional cycling team

18/06/2004 – 22/06/2004:

- Physiotherapist for the Crédit Agricole professional cycling team

02/05/04 – 17/05/04:

- Humanitarian Physiotherapy mission in Senegal for HANDISABLE

07/03/2004 – 14/03/2004:

- Physiotherapist for the Crédit Agricole professional cycling team

03/03/2003 – 02/05/2003:

- Humanitarian Physiotherapy mission in Vietnam for HANDICAP INTERNATIONAL

Qualifications

2016-2020:

- PhD in kinesiology (Western Ontario University – Canada)

2012-2015:

- Master's degree by research in Human movement science with honours (Université de Montpellier- France)

2011:

- Post graduate Diploma in postural control mechanism (Université Joseph Fourier – Grenoble1 - France)

2010:

- Post graduate Diploma in vestibular rehabilitation (Université Paris VI - France)

2009:

- Post graduate Diploma in Maxillo facial rehabilitation (Université de Montpellier - France)

2003:

- Bachelor's degree in physiotherapy (Université Catholique de Louvain la Neuve in Belgium)

2000:

- Saint CYR Coëtquidan Military Academy for French reserve officers (first Lieutenant)

1999:

- Bachelor's degree in sport science (Université de la Réunion - France)

Continuing professional development.

2016:

- Ultrasound course for physiotherapist (Julie Hides)
- Level 1 clinical integration Diploma from the Orthopaedic Division of the Canadian Physiotherapy Association

2012:

- Clinical assesment and manual therapy of the knee (international academy of orthopaedic Medecine United States)

- Clinical assesment and manual therapy of the shoulder (international academy of orthopaedic Medecine United States)
- Clinical assesment and manual therapy of the elbow (international academy of orthopaedic Medecine United States)
- Clinical assesment and manual therapy of the wrist and the hand (international academy of orthopaedic Medecine United States)
- Understanding and analyzing the randomized control trials (Rob Herbert)

2011:

- Introductory lower limb biomechanics certificate
- Medical Screening and triage (William Boissonnault)
- Hemodynamics for physiotherapists (Alan Taylor and Roger Kerry)
- Breathing Evaluation & Management certificate (Laurie Mclaughlin)

2010:

- Therapeutic exercice for cervical Spine disorders certificate (Deborah Falla)

2008:

- Neurodynamic solution instructor course (Michael Shacklock)

2007:

- Mc Kenzie level A
- Mc Kenzie Level B
- Neurodynamic for the lower quarter (Michael Shacklock)
- Neurodynamic for the upper quarter (Michael Shacklock)
- Sports physiotherapy Certificate (Université de Bourgogne)

2004-2005:

- Sports physiotherapy Certificate
- Myo-facial physiotherapy Certificate
- Breathing rehabilitation Certificate

Scholarships, Fellowships and Grants

2016-2020: PhD

- Mitacs Accelerate Fellowship: \$ 110,170.29
- WGRS – KINESIOLOGY: \$ 61,171.18
- Graduate Student Travel Grant: \$ 2400

Prizes and awards

2018:

- Second best student poster presentation: BioEm2018, Slovenia

2017:

- Second best student platform presentation: BioEm2017, China

Equipment and software experience

Electrophysiological Stimulation:

- Galvanic Vestibular Stimulation
- Extremely low frequency magnetic fields
- tDCS & tACS ((StarStim, Neuroelectrics, Spain)

Electrophysiologic Recording:

- Electroencephalography
- Pupillometry
- Eye tracking
- Vestibular testing: vHIT: otometrics. (Danemark). Videonystagmography (Framiral, Amplifon. Subjective Visual Vertical. Optokinetics Stimulatio.

Force Platforms:

- AMTI (USA)
- Intech (France)

Software and Computer Programming:

- Matlab
- Python
- Open CV
- Labview
- R
- Inkscape
- Blender

Professional Communications

Publications

- **Bouisset N**, Villard S, Legros A.2020 Vestibular Extremely low frequency magnetic and electric stimulation effects on human subjective visual vertical perception. *Journal of Neural Engineering*. (Under review: Brain Stimulation)
- **Bouisset N**, Villard S, Legros A.2020, Human Postural Control Under High Levels of Extremely Low Frequency Magnetic Fields. *IEEE ACCESS*
- **Bouisset N**, Villard S, Legros A.2020, Human Postural Responses to High Vestibular Specific Extremely Low Frequency Magnetic Stimulations. *IEEE ACCESS*
- Lagarde J, **Bouisset, N**. 2020. When is now in a distributed system? Animated motion (could) set the present in brain networks. (Submitted)
- Villard S, Allen A, **Bouisset N**, Corbacio M, Thomas A, Guerraz M, Legros A. 2018. Impact of extremely low-frequency magnetic fields on human postural control. *Exp. Brain Res*

Platform Presentations at Scientific Meetings- National

- **Bouisset N**., (2012) The neurodynamic approach in manual therapy. *First French Orthopaedic manual therapy congress*. Paris, France 10 2012
- **Bouisset, N**., Villard, S., Goulet D., Plante M., Souques M., Deschamps F., Ostiguy G., Lambrozo J., Legros A. Champs magnétiques d'extrêmement basses fréquences appliqués au système vestibulaire et contrôle de la posture. *EBF. Annual meeting of the Société Française de Radioprotection (SFRP), Montpellier, France. October 2nd, 2018*
- Villard, S., **Bouisset, N**., Goulet D., Plante M., Souques M., Deschamps F., Ostiguy G., Lambrozo J., Legros A. Effets de stimulations électriques magnétiques d'extrêmes basses fréquences sur la performance vestibulaire chez l'Homme. *EBF. Annual meeting of the Société Française de Radioprotection (SFRP), Montpellier, France. October 2nd, 2018*

Platform Presentations at Scientific Meetings- International

- **Bouisset N**, Villard S, Goulet D, Plante D, Souques M, Deschamps F, Ostiguy G, Lambrozo J & Legros A (2017). Human Vestibular System Exposed to Extremely Low Frequency Magnetic Fields up to 100 mT: a body sway investigation Annual Joint Meeting of the Bioelectromagnetics Society and the European BioElectromagnetics Association – BioEm2017, Hangzhou, China. 6/2017.

- Villard S, **Bouisset N**, Goulet D, Plante D, Souques M, Deschamps F, Ostiguy G, Lambrozo J & Legros A Acute effect of low frequency magnetic fields on the vestibular system: perception of verticality. Annual Joint Meeting of the Bioelectromagnetics Society and the European BioElectromagnetics Association – BioEm2017, Hangzhou, China. 6/2017.
- Villard S, **Bouisset N**, Goulet D, Plante D, Souques M, Deschamps F, Ostiguy G, Lambrozo J & Legros A. Extremely low frequency electric and magnetic stimulations on the vestibular performance in humans. Annual Joint Meeting of the Bioelectromagnetics Society and the European BioElectromagnetics Association – BioEm2018, Piran, Portoroz, Slovenia, June 25th – 29th, 2018
- **Bouisset N**, Villard S & Legros A. Postural Control Under Vestibular Extremely Low Frequency Magnetic Fields Stimulations. Cognitive and Motor Functions of the Vestibular System. Aix-Marseille University. Marseille, France. July 5th-6th.2018
- **Bouisset N**, Villard S, Goulet D, Plante D, Souques M, Deschamps F, Ostiguy G, Lambrozo J & Legros A (2019). Orientation and Disorientation Effects of a 50 mT Extremely Low Frequency Magnetic Fields on Human Postural Control. Annual Joint Meeting of the Bioelectromagnetics Society and the European BioElectromagnetics Association – BioEm2019, Montpellier, France, June 23– 28th, 2019
- **Bouisset N**, Villard S, Goulet D, Plante D, Souques M, Deschamps F, Ostiguy G, Lambrozo J & Legros A (2019). Probing Human Vestibulo-Autonomic System with Extremely Low Frequency Magnetic Fields: a pilot study. Annual Joint Meeting of the Bioelectromagnetics Society and the European BioElectromagnetics Association – BioEm2020, Oxford, United Kingdom, June 21– 26th, 2020 (Cancelled due to Covid-19)

Posters

- **Bouisset. N.**, Villard, S., Corbacio, M., Goulet, D., Plante, M., Souques, M., Deschamps, F., Ostiguy, G., Lambrozo, J., Guerraz, M., & Legros, A (2017). Can time varying magnetic fields impact the vestibular system? A body sway investigation. London Research day conference, London, Ontario, Canada
- **Bouisset. N.**, Villard, S., M., Goulet, D., Plante, M., Souques, M., Deschamps, F., Ostiguy, G., Lambrozo, J. & Legros, A (2018). Vestibular specific Time varying magnetic fields stimulation impact on human body sway. London Research day conference, London, Ontario, Canada
- **Bouisset N.**, Villard S. Corbacio, M. Goulet, D. Plante, M. Souques, M. Deschamps, F. Ostiguy G., Lambrozo J., Guerraz M., Legros A. Do Extremely Low Frequency Magnetic Field stimulations of the vestibular system modulate postural control in humans? Annual Joint Meeting of the Bioelectromagnetics Society and the European BioElectromagnetics Association – BioEm2018, Piran, Portoroz, Slovenia, June 25th – 29th, 2018

Workshops

- The neurodynamic approach in manual therapy: application to the upper quarter. *First French Orthopaedic manual therapy congress*. Paris, France 10 2012

Service

PROFESSIONAL AFFILIATIONS

- Société Française de Physiothérapie (SFP)
- Société Française de kinésithérapie Vestibulaire (SFKV)
- OMT-France (Orthopaedic Manual Therapy France)
- Bioelectromagnetic Society (BEMS)
- European Bioelectromagnetics Association (EBEA)

JOURNAL REVIEWER

- IEEE-Access
- Bioelectromagnetics
- Journal of manual and manipulative therapy
- EMC « Kinésithérapie-Médecine physique-Réadaptation »